UNIVERSITY OF CALIFORNIA
SANTA CRUZ

POTENTIAL AND EVIDENCE FOR LOCAL CLIMATE ADAPTATION IN CORALS

A dissertation submitted in partial satisfaction
of the requirements of

DOCTOR OF PHILOSOPHY in
ECOLOGY & EVOLUTIONARY BIOLOGY
by

Jaelyn T. Bos
August 2026

The Dissertation of Jaelyn T. Bos is approved:

_____
Professor Malin Pinsky, chair

_____
Professor Lisa McManus

_____
Professor Peter Raimondi

_____
Professor Isabel M. da Silva

_____
Donald Smith
Interim Vice Provost and
Dean of Graduate Studies

TABLE OF CONTENTS

LIST OF TABLES

LIST OF FIGURES

ABSTRACT

POTENTIAL AND EVIDENCE FOR LOCAL CLIMATE ADAPTATION IN CORALS

Jaelyn T. Bos

Climate change poses an existential threat to tropical corals, but corals vary in their thermal tolerance at multiple spatial scales. Here, I evaluate the spatial scales at which corals show potential and evidence for local temperature adaptation.

In Chapter 1, I evaluate the scale at which microclimates are detectable by comparing remotely sensed sea surface temperatures to data from in situ temperature loggers on reefs worldwide. I found that the remote dataset constitutes a good proxy for maximum monthly mean temperatures, but missed sub-daily variation as well as peak temperatures in the hottest microclimates. In Chapter 2, I used *Acropora tenuis* samples from the Philippines to evaluate isolation by distance patterns in both coral hosts and their algal symbionts. I found four near-panmictic taxa within our *Acropora cf. tenuis* samples, consistent with long (20km+) larval dispersal distances, but significant spatial structuring in their symbiotic algae. In Chapter 3, I looked for genetic variants correlated with temperature at both broad and fine spatial scales in samples of *Acropora. aff. divaricata* in Mozambique. I found two lineages, one of which was only collected in the hottest microclimate. These lineages differentiated most strongly at HES-1 locus, a genomic area described in *Acropora cf. hyacinthus* in American Samoa and putatively related to heat tolerance. I found strong genetic similarity at the HES-1 locus between lineages of *Acropora aff. divaricata* and

Acropora cf. hyacinthus collected in hot microclimates, consistent with incomplete lineage sorting or introgression.

Chapters 1 and 2 suggest that a mismatch between the broad scale at which Acropora disperse and show genetic variation, and the fine scales at which microclimates occur, may limit local adaptation. However, chapters 2 and 3 show mechanisms by which this difficulty may be overcome. These mechanisms include local adaptation by algal symbionts, as well as speciation and reproductive isolation between closely related *Acropora* lineages. The latter process may permit local adaptation by preventing gene swamping between lineages adapted to different microclimates. Chapter 3 also reveals a potentially adaptive allele shared across *Acropora* lineages, revealing another role that evolutionary processes play in coral responses to climate change.

DEDICATION

For my family, for my friends, and for everyone whose lives and livelihoods depend on coral reefs.

ACKNOWLEDGEMENTS

An adequate acknowledgement section would be longer than this dissertation. Thank you first to my advisor Malin Pinsky: I've learned so, so much from you, and am deeply grateful for both the support and the independence I was granted in the course of this PhD. Thank you also to the rest of my committee: Isabel Marques da Silva, Lisa McManus, and Peter Raimondi. Your unique strengths, generosity with your time, and tolerance for weird time zones, made this dissertation possible.

Just as importantly, thank you to the many students, postdocs, and researchers with whom I have shared a research group since 2020: Kyra Fitz, Jeewantha Bandara, Zoë Kitchel, René Clark, Katrina Catalano, Maya Zeff, Mikaela Salvador, Rae Fadlovich, Brendan Reid, Alexa Fredston, Aurore Maureaud, Mark Morales, Lucas Godoy, Marianne Dehasque, Meaghan Clark, and Roy Roberts. You're all incredible scientists and human beings and it's been such a privilege to have you in my life.

Thank you to the staff, faculty, and students at Rutgers University and at University of California, Santa Cruz. Thank you to warm student and postdoc communities at both universities, and thank you to Rutgers EcoGSA for being a wonderful launchpad to begin graduate school, even in the midst of a pandemic. Thank you especially to the many international students and researchers: you all make this country immeasurably richer, and I'm lucky to know you.

Thank you as well to the vibrant community at Lúrio University in Mozambique. Thank you to my undergraduate thesis students: Didi Minhote, Tomás

Cossa Jr., and Zulekha Jafar. Working with you all has been a delight, and I can't wait to see what you do next. Thanks to Dr. Bibiana Nassongole, an excellent scientist and a dear friend. It's a cliché to say that a dissertation wouldn't have happened without someone, but in this case, it's also true.

Finally, thank you to all of my friends and family. Thanks to my friends for continually inspiring me with your kindness, especially Fio Haire and Lucy Weinman. Thanks to Udari Peiris, Jeewantha Bandadara, and my perfect godson Teddy. Thanks to my Mozambican friends, and my RPCV friends, who understand the beauty as well as the challenges of working in this extraordinary country. Finally, thank you to my parents, Sara Bos and Nathan Bos, for deeply valuing education, but valuing me as a person even more. Thank you to my siblings Graham Bos and Bianca Bos, and sister in law Caroline Bos, for unwavering support, kindness, and fun.

This dissertation was made possible by a Rutgers School of Environmental and Biological Sciences Excellence Fellowship, a National Defense Science and Engineering Graduate Fellowship, and grants from the Philip Stephenson Foundation, the American Philosophical Society, the Rutgers Department of Ecology and Evolution, the University of California, Santa Cruz Academic Senate Committee on Research, and the Paul Angell Foundation.

PUBLICATION STATEMENT

The text of this dissertation includes reprints of published material:

Chapter 1:
J. T. Bos & M. L., Pinsky. Fine resolution satellite sea surface temperatures capture the conditions experienced by corals at monthly but not daily timescales. *Coral Reefs* 44, 423–434 (2025). https://doi.org/10.1007/s00338-024-02611-8.

Chapter 2:
J. T. Bos, L. C. McManus, R. Ravago-Gotanco, M. L. Pinsky. Contrasting patterns of seascape genetics in *Acropora cf. tenuis* and their symbiotic algae. *Molecular Ecology*, In Review. Published online at BioRxiv at https://doi.org/10.64898/2026.04.07.716991

INTRODUCTION

The last two centuries brought rapid changes for global biodiversity. Planetary-level changes in land use, resource extraction, and especially climate, have ushered in profound challenges and opportunities for organisms from trees to microbes, with serious consequences for both biodiversity and human society (Calvin et al., 2023; Ellis, 2015; Pauly et al., 2005). Many species will need to rapidly evolve if they are to survive in our changing world (Hoffmann & Sgrò, 2011; Wiens & Zelinka, 2024). Evolutionary rescue depends largely on genetic variants that already exist within species, which may be derived from landscape-level variation in populations' evolved environmental tolerances (Meek et al., 2023; Razgour et al., 2019). Such adaptive variation across space generally occurs at broad scales much larger than an individual organism's dispersal distance; however, the twenty first century has brought increasing understanding that fine-scale environmental heterogeneity may play an important role in species' climate change responses (Pinsky et al., 2025; Richardson et al., 2014; Slatkin, 1987).

Nowhere is understanding the spatial dynamics of evolutionary rescue more important than on coral reefs. Coral reefs play key roles in maintaining both global biodiversity and human society, hosting hundreds of thousands of species, providing livelihoods for millions of subsistence fishers, and contributing billions of dollars in economic value (Burke & Spalding, 2022; Fisher et al., 2015; Teh et al., 2013). However, reef-building corals face profound danger from climate change: the "fourth

global bleaching event" in 2023 and 2024 affected a majority of tropical reefs worldwide with "unprecedented" levels of heat stress and mass bleaching (Reimer et al., 2024). Broad scientific consensus asserts that coral reefs' survival depends on the ability of corals to rapidly evolve (McManus et al., 2021). Globally, coral bleaching temperatures increased by an estimated 0.5 degrees between 2007 and 2017 (Sully et al., 2019). However, this assemblage-level evolution may not be fast enough to keep pace with climate change (Lachs et al., 2023).

Ongoing evolution within coral species could be facilitated by genetic adaptations for elevated heat tolerance that already exist in wild coral populations (Bay et al., 2017). Such adaptive variation can certainly be found at broad spatial scales: coral communities in particularly hot regions, such as the Persian Gulf, can exhibit bleaching thresholds multiple degrees higher than those in cooler environments (Howells et al., 2016). Regional baseline temperature is so fundamental to heat tolerance that coral bleaching alerts are calculated relative to a summer baseline at that location, rather than in terms of absolute temperature (Liu et al., 2014). However, different regions may host markedly different coral assemblages, and adaptive alleles may move slowly across hundreds or even thousands of miles of environmental gradient (Ateweberhan & McClanahan, 2016; Vogt-Vincent et al., 2025). Intriguingly, genetic variation in coral heat tolerance can also exist at finer spatial scales, including within individual reefs. Hot microclimates on reefs sometimes host corals with genetic adaptations for elevated heat tolerance, and may serve as important reservoirs of heat adapted genotypes (Palumbi et al., 2014;

Thomas et al., 2022). The spatial scale of climate and genetic variation, the prevalence of microgeographic adaptive variation across taxa and environments, and the evolutionary mechanisms underlying such genetic variation remain under-explored.

My dissertation unpacks the spatial scales at which reef-building corals show both potential for, and evidence of, adaptation to climate conditions at fine geographic scales. First, in order to understand whether corals exhibit adaptive variation with microclimate, we must assess the spatial grain of available microclimates. In Chapter 1 I explore the spatial scale at which temperature varies on coral reefs, and to what extent reef temperatures can be accurately measured with remote sensing. I show that while 1-km2 remotely sensed temperatures are a good proxy for baseline "max monthly mean" temperatures, they are poor predictors of maximum temperatures at the hottest sites, as well as sub-diel temperature variation at all sites. The latter issue stems from the poor temporal resolution of daily satellite products, while the former also suggests that some hot microclimates are only detectable below the 1-km2 scale. Second, understanding the spatial scale at which local adaptation occurs, as well as how locally adapted alleles might spread, requires an understanding of seascape-level genetic connectivity. In Chapter 2, I consider the spatial scale of dispersal in corals from the genus *Acropora*, as well as their algal symbionts. I find long dispersal distances in coral hosts leading to near panmixia across the seascape, but lower dispersal distances and increased genetic structuring across space in their algal symbionts, suggesting the latter organisms as candidates

for fine-scale local adaptation. I also find that coral hosts all from the same putative species (*Acropora tenuis*) should actually be characterized as four genetically distinct taxa. Third, measuring the actual spatial scale of local climate adaptation requires sampling at multiple spatial scales corresponding to climatic differences. In Chapter 3, I look for patterns of genetic variation with temperature across multiple spatial scales in Mozambique, finding variation at a locus putatively involved in heat tolerance at both regional and microclimate scales. Interestingly, putatively adaptive variation at the same locus appears to have different evolutionary sources in closely related coral species, and the variant found in hot microclimates may be derived from introgression. Together, these chapters demonstrate that local adaptation at fine spatial scales can constitute a key evolutionary force shaping coral reef futures, while demonstrating the need for more research across diverse locations and taxa.

References

Ateweberhan, M., & McClanahan, T. R. (2016). Partitioning scleractinian coral diversity across reef sites and regions in the Western Indian Ocean. Ecosphere, 7(5), e01243. https://doi.org/10.1002/ecs2.1243

Bay, R. A., Rose, N. H., Logan, C. A., & Palumbi, S. R. (2017). Genomic models predict successful coral adaptation if future ocean warming rates are reduced. Science Advances, 3(11), e1701413. https://doi.org/10.1126/sciadv.1701413

Burke, L., & Spalding, M. (2022). Shoreline protection by the world's coral reefs: Mapping the benefits to people, assets, and infrastructure. Marine Policy, 146, 105311. https://doi.org/10.1016/j.marpol.2022.105311

Calvin, K., Dasgupta, D., Krinner, G., Mukherji, A., Thorne, P. W., Trisos, C., Romero, J., Aldunce, P., Barrett, K., Blanco, G., Cheung, W. W. L., Connors, S., Denton, F., Diongue-Niang, A., Dodman, D., Garschagen, M., Geden, O., Hayward, B., Jones, C., … Ha, M. (with Lee, H.). (2023). IPCC, 2023: Climate Change 2023: Synthesis Report. Contribution of Working Groups I, II and III to the Sixth Assessment Report of the Intergovernmental Panel on

Climate Change [Core Writing Team, H. Lee and J. Romero (eds.)]. IPCC, Geneva, Switzerland. (P. Arias, M. Bustamante, I. Elgizouli, G. Flato, M. Howden, C. Méndez-Vallejo, J. J. Pereira, R. Pichs-Madruga, S. K. Rose, Y. Saheb, R. Sánchez Rodríguez, D. Ürge-Vorsatz, C. Xiao, N. Yassaa, J. Romero, J. Kim, E. F. Haites, Y. Jung, R. Stavins, … C. Péan, Eds.; First). Intergovernmental Panel on Climate Change (IPCC). https://doi.org/10.59327/IPCC/AR6-9789291691647

Ellis, E. C. (2015). Ecology in an anthropogenic biosphere. Ecological Monographs, 85(3), 287–331. https://doi.org/10.1890/14-.1

Fisher, R., O'Leary, R. A., Low-Choy, S., Mengersen, K., Knowlton, N., Brainard, R. E., & Caley, M. J. (2015). Species Richness on Coral Reefs and the Pursuit of Convergent Global Estimates. Current Biology, 25(4), 500–505. https://doi.org/10.1016/j.cub.2014.12.022

Hoffmann, A. A., & Sgrò, C. M. (2011). Climate change and evolutionary adaptation. Nature, 470(7335), 479–485. https://doi.org/10.1038/nature09670

Howells, E. J., Abrego, D., Meyer, E., Kirk, N. L., & Burt, J. A. (2016). Host adaptation and unexpected symbiont partners enable reef‐building corals to tolerate extreme temperatures. Global Change Biology, 22(8), 2702–2714. https://doi.org/10.1111/gcb.13250

Lachs, L., Donner, S. D., Mumby, P. J., Bythell, J. C., Humanes, A., East, H. K., & Guest, J. R. (2023). Emergent increase in coral thermal tolerance reduces mass bleaching under climate change. Nature Communications, 14(1), 4939. https://doi.org/10.1038/s41467-023-40601-6

Liu, G., Heron, S., Eakin, C., Muller-Karger, F., Vega-Rodriguez, M., Guild, L., De La Cour, J., Geiger, E., Skirving, W., Burgess, T., Strong, A., Harris, A., Maturi, E., Ignatov, A., Sapper, J., Li, J., & Lynds, S. (2014). Reef-Scale Thermal Stress Monitoring of Coral Ecosystems: New 5-km Global Products from NOAA Coral Reef Watch. Remote Sensing, 6(11), 11579–11606. https://doi.org/10.3390/rs61111579

McClanahan, T. R., Darling, E. S., Maina, J. M., Muthiga, N. A., 'agata, S. D., Jupiter,
S. D., Arthur, R., Wilson, S. K., Mangubhai, S., Nand, Y., Ussi, A. M., Humphries, A. T., Patankar, V. J., Guillaume, M. M. M., Keith, S. A., Shedrawi, G., Julius, P., Grimsditch, G., Ndagala, J., & Leblond, J. (2019). Temperature patterns and mechanisms influencing coral bleaching during the 2016 El Niño. Nature Climate Change, 9(11), 845–851. https://doi.org/10.1038/s41558-019-0576-8

McManus, L. C., Forrest, D. L., Tekwa, E. W., Schindler, D. E., Colton, M. A., Webster, M. M., Essington, T. E., Palumbi, S. R., Mumby, P. J., & Pinsky, M. L. (2021). Evolution and connectivity influence the persistence and recovery of coral reefs under climate change in the Caribbean, Southwest Pacific, and Coral Triangle. Global Change Biology, 27(18), 4307–4321. https://doi.org/10.1111/gcb.15725

Meek, M. H., Beever, E. A., Barbosa, S., Fitzpatrick, S. W., Fletcher, N. K., Mittan-Moreau, C. S., Reid, B. N., Campbell-Staton, S. C., Green, N. F., & Hellmann, J. J. (2023). Understanding Local Adaptation to Prepare Populations for Climate Change. BioScience, 73(1), 36–47. https://doi.org/10.1093/biosci/biac101

Palumbi, S. R., Barshis, D. J., Traylor-Knowles, N., & Bay, R. A. (2014). Mechanisms of reef coral resistance to future climate change. Science, 344(6186), 895–898. https://doi.org/10.1126/science.1251336

Pauly, D., Watson, R., & Alder, J. (2005). Global trends in world fisheries: Impacts on marine ecosystems and food security. Philosophical Transactions of the Royal Society B: Biological Sciences, 360(1453), 5–12. https://doi.org/10.1098/rstb.2004.1574

Pinsky, M. L., Hillebrand, H., Chase, J. M., Antão, L. H., Hirt, M. R., Brose, U., Burrows, M. T., Gauzens, B., Rosenbaum, B., & Blowes, S. A. (2025). Warming and cooling catalyse widespread temporal turnover in biodiversity. Nature, 638(8052), 995–999. https://doi.org/10.1038/s41586-024-08456-z

Razgour, O., Forester, B., Taggart, J. B., Bekaert, M., Juste, J., Ibáñez, C., Puechmaille, S. J., Novella-Fernandez, R., Alberdi, A., & Manel, S. (2019). Considering adaptive genetic variation in climate change vulnerability assessment reduces species range loss projections. Proceedings of the National Academy of Sciences, 116(21), 10418–10423. https://doi.org/10.1073/pnas.1820663116

Reimer, J. D., Peixoto, R. S., Davies, S. W., Traylor-Knowles, N., Short, M. L., Cabral-Tena, R. A., Burt, J. A., Pessoa, I., Banaszak, A. T., Winters, R. S., Moore, T., Schoepf, V., Kaullysing, D., Calderon-Aguilera, L. E., Wörheide, G., Harding, S., Munbodhe, V., Mayfield, A., Ainsworth, T., … Voolstra, C. R. (2024). The Fourth Global Coral Bleaching Event: Where do we go from here? Coral Reefs, 43(4), 1121–1125. https://doi.org/10.1007/s00338-024-02504-w

Richardson, J. L., Urban, M. C., Bolnick, D. I., & Skelly, D. K. (2014).

Microgeographic adaptation and the spatial scale of evolution. Trends in Ecology & Evolution, 29(3), 165–176. https://doi.org/10.1016/j.tree.2014.01.002

Slatkin, M. (1987). Gene Flow and the Geographic Structure of Natural Populations. Science, 236(4803), 787–792. https://doi.org/10.1126/science.3576198

Sully, S., Burkepile, D. E., Donovan, M. K., Hodgson, G., & Van Woesik, R. (2019). A global analysis of coral bleaching over the past two decades. Nature Communications, 10(1), 1264. https://doi.org/10.1038/s41467-019-09238-2

Teh, L. S. L., Teh, L. C. L., & Sumaila, U. R. (2013). A Global Estimate of the Number of Coral Reef Fishers. PLoS ONE, 8(6), e65397. https://doi.org/10.1371/journal.pone.0065397

Thomas, L., Underwood, J. N., Rose, N. H., Fuller, Z. L., Richards, Z. T., Dugal, L., Grimaldi, C. M., Cooke, I. R., Palumbi, S. R., & Gilmour, J. P. (2022). Spatially varying selection between habitats drives physiological shifts and local adaptation in a broadcast spawning coral on a remote atoll in Western Australia. Science Advances, 8(17), eabl9185. https://doi.org/10.1126/sciadv.abl9185

Vogt-Vincent, N. S., Pringle, J. M., Cornwall, C. E., & McManus, L. C. (2025). Anthropogenic climate change will likely outpace coral range expansion. Science Advances, 11(23), eadr2545. https://doi.org/10.1126/sciadv.adr2545

Wiens, J. J., & Zelinka, J. (2024). How many species will Earth lose to climate change? Global Change Biology, 30(1), e17125. https://doi.org/10.1111/gcb.17125

Chapter 1

Fine resolution satellite sea surface temperatures capture the conditions experienced by corals at monthly but not daily time scales.

Bos, J.T.[1] & Pinsky, M.L.[1]

1. University of California at Santa Cruz, Ecology and Evolutionary Biology Department, 130 McAllister Way, Santa Cruz, CA 95060, U.S.A.

Published 16 January 2025 in *Coral Reefs*
https://doi.org/10.1007/s00338-024-02611-8

Abstract

Water temperature is a strong driver of growth, survival, and local adaptation in corals, but our knowledge of the temperatures experienced by corals on reefs worldwide remains limited. While *in situ* temperature loggers can provide high quality data, they are relatively expensive to place and retrieve. Alternatively, remotely sensed sea surface temperature data is globally available but may be a biased representation of the temperatures experienced by corals. Here, we compared data from 314 temperature loggers on coral reefs to the ~1 km^2 resolution remotely sensed Multi-scale Ultra-high Resolution Sea Surface Temperature (MUR) product from NASA. We found good agreement (Pearson's $r = 0.95$) between maximum monthly mean temperatures calculated from remote and *in situ* data, with 84% of temperatures within 0.5 °C of each other. However, remotely sensed temperature did not effectively capture sub-diel temperature fluctuations and the highest peak temperatures that may be most dangerous for corals. Predictions of *in situ* temperatures were significantly but weakly improved by a consideration of reef geomorphology. Ultimately, we found that remotely sensed temperatures can accurately represent the monthly conditions experienced by most corals, but should be used with caution at finer temporal scales.

1. 1 Introduction

Climate varies on multiple scales. While broad climate patterns define biomes, spatial temperature variation also occurs within regions and even habitats.

"Microclimates" exist across scales from centimeters to meters in ecosystems as diverse as forests, mountains, and the intertidal zone, and they can complicate our understanding of climate change impacts by serving to either buffer or exacerbate the effects of rising regional temperatures on individual organisms (Seabra et al. 2011; Verrall and Pickering 2020; Zellweger et al. 2020). Microclimates also exist on coral reefs, and a growing body of research suggests that microclimate variation plays a key role in determining thermal tolerance in corals (Barshis et al. 2013; Palumbi et al. 2014; Schoepf et al. 2015). However, accurately mapping *in situ* temperatures on coral reefs remains challenging. Here we assess the utility of a globally-available remote sensing product for predicting geographically fine-scale temperatures on coral reefs.

Coral reefs occur in more than one hundred countries and territories in every tropical ocean basin (UNEP-WCMC et al. 2018). This broad range naturally leads to substantial differences in temperature between reefs, with some regions such as the Red Sea and the Persian Gulf exhibiting summer temperatures multiple degrees warmer than those found elsewhere in the world (Howells et al. 2012). However, temperature differences also exist at finer spatial scales. *In situ* temperatures on coral reefs depend not only on regional climate patterns but also on within-reef processes including tidal cycling and wave action (MacKellar 2013; Bachman 2022). These fine-scale processes affect both long-term temperature averages and sub-diel temperature variability (Reid et al. 2020). Sites separated by as little as 200 meters can have daily temperature ranges that differ substantially, from less than 1 °C to as

great as 5 °C (Davis et al. 2011). Ultimately, the temperature regime experienced by an individual coral results from the combination of regional processes, within-reef water circulation, depth (Cyronak et al. 2020), and atmospheric conditions, including clouds (Leahy et al. 2013). As a result, regional temperature averages may differ substantially from the temperature actually experienced by an individual coral animal in its microclimate (Thomas et al. 2022).

Microclimate variations in temperature have clear effects on growth, survival, and local genetic adaptation in corals. Differences in thermal tolerance between populations of conspecific corals inhabiting different parts of the same reefs have been documented in *Porites* in Florida (Kenkel 2015), *Pocillopora* in Australia (Marhoefer et al. 2021), and *Acropora* in American Samoa (Palumbi et al. 2014), among others. Furthermore, physiological differences between corals in different microclimates have in some cases been explicitly linked to genetic differences in coral animals (Palumbi et al. 2014; Thomas et al. 2022) or symbionts (Hoadley et al. 2019). Multiple studies suggest that natural variation in heat tolerance between coral populations may be a key factor contributing to climate resilience of coral reefs (Kleypas et al. 2016; McManus et al. 2021), emphasizing the importance of accurately assessing temperature landscapes on reefs.

Studies make use of multiple temperature metrics to delineate microclimates, though a subset of metrics are particularly common. First, maximum monthly mean (MMM) temperatures are commonly used as baselines in coral bleaching studies and are closely related to local heat tolerance in coral assemblages (Kayanne 2017).

MMM temperatures are equal to mean water temperatures during the hottest month of the year, usually calculated across a timespan of several years (Liu, Gang et al. 2017). Heat acclimation and local climate adaptation in corals can also respond to peak daily temperatures (Thomas et al. 2018; Marhoefer et al. 2021). Third, heat adaptation in corals can relate to daily temperature ranges, with corals that experience wider ranges also having more protection against bleaching (Kenkel et al. 2015; Safaie et al. 2018). This latter observation suggests that the difference between local daily maximum and minimum temperatures may have significant effects on coral health.

Measuring local temperatures on coral reefs usually involves the placement of *in situ* temperature loggers, a process that can be expensive and time consuming (Colin and Johnston 2020). Consequently, many coral reefs, particularly in remote areas, lack *in situ* temperature measurements entirely. By contrast, remotely sensed data is often globally available and free to researchers. For example, global remotely-sensed sea surface temperature data from NOAA has long been used to both explain and predict coral bleaching (Gleeson and Strong 1995). However, it remains unclear to what extent remotely sensed products are accurate, precise, and unbiased predictors of *in situ* temperatures on coral reefs because of differences between the ocean surface observed by satellites and the more complex conditions experienced by corals. Comparison of maximum monthly mean temperatures calculated from *in situ* loggers and NOAA's 5 km^2 Coral Reef Watch remote sea surface temperature product in American Samoa revealed a greater than 0.5 °C difference between the two metrics (Klepac and Barshis 2022). Similarly, a comparison of the NOAA product with *in situ*

loggers in Belize noted mean offsets of greater than 0.5 °C that varied seasonally, despite high linear correlations between remote and *in situ* temperatures (Castillo et al. 2012). A comparison between the NOAA product and *in situ* data using 17 temperature loggers in Kiritimati also found strong linear correlations in long term averages but spatially localized multi-degree differences between the remote and *in situ* calculations during cold upwelling events (Claar et al. 2019). These local examples suggest possible discrepancies between *in situ* and remotely sensed temperatures more broadly; however, comparison of *in situ* and remotely sensed temperatures across reefs in multiple geographic regions or with more modern and higher resolution SST products is lacking.

Here, we compared *in situ* temperature records on coral reefs to the 0.01 degree resolution *Multi-scale Ultra-high Resolution Sea Surface Temperature* (MUR) dataset from NASA. We examined three temperature metrics linked to local adaptation in corals: maximum monthly mean temperature (MMM), maximum monthly 99th percentile temperature (peak annual temperature), and mean daily temperature range (DTR). We found that remotely sensed MMMs closely correlated with those calculated *in situ*, but remotely sensed data missed the highest annual temperatures and failed to predict daily temperature ranges.

1.2 Materials and Methods

We tested the accuracy and bias of remotely sensed temperature on coral reefs by comparing it to an assembled dataset of *in situ* temperature loggers. We calculated

each temperature metric separately from both the remote and *in situ* data. We also assessed how bias differed across latitude, depth, and reef geomorphology.

1.2.1 Data sources

We obtained remotely sensed sea surface temperature from the *Multi-scale Ultra-high Resolution (MUR) Sea Surface Temperature* dataset (NASA/JPL 2015). MUR is a daily sea surface temperature product at a spatial resolution of 0.01 degrees by 0.01 degrees, or approximately one kilometer by one kilometer, available beginning in 2002. The dataset is a processed product that includes data from MODIS satellites and from Advanced Very High Resolution Radiometer (AVHRR) and microwave sensors carried by a variety of satellites, all of which has been calibrated to *in situ* data from the NOAA buoy network (Chin et al. 2017). The daily remotely sensed SST product is designed to represent "bulk" temperatures in the mixed layer of the ocean; roughly 10 meters deep to just below the "skin" at the sea-air interface. The product uses only remote sensed data taken at night (Chin et al. 2017; Koutantou et al. 2023).

We used *in situ* temperature logger records on coral reefs from a variety of sources. *In situ* temperatures are typically recorded using battery-powered submerged temperature loggers that can be left on reefs to record temperatures at set time intervals for several months or years and later recovered (Colin and Johnston 2020). Here, we use temperature logger data from Australia, several Pacific islands, Puerto Rico, the Virgin Islands, the South China Sea, Florida, and Panama, for an incomplete

but broad representation of temperatures on global coral reefs over the last twenty years (Fig 1.1). After filtering, we used data from 314 loggers (Table 1.1).

We also obtained additional environmental data for the location of each temperature logger. We downloaded reef geomorphology data from the Allen Coral Atlas (Allen Coral Atlas 2022), which uses "geomorphic classes" to qualitatively characterize reef zones by their physical form, such as lagoons, reef crests, and reef flats, and maps these features on a 10 m^2 scale on reefs up to 15 meters deep. We also used the global coastlines dataset from OpenStreetMap (OpenStreetMap contributors 2024) to calculate distance between loggers and the shore.

1.2.2 Logger data preprocessing

All temperature logger records included metadata with latitude and longitude, and many but not all metadata records included the logger depth (Table 1.1). We matched logger locations to Allen Coral Atlas geomorphic data and discarded the 54% of logger points (513 removed of 955) that fell outside the area for which the Allen Coral Atlas defined geomorphic classes.. We trimmed the temporal extent of the logger data to match that of the sea surface temperatures (June 2002 to January 2020) where necessary. We filtered the frequency of each logger's measurement to one data point every 30 minutes to equalize temporal resolution between loggers. For each logger, we discarded data from any day with fewer than 24 timepoints and any month with fewer than 15 days of data. Next, we discarded data from loggers with

fewer than 12 continuous months of data, leaving us with 9.9 million total logged hours of data across 314 loggers.

We calculated MMM temperature, peak annual temperature, and DTR for each logger. MMM temperatures were calculated by taking the mean temperature of each calendar month (i.e. January, February, etc.) across the entire logged timeframe and selecting the hottest mean month. For peak annual temperature, we used a similar process but calculated the 99th percentile temperature of each calendar month rather than the mean, then took the maximum of those. This gave us a proxy for maximum annual temperature, while filtering out the highest temperatures that may be caused by instrument error or other anomalies. Finally, for DTR we calculated the daily minimum and maximum temperatures for each logger across the entire logged timeframe, subtracted the minimum from the maximum, and took the mean across all daily differences.

We processed remotely sensed SST for each logger point by trimming the MUR data to the same temporal extent as the logger data. We then used the temporally trimmed data to calculate MMM, peak annual temperature, and mean weekly temperature variation. We calculated the peak annual temperature by taking the highest temperature across the entire time frame, since the MUR SST has a one-day temporal resolution. We used hottest daily temperature instead of 99th percentile temperature due to the greater quality control and coarser spatial precision of the remotely sensed data compared to the *in situ* data. Mean weekly temperature variation was calculated by taking the maximum and minimum temperatures of each

calendar week (Sunday - Saturday), subtracting the minimum from the maximum, and taking the mean of all of the differences. We used mean weekly temperature range in lieu of mean daily temperature range since remote SST is not available at sub-daily timescales. We chose this timescale because one week should encompass most of a tidal cycle while minimizing seasonal variation that would be associated with longer timescales.

We used the Allen Coral Atlas to define the reef "geomorphic class" at each logger point. Finally, we calculated distance to shore for each logger point using the OpenStreetMap coastlines and the "great circle" distance function from Python's Xarray-Spatial library. All data preprocessing and analysis was performed in Python 3.8.3. Scripts are available at https://github.com/pinskylab/logger_remote_temps.

1.2.3 Statistics

Prior to processing, we normalized the "distance to shore" data by taking the natural logarithm of one plus the distance. To understand linear relationships between variables, we calculated Pearson's correlation coefficient (r). For factor-level relationships between geomorphic classes and temperatures, we calculated H statistics and P values using Kruskal-Wallis tests in the scipy.stats library version 1.11.4.

To test our ability to predict *in situ* MMM and peak temperatures, we fit linear models to predict each *in situ* temperature metric from all of the remotely sensed variables, including distance to shore, an interaction term of remote MMM and distance to shore, and all geomorphic classes. We selected models by stepwise

addition based on cross-validated R^2 score, performed with default parameters in scikit-learn library version 1.0.2.

Here, we define "accuracy" of each model as the mean absolute difference between the predicted value and actual *in situ* value of each temperature metric. We define "bias" as the difference in means between predicted values and actual *in situ* values. Therefore, a measure may be unbiased but inaccurate if predicted values are far from the actual values but evenly split between positive and negative differences.

1.3 Results

For the commonly used MMMs, we found a close linear relationship between *in situ* and remote temperatures (Pearson's $r = 0.95$, linear regression slope of 1.001 ± 0.001, n = 314, Fig. 1.2a). Remotely sensed MMMs averaged 0.04 °C cooler than *in situ*, with a standard deviation of the difference of 0.47 °C ($n = 314$ loggers). The maximum absolute difference was for a logger in the southern Great Barrier Reef, which had a MMM 2.56 °C warmer than the remotely sensed MMM. Across all 314 comparisons of MMM, 96% of the remotely sensed values were within 1 °C of the *in situ* values, and 84% were within 0.5 °C (n = 314, Fig. 1.2b).

We tested whether the bias of remotely sensed MMMs differed across gradients of latitude, depth, distance to shore, or geomorphology. There was no clear relationship with either latitude (see Supplemental Fig. 1.1a) or distance to shore (Supplemental Fig. 1.1b). For the loggers with associated depth measurements, deeper loggers exhibited colder MMMs relative to the remotely sensed MMMs (Fig.

1.3a). However, the linear correlation with depth relationship was weak (Pearson's r = -0.402 ± 0.052, n = 277). There was a weak relationship between bias and geomorphic class, and both terrestrial reef flats and outer reef flats each had *in situ* MMMs that were 0.27 °C hotter than remote MMMs on average (Fig. 1.3b). A Kruskal-Wallis test of bias vs. geomorphic class was statistically significant (n = 314, H = 19.8, p = 0.02).

We tested whether latitude, distance from shore, and geomorphic class together helped to explain additional variation in *in situ* temperatures. The model selection routine identified a linear model that included distance to shore, an interaction term of remote MMM and distance to shore, and three geomorphic classes (outer reef flat, shallow lagoon, and an aggregate of all other geomorphic classes). The model suggested that *in situ* MMMs were colder relative to remotely sensed MMM at sites further from shore, though less so on outer reef flats, and warmer in shallow lagoons. However, the improvement in cross-validated R^2 was negligible (only 0.004, see Table A1.1).

After comparing *in situ* and remote MMMs, we assessed the similarity of peak annual temperatures measured *in situ* and remotely. The mean difference between *in situ* and remote peak annual temperatures was 0.23°C, with the *in situ* temperatures hotter than the remote temperatures. These metrics showed weaker linear correlation than did remote and *in situ* MMMs, especially at the highest temperatures (Pearson's r = 0.83, Fig. 1.4a). In addition, this fit was not consistent across the full range of temperatures. *In situ* peak annual temperatures below 31 °C (70% of logged

temperatures, n=223) correlated closely with the remote peak annual temperatures (r = 0.88), but above this temperature, higher *in situ* temperatures were only weakly associated with higher remotely sensed temperatures (r =0.21, n= 91).

Similarly to MMMs, we evaluated potential sources of bias in the remotely sensed peak annual temperatures, including latitude, depth, distance to shore, and geomorphology (see Fig. A1.2). We found no clear bias by latitude or distance to shore. The difference between *in situ* and remotely sensed peak annual temperatures showed a negative but nonlinear relationship with depth, with *in situ* peak annual temperatures up to 4 °C hotter than remote sensing for depths <5 m, and closer to 1 °C cooler for depths >20 m (Fig. 1.5a). The bias was moderately correlated with the natural log of depth (Pearson's r = -0.56). Geomorphic class was a stronger predictor of bias, with inner reef flats consistently hotter than remotely sensed maxima (Kruskal-Wallis of *in situ* vs. remote differences across geomorphic classes, n = 314, H = 58.7, $p=2.4x10^{-9}$, Fig. 1.5b). Statistical models predicting peak temperatures from remotely sensed variables performed less well than those predicting MMMs (see Table A1.2).

Finally, we examined the relationship between daily temperature range and each of the remotely sensed temperature metrics (MMM, maximum annual temperature, and weekly temperature range), and found no strong relationship with any of them (all Pearson's r < 0.1). There were notable relationships between daily temperature range and both geomorphic class (Kruskal-Wallis H= 71.67, $p = 7x10^{-12}$, n =314) and the natural logarithm of depth (Pearson's R = -0.51, n =277). Inner reef

flats had the highest mean DTR (1.4°C), and both outer reef flats and shallow lagoons also had mean DTRs above 1 °C. All other geomorphic classes had mean DTRs between 0.5 and 1 °C (see Fig. A1.3). Furthermore, daily temperature range was correlated with the difference between *in situ* and remote maximum temperatures, suggesting that some of the sites with high daily temperature range may be the same as the sites with high maximum temperatures missed by the remotely sensed data. However, these relationships gave us little ability to predict *in situ* daily temperature ranges from remotely sensed data (see Table A1.3).

1.4 Discussion

This study evaluated how closely temperature metrics relevant to coral thermal adaptation calculated from the remotely sensed 1 km^2 NASA-MUR dataset resembled those calculated from *in situ* temperature loggers on coral reefs. Overall, we found that remotely sensed sea surface temperature was in many cases a good proxy for in situ temperatures on coral reefs, though the accuracy and bias depended on both the specific temperature metric and within-reef geomorphic features.

In particular, we found remotely sensed temperatures to be effective proxies for MMMs calculated *in situ*. In particular, the <0.1 °C difference in means for remote and *in situ* data suggests that the subsurface corrections applied by NASA for buoy depth are appropriate and effective in coral reef environments. This is especially notable since the 1 km^2 resolution MUR data, while more spatially precise than many other remotely sensed SST products, is still coarser grained than many of the

oceanographic processes known to contribute to variation in reef temperatures and coral bleaching. Water circulation on reefs depends on fine-scale patterns including internal waves, turbulence, and tides, all of which can result in temperature variation on fine spatial scales (Herdman et al. 2015; Reid et al. 2020; Davis et al. 2021). For example, a 2008 study on Mo'orea by Lenihan *et al* found differences in current speed and corresponding differences in coral bleaching at spatial scales as fine as meters and even centimeters (Lenihan et al. 2008).

Most MMM temperatures calculated from SST were within 0.5 °C of those calculated *in situ* and nearly all were within 1 °C, similar to results collected by Claar on Kiritimati (2019). Since bleaching predictions are often calculated from SSTs that are more than 1 °C above MMM temperature (Liu, Gang et al. 2017), accurately measuring baseline temperatures to within one degree is helpful for a meaningful understanding of heat adaptation in corals. The close agreement between remote and *in situ* temperatures is in contrast to the Klepac (2022) study, which found a greater than 0.5 °C offset between *in situ* and remote temperature. However, the latter study used daily temperature averages rather than maximum monthly means, and the 5 km x 5 km NOAA Coral Reef Watch sea surface temperature in lieu of the finer-scale NASA-MUR dataset used here. The highly linear relationship between remote and *in situ* MMMs found here suggests comparable accuracy between the highest and lowest extrema of the temperature range, as well as the median temperatures. Moreover, this relationship proved unbiased by latitude, indicating that remotely sensed MMMs may be equally appropriate for tropical and subtropical reefs.

Remotely sensed sea surface temperature proved less effective for measuring peak annual temperatures than maximum monthly means and unsuitable for estimating daily temperature range. Peak annual temperatures measured *in situ* agreed well with those measured remotely for cooler locations, showing a linear relationship similar to that seen between *in situ* and remote MMMs. However, for the 30% of logger points with the highest *in situ* peak temperatures (>31 °C), the remote peak annual temperature substantially underestimated the *in situ* peak temperature. The magnitude of this underestimate increased with increasing *in situ* temperature. These sites where *in situ* peak annual temperatures were hotter than remote peak annual temperatures also had disproportionately high daily temperature ranges, suggesting that these hottest peak temperatures may occur as part of high frequency temperature fluctuations. Since NASA-MUR is a daily product, it has an inherently limited ability to detect sub-diel variation, a well-established issue with remote sea surface temperature products (Leichter 2006). We refer to the sites with high peak annual temperatures underestimated by remote sensing and high daily temperature ranges as "highly variable sites".

Consistent with past research on heat fluxes in coral reefs, these highly variable sites were disproportionately shallow (Leichter et al. 2006). High frequency temperature variability strongly depends on reef geomorphology at scales as fine as meters, even where average temperatures are similar between sites. These differences in temperature variability appear to correspond to differences in water retention time, depth, and turbulence (Guadayol et al. 2014). These findings are consistent with our

data, as we saw strong relationships between geomorphic class and both peak annual temperatures and daily temperature range. However, the literature also shows that the relationship between temperature and specific geomorphic classes differs by location. For example, studies in the Red Sea show the highest levels of high frequency temperature variation on wave-protected reef flats (Davis et al. 2011), whereas studies of Dongsha Atoll in the South China show the opposite pattern, with wave-exposed reef crests exhibiting more temperature variation than the protected reef flat (Reid et al. 2020). This inconsistency hampers our ability to use remotely sensed geomorphic classes to predict either peak temperatures or daily temperature range across different reefs.

Any interpretation of these results must also consider known issues in these datasets. The existence of a logger in New Caledonia at greater than 50 meters depth within areas defined as "reef" by the Allen Coral Atlas reveals inaccuracies in the Allen Coral Atlas dataset, including its delineation of geomorphic classes. This logger in particular seems to have been placed at the deep end of a steep drop off and most likely does not represent a living coral area. Similarly, the lack of accurate, easily accessible depth data for most reef areas (and the lack of depth metadata for 37 of the loggers) means that many of our analyses included no direct measurement of the most important determinants of *in situ* water temperatures. We compensated for this omission by including geomorphic classes, which the Allen Coral Atlas defines partially by depth, and by post-hoc analysis of depth effects using loggers with defined depths. Increased availability of fine-scale bathymetric maps for coral reefs

worldwide would enable researchers to better incorporate depth into future temperature predictions.

The *in-situ* temperature loggers used in this study were assembled from various other studies and long-term monitoring projects, none of which were specifically designed for comparison with remote temperatures, leading to multiple potential issues. First, different loggers covered substantially different timeframes, some of which were as short as one year. While we compensated for this issue by temporally trimming remote temperatures to match the *in situ* dataset at each point, longer and more consistent timeframes would give us a better sense for how medium-term climate fluctuations affect concordance between *in situ* and remote data (e.g., El Niño cycles). This is particularly true for the calculation of maximum monthly means, which are typically defined across decades-long historical timeframes. Similarly, the spatial distribution of loggers varied substantially by site, with some loggers in Palau spaced closer than 2.5 meters and other loggers, such as the one in the Phoenix Islands Protected Area, totally isolated. Additional research comparing *in situ* and remotely sensed temperature products, especially using dense networks of temperature loggers in geomorphically complex reef areas, could improve our understanding of temperature variation at fine spatial scales. For example, recent work in Australia (Brown et al. 2023) and Hawai'i (Gorospe and Karl 2011) both use dense networks of temperature loggers on coral reefs to link fine-scale differences in coral bleaching to temperature fluctuations caused by local geomorphology and meter-scale hydrodynamic processes. Further studies such as

these are especially important for improving our ability to predict peak daily temperatures and related metrics such as sub-diel temperature variability.

Relatedly, additional research into which temperature metrics best predict thermal tolerance in corals, and whether that differs by factors such as geographic region or coral species, will allow us to refine the use of remotely sensed temperatures. MMM remains commonly used in coral studies for good reason: it is empirically linked to coral thermal tolerance and allows for effective calculation of heat stress above baseline, as with degree heating weeks. For studies relying on MMMs or related DHWs, remotely sensed temperatures may well be adequate substitutes for those measured *in situ.* Still, recent research suggests that both peak temperatures and sub-diel variability can play key roles in determining coral heat tolerance (Bay and Palumbi 2014; Thomas et al. 2018). The large (>1 °C) differences between remote and *in situ* temperature maxima for inner reef flats in particular indicate that remote data should still be used cautiously or not at all to approximate maximum temperature in shallow nearshore environments.

Overall, the NASA MUR dataset is a useful dataset for the study of fine-scale climates on coral reefs, albeit with some important limitations. The 25-fold improvement in spatial precision as compared to the more commonly used NOAA Coral Reef Watch dataset means that the NASA-MUR is an important tool for the study of microclimate adaptation in corals and could be more widely used by coral reef scientists for this purpose. Additionally, the availability of the entire dataset on Amazon Web Services in a cloud-computing format (Zarr) reduces the required

computational and memory overhead for analysis, a clear benefit for scientists and practitioners. Finally, the further development of remotely sensed temperature products open new avenues for comparison with *in situ* data. For example, the Ecostress 70 meter by 70 meter satellite temperature product is now intermittently available in select coastal locations and provides a dramatic improvement in spatial resolution over the NASA-MUR product (Weidberg 2021). The broad availability of an ever-improving suite of remotely sensed ocean temperature products has incredible potential to facilitate a previously arduous and important aspect of coral reef science.

Acknowledgements

This study was made possible by funding from a Rutgers School of Environmental and Biological Sciences Fellowship (JTB), a National Defense Science and Engineering Graduate Fellowship (JTB), and the Paul M. Angell Foundation (MLP and JTB). The authors gratefully thank the researchers and institutions that have generously made their data publicly available, including the Allen Coral Atlas, NASA, AIMS, NOAA, USGS, the ReefTEMPS network, the Smithsonian Tropical Research Institute, the Biological and Chemical Oceanography Data Management Office at Woods Hole Oceanographic Institution, Dr. Anne L. Cohen at Woods Hole Oceanographic Institution, Dr. Stephen Palumbi at Stanford University, and Dr. Kim Cobb at the Georgia Institute of Technology.

References

Allen Coral Atlas (2022) Imagery, maps and monitoring of the world's tropical coral reefs.

Australian Institute of Marine Science (2017) AIMS Sea Water Temperature Observing System (AIMS Temperature Logger Program). doi.org/10.25845/5b4eb0f9bb848

Barshis DJ, Ladner JT, Oliver TA, Seneca FO, Traylor-Knowles N, Palumbi SR (2013) Genomic basis for coral resilience to climate change. Proc Natl Acad Sci 110:1387–1392. 10.1073/pnas.1210224110

Bay RA, Palumbi SR (2014) Multilocus Adaptation Associated with Heat Resistance in Reef-Building Corals. Curr Biol 24:2952–2956. doi.org/10.1016/j.cub.2014.10.044

Brown KT, Eyal G, Dove SG, Barott KL (2023) Fine-scale heterogeneity reveals disproportionate thermal stress and coral mortality in thermally variable reef habitats during a marine heatwave. Coral Reefs 42:131–142. doi.org/10.1007/s00338-022-02328-6.

Castillo KD, Ries JB, Weiss JM, Lima FP (2012) Decline of forereef corals in response to recent warming linked to history of thermal exposure. Nat Clim Change 2:756–760. doi.org/10.1038/nclimate1577

Chin TM, Vazquez-Cuervo J, Armstrong EM (2017) A multi-scale high-resolution analysis of global sea surface temperature. Remote Sens Environ 200:154–169. doi.org/10.1016/j.rse.2017.07.029

Claar DC, Cobb KM, Baum JK (2019) In situ and remotely sensed temperature comparisons on a Central Pacific atoll. Coral Reefs 38:1343–1349. doi.org/10.1007/s00338-019-01850-4

Cobb KM, Gates RD (2016) RAPID: Tracking coral reef impacts of the 2014/2015 El Nino event in Kiritimati. https://www.bco-dmo.org/dataset/659999. Accessed 28 February 2023.

Cohen AL (2013) Dongsha Atoll temperature. https://www.bco-dmo.org/dataset/560618. Accessed 19 January 2023.

Colin PL, Johnston TMS (2020) Measuring Temperature in Coral Reef Environments: Experience, Lessons, and Results from Palau. J Mar Sci Eng 8:680. doi.org/10.3390/jmse8090680

Coral Reef Ecosystem Program; Pacific Islands Fisheries Science Center (2017) National Coral Reef Monitoring Program: Water Temperature Data from Subsurface Temperature Recorders (STRs) deployed at coral reef sites in

American Samoa from 2012-03-21 to 2015-03-25 (NCEI Accession 0162246). NOAA National Centers for Environmental Information. Dataset. https://www.ncei.noaa.gov/archive/accession/0162246. Accessed March 2021.

Coral Reef Ecosystem Program; Pacific Islands Fisheries Science Center (2017) National Coral Reef Monitoring Program: Water Temperature Data from Subsurface Temperature Recorders (STRs) deployed at coral reef sites in the Hawaiian Archipelago from 2008-09-20 to 2013-09-14 (NCEI Accession 0162219). NOAA National Centers for Environmental Information. Dataset. https://www.ncei.noaa.gov/archive/accession/0162219. Accessed March 2021.

Coral Reef Ecosystem Program; Pacific Islands Fisheries Science Center (2017) National Coral Reef Monitoring Program: Water Temperature Data from Subsurface Temperature Recorders (STRs) deployed at coral reef sites in the Hawaiian Archipelago from 2013-07-13 to 2016-09-28 (NCEI Accession 0162216). NOAA National Centers for Environmental Information. Dataset. https://www.ncei.noaa.gov/archive/accession/0162216. Accessed March 2021.

Coral Reef Ecosystem Program; Pacific Islands Fisheries Science Center (2017) Water temperature data from Subsurface Temperature Recorders (STRs) deployed at coral reef sites in Batangas, Philippines from 2012-03-13 to 2015-05-28 (NCEI Accession 0163746). NOAA National Centers for Environmental Information. Dataset. https://www.ncei.noaa.gov/archive/accession/0163746. Accessed March 2021.

Coral Reef Ecosystem Program; Pacific Islands Fisheries Science Center (2017) National Coral Reef Monitoring Program: Water Temperature Data from Subsurface Temperature Recorders (STRs) deployed at coral reef sites in the Pacific Remote Island Areas from 2012-03-04 to 2015-11-12 (NCEI Accession 0162217). NOAA National Centers for Environmental Information. Dataset. https://www.ncei.noaa.gov/archive/accession/0162217. Accessed March 2021.

Coral Reef Ecosystem Program; Pacific Islands Fisheries Science Center (2017) Water temperature data from subsurface temperature recorders (STRs) deployed at coral reef sites in Timor-Leste from 2012-10-15 to 2014-10-09 (NCEI Accession 0168931). [indicate subset used]. NOAA National Centers for Environmental Information. Dataset. https://www.ncei.noaa.gov/archive/accession/0168931. Accessed March 2021.

Coral Reef Ecosystem Program; Pacific Islands Fisheries Science Center (2017) National Coral Reef Monitoring Program: Water Temperature Data from Subsurface Temperature Recorders (STRs) deployed at coral reef sites at Wake Island from 2011-03-22 to 2014-03-19 (NCEI Accession 0162218).

NOAA National Centers for Environmental Information. Dataset. https://www.ncei.noaa.gov/archive/accession/0162218. Accessed March 2021.

Cyronak T, Takeshita Y, Courtney TA, DeCarlo EH, Eyre BD, Kline DI, Martz T, Page H, Price NN, Smith J, Stoltenberg L, Tresguerres M, Andersson AJ (2020) Diel temperature and pH variability scale with depth across diverse coral reef habitats. Limnol Oceanogr Lett 5:193–203.

Davis KA, Lentz SJ, Pineda J, Farrar JT, Starczak VR, Churchill JH (2011) Observations of the thermal environment on Red Sea platform reefs: a heat budget analysis. Coral Reefs 30:25–36. doi.org/10.1007/s00338-011-0740-8

Davis KA, Pawlak G, Monismith SG (2021) Turbulence and Coral Reefs. Annu Rev Mar Sci 13:343–373. doi.org/10.1146/annurev-marine-042120-071823

Ecosystem Sciences Division, Pacific Islands Fisheries Science Center (2020) National Coral Reef Monitoring Program: Water temperature data from subsurface temperature recorders (STRs) deployed at coral reef sites in the Hawaiian Archipelago from 2013-07-14 to 2019-09-05 (NCEI Accession 0210383). NOAA National Centers for Environmental Information. Dataset. https://www.ncei.noaa.gov/archive/accession/0210383. Accessed March 2021.

Ecosystem Sciences Division, Pacific Islands Fisheries Science Center (2020) National Coral Reef Monitoring Program: Water temperature data from subsurface temperature recorders (STRs) deployed at coral reef sites across the Marianas Archipelago with time-series spanning 2011-04-20 to 2017-06-20 (NCEI Accession 0176112).NOAA National Centers for Environmental Information. Dataset. https://www.ncei.noaa.gov/archive/accession/0176112. Accessed March 2021.

Ecosystem Sciences Division, Pacific Islands Fisheries Science Center (2020) National Coral Reef Monitoring Program: Water temperature data from subsurface temperature recorders (STRs) deployed at coral reef sites in the Pacific Remote Islands Marine National Monument from 2014-03-16 to 2017-04-22 (NCEI Accession 0176111). NOAA National Centers for Environmental Information. Dataset. https://www.ncei.noaa.gov/archive/accession/0176111. Accessed March 2021.

Fox MD, Cohen AL (2022) Hourly temperature data from deployments between 2012 and 2018 from three of the Phoenix Islands. doi.org/10.26008/1912/BCO-DMO.863421.1

Gleeson MW, Strong AE (1995) Applying MCSST to coral reef bleaching. Adv Space Res 16:151–154. doi.org/10.1016/0273-1177(95)00396-V

Gorospe KD, Karl SA (2011) Small-Scale Spatial Analysis of *In Situ* Sea Temperature throughout a Single Coral Patch Reef. J Mar Biol 2011:1–12. doi.org/10.1155/2011/719580

Grossman E, Marrack L (2019) Nearshore water properties and estuary conditions along the coral reef coastline of west Hawaii Island (2010-2014). doi.org/10.5066/F7154FJQ

Guadayol Ò, Silbiger NJ, Donahue MJ, Thomas FIM (2014) Patterns in Temporal Variability of Temperature, Oxygen and pH along an Environmental Gradient in a Coral Reef. PLoS ONE 9:e85213. doi.org/10.1371/journal.pone.0085213

Herdman LMM, Hench JL, Monismith SG (2015) Heat balances and thermally driven lagoon‐ocean exchangeson a tropical coral reef system (M oorea, F rench P olynesia). J Geophys Res Oceans 120:1233–1252. doi.org/10.1002/2014JC010145

Hoadley KD, Lewis AM, Wham DC, Pettay DT, Grasso C, Smith R, Kemp DW, LaJeunesse TC, Warner ME (2019) Host–symbiont combinations dictate the photo-physiological response of reef-building corals to thermal stress. Sci Rep 9:9985. doi.org/10.1038/s41598-019-46412-4

Howells EJ, Beltran VH, Larsen NW, Bay LK, Willis BL, Van Oppen MJH (2012) Coral thermal tolerance shaped by local adaptation of photosymbionts. Nat Clim Change 2:116–120. https://doi.org/10.1038/nclimate1330

Kayanne H (2017) Validation of degree heating weeks as a coral bleaching index in the northwestern Pacific. Coral Reefs 36:63–70. doi.org/10.1007/s00338-016-1524-y

Kenkel CD, Almanza AT, Matz MV (2015) Fine-scale environmental specialization of reef-building corals might be limiting reef recovery in the Florida Keys. Ecology 96:3197–3212. doi.org/10.1890/14-2297.1

Klepac CN, Barshis DJ (2022) High-resolution in situ thermal metrics coupled with acute heat stress experiments reveal differential coral bleaching susceptibility. Coral Reefs 41:1045–1057. doi.org/10.1007/s00338-022-02276-1

Kleypas JA, Thompson DM, Castruccio FS, Curchitser EN, Pinsky M, Watson JR (2016) Larval connectivity across temperature gradients and its potential effect on heat tolerance in coral populations. Glob Change Biol 22:3539–3549. doi.org/10.1111/gcb.13347

Koutantou K, Brunner P, Vazquez-Cuervo J (2023) Validation of NASA Sea Surface Temperature Satellite Products Using Saildrone Data. Remote Sens 15:2277. doi.org/10.3390/rs15092277

Leahy SM, Kingsford MJ, Steinberg CR (2013) Do Clouds Save the Great Barrier Reef? Satellite Imagery Elucidates the Cloud-SST Relationship at the Local Scale. PLoS ONE 8:e70400. doi.org/10.1371/journal.pone.0070400

Leichter JJ, Helmuth B, Fischer AM (2006) Variation beneath the surface: Quantifying complex thermal environments on coral reefs in the Caribbean, Bahamas and Florida. J Mar Res 64:563–588. doi.org/10.1357/002224006778715711

Lenihan H, Adjeroud M, Kotchen M, Hench J, Nakamura T (2008) Reef structure regulates small-scale spatial variation in coral bleaching. Mar Ecol Prog Ser 370:127–141. doi.org/10.3354/meps07622

Liu, Gang, Skirving,William J, Geiger, Erick F., De La Cour, Jacqueline L., Marsh, Ben L., Heron, Scott F., Tirak, Kyle V., Strong, Alan E., Eakin, C. Mark (2017) NOAA Coral Reef Watch's 5km Satellite Coral Bleaching Heat Stress Monitoring Product Suite Version 3 and Four-Month Outlook Version 4. Reef Encount 32:39–45.

Manzello, Derek; Enochs, Ian; Dutra, Elizabeth; Kolodziej, Graham; Jankulak, Mike (2018) National Coral Reef Monitoring Program: Water temperature data from subsurface temperature recorders (STRs) deployed at coral reef sites in Florida's Biscayne National Park in 2014-08-29 to 2017-12-20 (NCEI Accession 0177773).NOAA National Centers for Environmental Information. Dataset. https://www.ncei.noaa.gov/archive/accession/0177773. Accessed March 2021.

Manzello, Derek; Enochs, Ian; Dutra, Elizabeth; Kolodziej, Graham; Jankulak, Mike (2018) National Coral Reef Monitoring Program: Water temperature data from subsurface temperature recorders (STRs) deployed at coral reef sites in St. Thomas and St. John from 2014-06-30 to 2017-08-15 (NCEI Accession 0177772).NOAA National Centers for Environmental Information. Dataset. https://www.ncei.noaa.gov/archive/accession/0177772. Accessed March 2021.

Manzello, Derek; Enochs, Ian; Dutra, Elizabeth; Morris, John; Kolodziej, Graham; Jankulak, Mike; Hendee, James; National Oceanic and Atmospheric Administration; Cooperative Institute for Marine and Atmospheric Studies (2018) National Coral Reef Monitoring Program: Water Temperature Data from Subsurface Temperature Recorders (STRs) deployed at coral reef sites along the Florida Keys Reef Tract from 2013-12-02 to 2016-12-13 (NCEI

Accession 0171796). NOAA National Centers for Environmental Information. Dataset. https://www.ncei.noaa.gov/archive/accession/0171796. Accessed March 2021.

Manzello, Derek; Enochs, Ian; Dutra, Elizabeth; Morris, John; Kolodziej, Graham; Hendee, James; Jankulak, Mike; National Oceanic and Atmospheric Administration; Cooperative Institute for Marine and Atmospheric Studies (2018) National Coral Reef Monitoring Program: Water Temperature Data from Subsurface Temperature Recorders (STRs) deployed at coral reef sites in St. Croix, U.S. Virgin Islands from 2013-09-09 to 2016-09-14 (NCEI Accession 0171794). NOAA National Centers for Environmental Information. Dataset. https://www.ncei.noaa.gov/archive/accession/0171794. Accessed March 2021.

Manzello, Derek; Enochs, Ian; Kolodziej, Graham; Besemer, Nicole; Jankulak, Mike (2020). National Coral Reef Monitoring Program: Water Temperature Data from Subsurface Temperature Recorders (STRs) deployed at coral reef sites in St. Croix, USVI in 2016-09-12 to 2019-09-12 (NCEI Accession 0209241). NOAA National Centers for Environmental Information. Dataset. https://www.ncei.noaa.gov/archive/accession/0209241. Accessed March 2021.

Marhoefer SR, Zenger KR, Strugnell JM, Logan M, Van Oppen MJH, Kenkel CD, Bay LK (2021) Signatures of Adaptation and Acclimatization to Reef Flat and Slope Habitats in the Coral *Pocillopora damicornis*. Front Mar Sci 8:704709. doi.org/10.3389/fmars.2021.704709

McManus LC, Forrest DL, Tekwa EW, Schindler DE, Colton MA, Webster MM, Essington TE, Palumbi SR, Mumby PJ, Pinsky ML (2021) Evolution and connectivity influence the persistence and recovery of coral reefs under climate change in the Caribbean, Southwest Pacific, and Coral Triangle. Glob Change Biol 27:4307–4321. doi.org/10.1111/gcb.15725

NASA/JPL (2015) GHRSST Level 4 MUR Global Foundation Sea Surface Temperature Analysis (v4.1). doi.org/10.5067/GHGMR-4FJ04

OpenStreetMap contributors (2024) OpenStreetMap Coastlines. Accessed 22 March 2023. https://www.openstreetmap.org/

Palumbi SR (2021) Water temperature records for Acropora hyacinthus coral colonies located in either patch or fore reefs of the Palau Archipeglo from November 2017 to January 2020. doi.org/10.26008/1912/BCO-DMO.772445.2

Palumbi SR, Barshis DJ, Traylor-Knowles N, Bay RA (2014) Mechanisms of reef coral resistance to future climate change. Science 344:895–898.

doi.org/10.1126/science.1251336

Physical Monitoring Program of the Smithsonian Tropical Research Institute Underwater Temperature Sensor Data, Panama. https://biogeodb.stri.si.edu/physical_monitoring/research/sst. Accessed 3 March 2023.

Reid EC, Lentz SJ, DeCarlo TM, Cohen AL, Davis KA (2020) Physical Processes Determine Spatial Structure in Water Temperature and Residence Time on a Wide Reef Flat. J Geophys Res Oceans 125:e2020JC016543. doi.org/10.1029/2020JC016543

Safaie A, Silbiger NJ, McClanahan TR, Pawlak G, Barshis DJ, Hench JL, Rogers JS, Williams GJ, Davis KA (2018) High frequency temperature variability reduces the risk of coral bleaching. Nat Commun 9:1671. doi.org/10.1038/s41467-018-04074-2

Schoepf V, Grottoli AG, Levas SJ, Aschaffenburg MD, Baumann JH, Matsui Y, Warner ME (2015) Annual coral bleaching and the long-term recovery capacity of coral. Proc R Soc B Biol Sci 282:20151887. doi.org/10.1098/rspb.2015.1887

Seabra R, Wethey DS, Santos AM, Lima FP (2011) Side matters: Microhabitat influence on intertidal heat stress over a large geographical scale. J Exp Mar Biol Ecol 400:200–208. doi.org/10.1016/j.jembe.2011.02.010

Thomas L, Rose NH, Bay RA, López EH, Morikawa MK, Ruiz-Jones L, Palumbi SR (2018) Mechanisms of Thermal Tolerance in Reef-Building Corals across a Fine-Grained Environmental Mosaic: Lessons from Ofu, American Samoa. Front Mar Sci 4:434. doi.org/10.3389/fmars.2017.00434

Thomas L, Underwood JN, Rose NH, Fuller ZL, Richards ZT, Dugal L, Grimaldi CM, Cooke IR, Palumbi SR, Gilmour JP (2022) Spatially varying selection between habitats drives physiological shifts and local adaptation in a broadcast spawning coral on a remote atoll in Western Australia. Sci Adv 8:eabl9185. doi.org/10.1126/sciadv.abl9185

UNEP-WCMC, WorldFish Centre, WRI (2018) Global distribution of warm-water coral reefs, compiled from multiple sources including the Millennium Coral Reef Mapping Project. Version 4.0. Includes contributions from IMaRS-USF and IRD (2005), IMaRS-USF (2005) and Spalding et al. (2001). doi.org/10.34892/t2wk-5t34

Varillon D, Fiat S, Magron F, Allenbach M, Hoibian T, De Ramon N'Yeurt A,

Ganachaud A, Aucan J, Pelletier B, Hocdé R (2019) ReefTEMPS : The Pacific Island coastal ocean observation network. doi.org/10.17882/55128

Verrall B, Pickering CM (2020) Alpine vegetation in the context of climate change: A global review of past research and future directions. Sci Total Environ 748:141344. doi.org/10.1016/j.scitotenv.2020.141344

Zellweger F, De Frenne P, Lenoir J, Vangansbeke P, Verheyen K, Bernhardt-Römermann M, Baeten L, Hédl R, Berki I, Brunet J, Van Calster H, Chudomelová M, Decocq G, Dirnböck T, Durak T, Heinken T, Jaroszewicz B, Kopecký M, Máliš F, Macek M, Malicki M, Naaf T, Nagel TA, Ortmann-Ajkai A, Petřík P, Pielech R, Reczyńska K, Schmidt W, Standovár T, Świerkosz K, Teleki B, Vild O, Wulf M, Coomes D (2020) Forest microclimate dynamics drive plant responses to warming. Science 368:772–775. doi.org/10.1126/science.aba6880

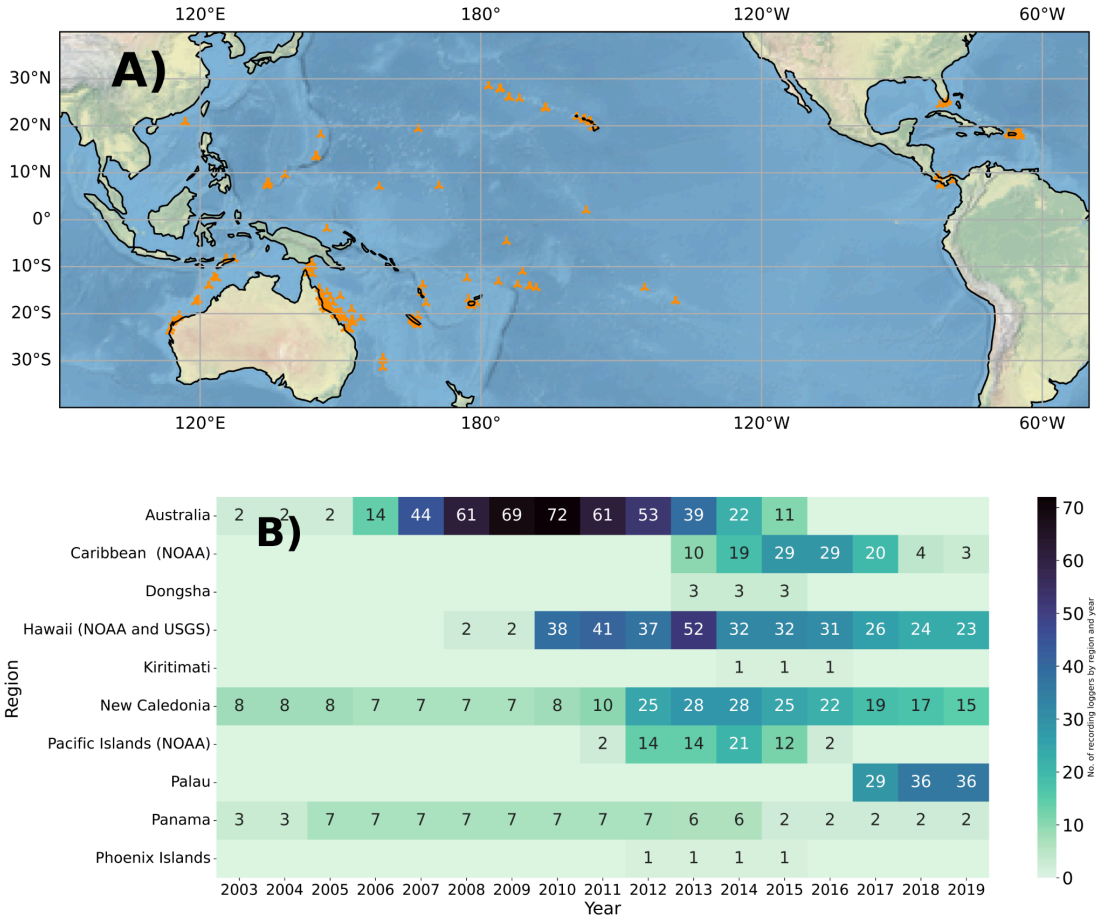

Fig. 1.1 Temperature loggers retained for analysis by location (a) and date ranges (b).

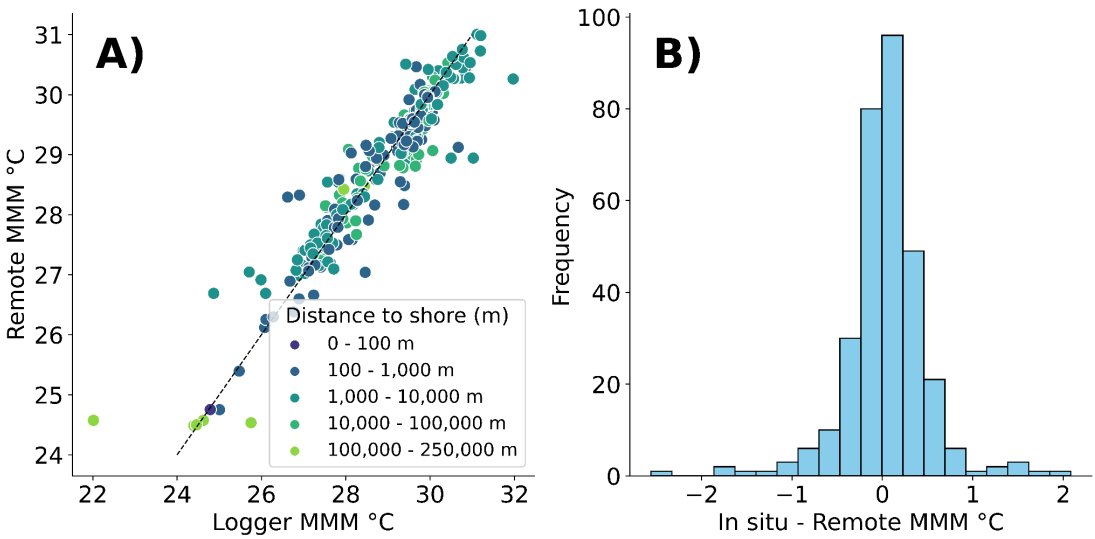

Fig. 1.2 Maximum monthly mean (MMM) temperatures from remote sensing were closely correlated with those from *in situ* temperature loggers. The dashed line shows a hypothetical 1:1 relationship between *in situ* and remotely sensed temperatures (a). Most *in situ* MMMs were within one degree of remotely sensed MMM (b). Values to the right indicate *in situ* MMMs that were hotter than remotely sensed values.

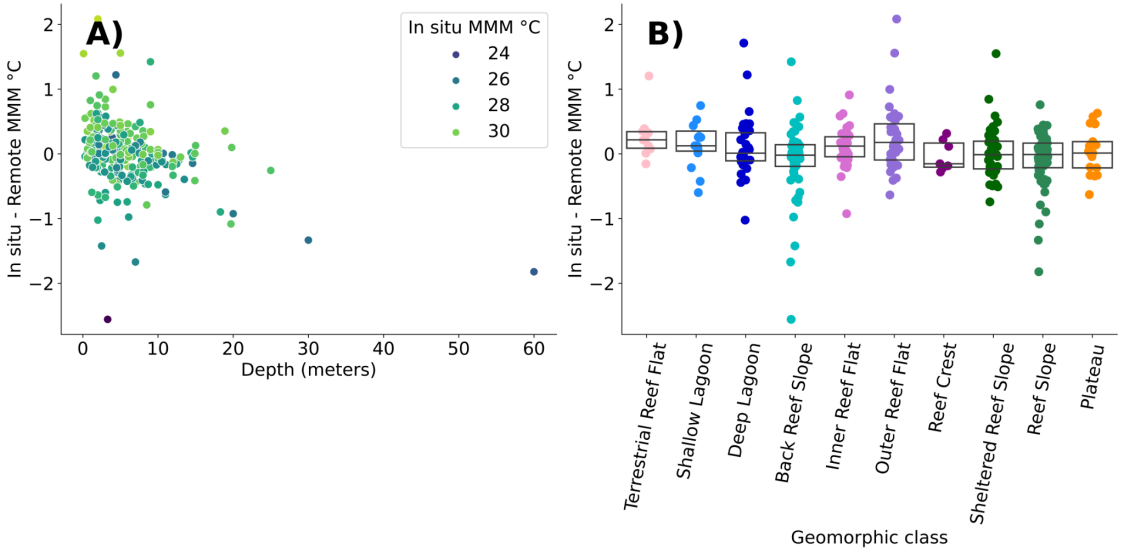

Fig. 1.3. The difference between *in situ* and remotely sensed MMMs varied with depth (a) and geomorphic class (b).

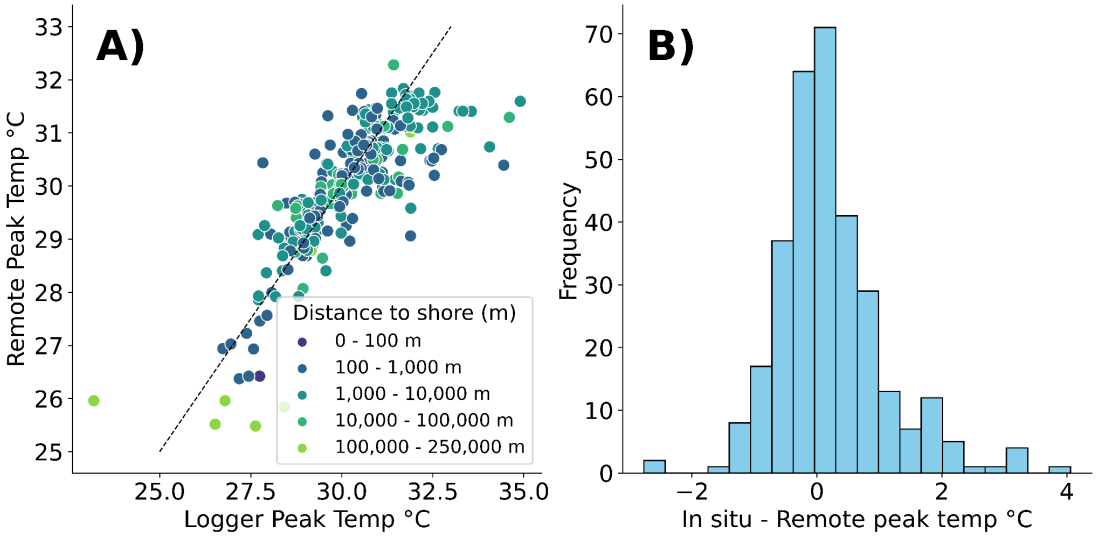

Fig. 1.4. (a) Peak annual temperature from remotely sensed sea surface temperatures systematically underestimated the hottest *in situ* peak annual temperatures. (b) Histogram of *in situ* minus remotely sensed peak temperatures.

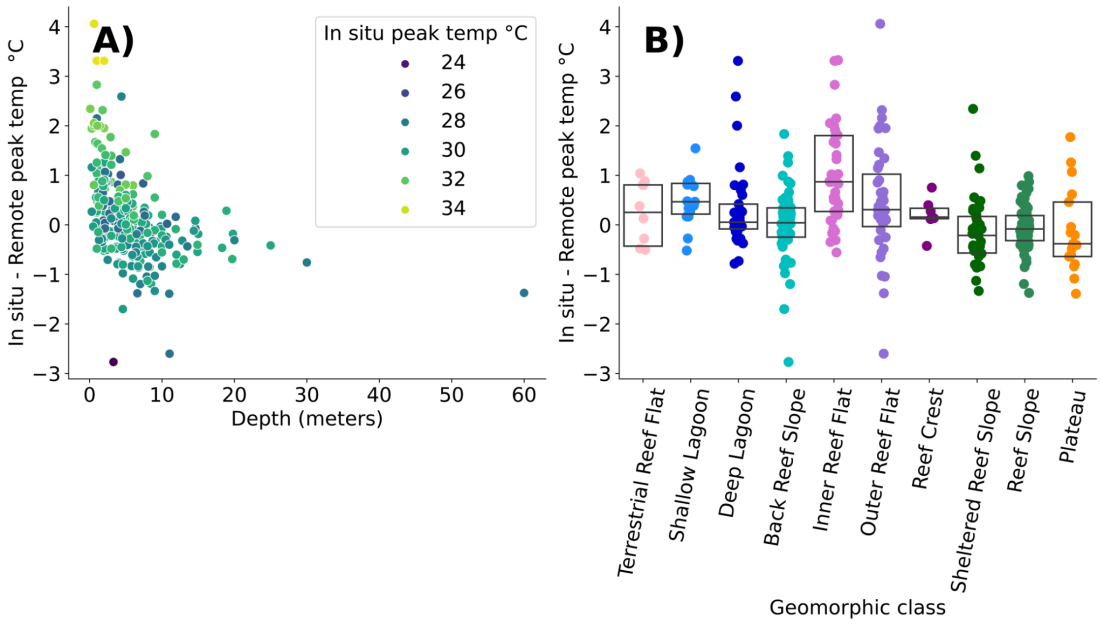

Fig. 1.5. The difference between in situ and remotely sensed peak temperatures varied with depth (a) and geomorphic class (b).

Region	Institution	Loggers in unfiltered dataset	Loggers kept post-filtering	Depth range (meters)	Reference(s)
Hawai'i, U.S. Pacific Territories, Puerto Rico, U.S. Virgin Islands, Florida	U.S. National Oceanographic and Atmospheric Administration (NOAA)	412	104	0.6 - 25.0	(Coral Reef Ecosystem Program, Pacific Islands Fisheries Science Center, 2017) (Ecosystem Sciences Division, Pacific Islands Fisheries Science Center, 2020) (Manzello et al 2018; 2020)
Hawai'i	U.S. Geological Survey (USGS)	32	14	0.3 - 14.6	(Grossman and Marrack 2019)
Australia (inc. Great Barrier Reef, Western Australia, and Coral Sea)	Australian Institute of Marine Science	306	113	0.1 - 19.7	(Australian Institute of Marine Science 2017)
Palau	Stanford University	90	36	No depth data	(Palumbi 2021)
New Caledonia	ReefTEMPS	94	35	1.0 - 60.0	(Varillon et al. 2019)
Panama	Smithsonian Tropical Research	18	7	1.0 - 18.3	(Physical Monitoring Program of the Smithsonian

	Institute				Tropical Research Institute)
Dongsha Atoll, South China Sea	Woods Hole Oceanographic Institution	5	3	1.0 - 5.0	(Cohen 2013)
Kiritimati, Northern Line Islands	Georgia Institute of Technology	2	1	No depth data	(Cobb and Gates 2016)
Phoenix Islands	Woods Hole Oceanographic Institution	4	1	8.0	(Fox and Cohen 2022)

Table 1.1. Sources of *in situ* temperature logger data.

APPENDICES

Appendix 1: Chapter 1 supplemental material

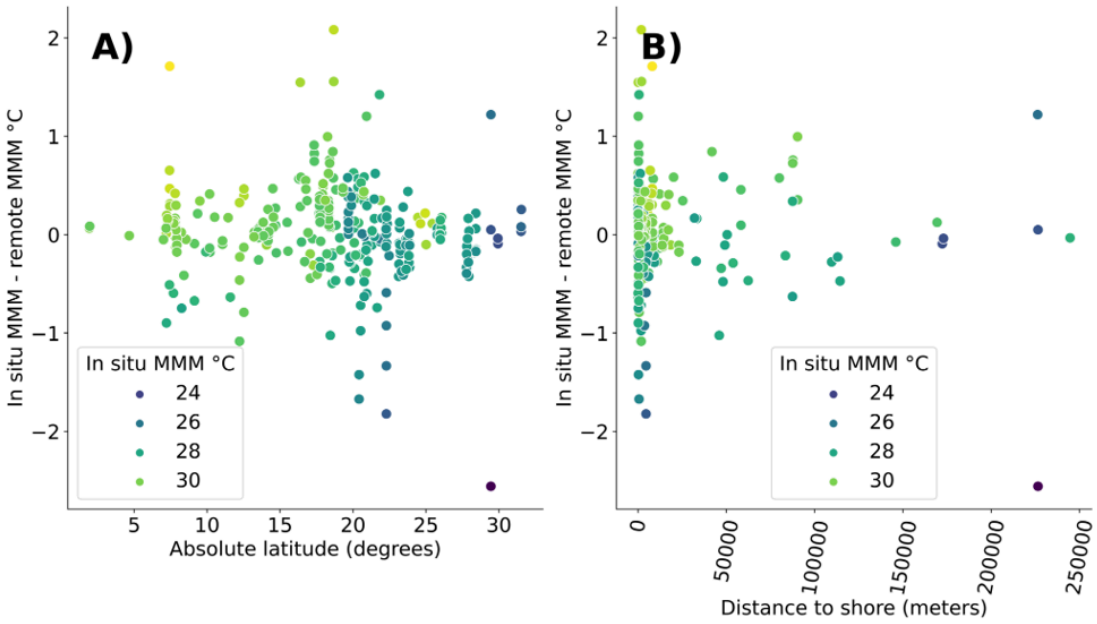

Fig. A1.1. There was no clear linear relationship between the *in situ* vs. remotely sensed MMM differences and either latitude (A; Pearson's r = -0.087) or distance to shore (B;Pearson's r = -0.063).

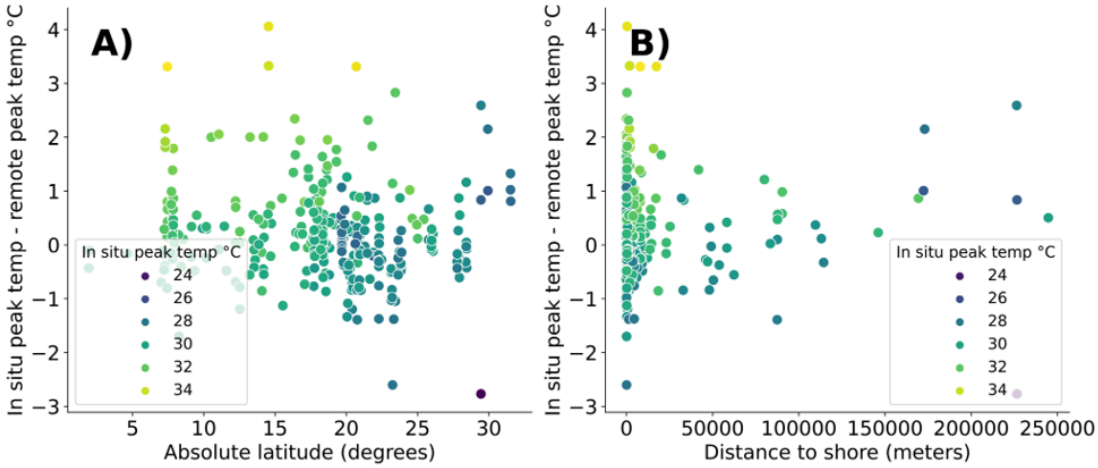

Fig. A1.2. There was no clear relationship between the *in situ* vs. remotely sensed peak temperature differences and either latitude (a; Pearson's r = -0.101) or distance to shore (b; 0.062).

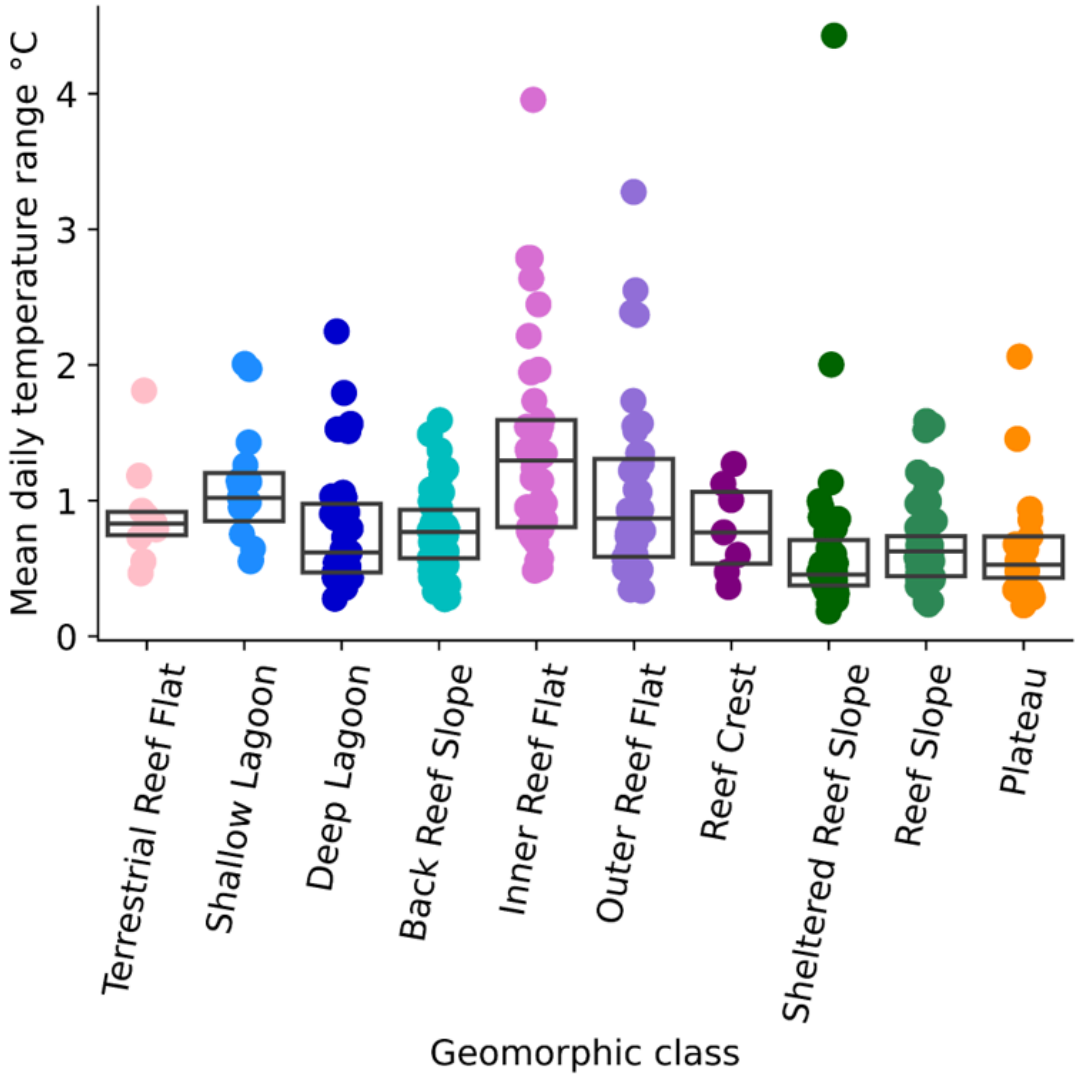

Fig. A1.3. Mean daily temperature range varied with remotely sensed geomorphic class (Kruskal-Wallis H= 71.67, p = 7 x 10^{-12}, n =314)

Independent variable(s)	Model type	Mean cross-validated R^2
Remote MMM	Linear	0.8803
Remote MMM, latitude	Linear	0.8753
Remote MMM, log distance to shore	Linear	0.8803
Remote MMM, log distance to shore, interaction	Linear	0.8805
Remote MMM, log distance to shore, Remote MMM * log distance to shore, is outer reef flat	Linear	0.8844
Remote MMM * log distance to shore, is outer reef flat, is shallow lagoon	Linear	0.8846
Remote MMM, log distance to shore, each geomorphic class	Random Forest	0.8297
Remote MMM, log distance to shore, each geomorphic class	Linear	0.8780

Table A1.1. Model parameters and cross-validated R^2 for *in situ* MMM temperatures. Each geomorphic class (e.g., "is outer reef flat) is coded as 1 or 0 for whether a location is in that class or not (respectively).

Independent variable(s)	Model type	Mean cross-validated R^2
Remote MMM	Linear	0.574
Remote peak temperature	Linear	0.629
Remote peak temperature, latitude	Linear	0.622
Remote peak temperature, log distance to shore	Linear	0.623
Remote peak temperature, is inner reef flat	Linear	0.649
Remote peak temperature, is inner reef flat, is outer reef flat	Linear	0.661
Remote peak temperature, is inner reef flat, is outer reef flat, is shallow lagoon	Linear	0.666
Remote peak temperature, each geomorphic class	Linear	0.644
Remote peak temperature, each geomorphic class	Random forest	0.650
Remote peak temperature, log distance to shore, each geomorphic class	Random forest	0.645

Table A1.2. Model parameters and results for *in situ* peak annual temperatures. Details as in Supplemental Table 1.

Independent variable(s)	Model type	Mean cross-validated R^2
Remote mean weekly temperature range	Linear	-0.355
Remote maximum monthly mean temperature	Linear	-0.387
Remote peak annual temperature	Linear	-0.349
Log distance to shore	Linear	-0.365
Each geomorphic class	Linear	-0.327
Each geomorphic class	Random forest	-0.326
Back reef slope	Linear	-0.438
Is reef slope	Linear	-0.277
Sheltered reef slope	Linear	-0.338
Deep lagoon	Linear	-0.388
Shallow lagoon	Linear	-0.333
Outer reef flat	Linear	-0.318
Inner reef flat	Linear	-0.343
Terrestrial reef flat	Linear	-0.360
Reef crest	Linear	-0.357
Plateau	Linear	-0.361

Table A1.3. Model parameters and results for *in situ* mean DTR. Details as in Supplemental Table 1.

Supplemental text: Modeling *in situ* temperature metrics from remotely sensed data

Maximum monthly mean temperatures

We used multiple model types and remotely sensed variables to model and predict *in situ* MMMs. We selected models with the highest mean cross-validated R^2, which involved iteratively fitting the model using a randomly selected 80% of the data, calculating the R^2 value of the same model on the remaining 20% of the data, repeating this procedure five times, then calculating the mean of all five R^2 values. This procedure helps avoid overfitting (Lever 2016). We specifically fit the models on independent variables that could be remotely sensed from space and for which datasets covering all or most of global coral reefs are publicly available. We fit both linear and random forest models. The input variables, model type, mean cross-validated R^2 value, and variable coefficients (where relevant) are reported in Table A1.1. We created dummy variables for each geomorphic class, setting the variable equal to 1 if the point fell within that geomorphic class (for example, a shallow lagoon), and otherwise equal to zero.

We first fit each model using only remotely sensed temperature and reported the cross-validated R^2 (Table A1.1). We then added other variables in a stepwise manner, selecting the best model using cross-validated R^2. For geomorphic classes, we fit a model using the dummy variable for each individual geomorphic class in addition to the other parameters chosen in previous step(s). For any geomorphic class that improved the model, we then conducted an additional round of model model fitting and evaluation adding each remaining geomorphic class one at a time. We also

fit a random forest model using all of the potential dependent variables and reported the mean cross-validated R^2 value.

Peak annual temperatures

We repeated the same procedure described above to fit models with the 99th percentile annual *in situ* temperature (hereafter "peak annual temperature") as the dependent variable (Table A1.2).

Mean daily temperature range

Finally, we fit both linear and random forest models to predict mean daily temperature range (DTR). We found no models with positive predictive power in cross validation; in fact, all of the mean cross validated R^2 values were negative (Table A1.3). While mean DTR appears somewhat related to geomorphic class (see Kruskal-Wallis test results in main text), we were unable to predict mean DTR from any remotely sensed variables.

References

Lever J, Krzywinski M, Altman N (2016) Model selection and overfitting. Nat Methods 13:703–704

Chapter 2

Contrasting patterns of seascape genetics in *Acropora cf. tenuis* and their symbiotic algae.

Bos, J.T.[1], McManus, L.C.[2], Ravago-Gotanco, R.[3], Pinsky, M.L.[1]

1. Department of Ecology & Evolutionary Biology, University of California Santa Cruz, 130 McAllister Way, Santa Cruz, California 95060, U.S.A.
2. Hawai‘i Institute of Marine Biology, 46-007 Lilipuna Rd, Kāne’ohe, Hawai’i, 96744, U.S.A.
3. Marine Science Institute, University of the Philippines,Velasquez St., Diliman, Quezon City 1101, Philippines.

Abstract

Theory suggests that pairs of mutualist species will often co-disperse and share the same dispersal patterns, though the extent to which this happens remains unclear. Photosynthetic corals constitute an example of this dynamic, as they rely on algal symbionts to meet their energetic needs, yet many acquire their symbionts environmentally after their larval dispersal phase. Consequently, corals and their symbionts may exhibit similar or contrasting patterns of genetic variation across the seascape, with implications for their evolutionary and ecological processes. Here, we densely sample corals of the key reef-building taxon *Acropora cf. tenuis* and their algal symbionts across a reefscape in the central Philippines to examine genetic variation across space. Four distinct coral taxa show genetic evidence of long distance dispersal, including weak or absent isolation by distance signals and parent-offspring pairs at widely spaced sites. These coral taxa all host a single group of algal symbionts from the genus *Cladocopium*, which shows landscape genetic structure independent from its coral hosts. In fact, *Cladocopium* genetics vary with both latitude and depth, potentially indicating genome-wide local adaptation at a finer spatial scale than that seen in their hosts. Genetic variation at markedly different spatial scales between host and symbiont may be beneficial for hosts if these differences enable them to acquire symbionts adapted to their settlement environments.

2.1. Introduction

The spatial scale of genetic variation differs widely between species, from globally panmictic dragonflies to tuataras that exhibit genetic structuring on the sub-kilometer scale (Moore et al., 2008; Troast et al., 2016). These contrasting patterns stem partially from differences in dispersal. Longer dispersal distances can lead to higher connectivity and more homogeneity between sites, blunting the effects of drift and inbreeding for smaller populations. Shorter dispersal may enable spatial heterogeneity and local adaptation as populations evolve to tolerate their immediate environment (Slatkin, 1987). However, patterns of genetic variation may also be driven by co-dispersal among closely associated species, such as mutualistic pairs or host-microbe holobionts. How dispersal shapes landscape genetic structure in such associations remains poorly understood (Hand et al., 2015).

Some theorists have suggested that the evolution of mutualisms should rely heavily on parent to child transmission of symbiotic partners, and therefore codispersal of the mutualist pair (Ewald, 1987). This is certainly true in some cases. A wide variety of terrestrial plants, for example, transmit their mycorrhizal partners directly from parent to offspring (Johnston-Monje et al., 2021; Laurent‐Webb et al., 2024). However, the real world provides contradictory examples, including the many species of corals that acquire their algal obligate symbionts environmentally, a situation that some authors have described as a “paradox” (Hartmann et al., 2017). Environmental acquisition of mutualist symbionts occurs across taxa, and is

especially common in the marine realm, including in many species of corals (Russell, 2019). Photosynthetic corals play critical roles in maintaining global biodiversity and human wellbeing, and depend on algal symbionts for their nutrition and survival (Fisher et al., 2015; Mellin et al., 2022). While corals and symbionts form obligate mutualist associations, they can disperse separately, making them an ideal study system to understand the extent to which mutualists show similar patterns of dispersal.

Most reef-building corals depend on photosynthetic algae living within their tissues to produce up to 95% of the carbohydrates they need to survive (Muscatine & Cernichiari, 1969). These algal symbionts belong to multiple genera, and individual corals can acquire symbionts in one of two ways. “Brooding” species of corals transmit their symbionts vertically from parent to offspring, producing larger larvae that carry their own symbionts. By contrast, “broadcast” spawning corals release gametes directly into the water column, where they form smaller larvae that acquire symbionts from the environment post-settlement (Harii et al., 2009). The second life history strategy, employed by corals of the genus *Acropora*, leads to the potential for corals and their algal symbionts to exhibit different patterns of genetic variation across space (Boutet & Schierwater, 2021). However, the extent to which corals and their symbionts show similar or disparate patterns of dispersal remains unclear.

Fortunately, population genetic methods allow direct observation of patterns of spatial genetic variation, as well as indirect inference about dispersal through isolation by distance methods (Pinsky et al., 2017). For example, analyses of

Stylophora pistillata and *Pocillopora verrucosa* on the Great Barrier Reef found far higher cross-reef connectivity and genetic homogeneity in the latter species, with estimated mean dispersal distances of 2100 to 5200 meters in *P. verrucosa* but just 23 to 102 meters in *S. pistillata* (Meziere et al., 2025). Algal symbionts of corals may or may not show the same level of connectivity as their hosts. Some evidence shows algal symbionts exhibiting genetic differentiation at finer spatial scales than their coral hosts (Davies et al., 2020). This could imply consistent differences in both connectivity and local adaptation between corals and their symbionts.

Our limited understanding of how landscape genetic patterns differ between corals and their algal symbionts is especially critical for corals of the genus *Acropora*. This keystone genus of branching corals associates with a variety of algal symbiont strains acquired environmentally after their larval dispersal phase (Cumbo et al., 2013). All species of *Acropora* are broadcast spawners, and their asymbiotic larvae drift in the water column for days to weeks before settling (Nishikawa et al., 2003). *Acropora* in the Indo-Pacific, including the Philippines, mostly associate with symbionts from genus *Cladocopium*, though they can also associate with symbionts of other genera (Davies et al., 2020; Matias et al., 2023; Matsuda et al., 2022; Torres et al., 2021). *Acropora* are sensitive to heat waves and face a growing threat from anthropogenic climate change (Pratchett et al., 2013). In addition, some *Acropora* populations exhibit local genetic adaptation to higher temperatures at both the regional and intra-reef scales, as do their algal symbionts (Howells et al., 2012; McClanahan et al., 2020; Thomas et al., 2018). Consequently, understanding

Acropora landscape genetics matters for applied conservation questions concerning connectivity, reserve design, and adaptation to anthropogenic change (Arafeh-Dalmau et al., 2023).

Here, we examine landscape genomic patterns of *Acropora cf. tenuis* and its algal symbionts in the central Philippines to test whether host and symbiont exhibit congruent or disparate dispersal patterns. The samples for this study are from the Philippines, which is situated within the Coral Triangle, known as the global epicenter of marine biodiversity (J. (Charlie) E. N. Veron et al., 2011). Our spatially dense sampling took place along two different two hundred kilometer stretches of reefscape on Cebu and Leyte islands, which facilitated assessment of isolation by distance patterns. Prior study of multiple species of reef-dwelling anemonefish across this same seascape found clear isolation by distance patterns and estimated dispersal kernel spreads on the order of 10 kilometers (Catalano et al., 2021; Fitz et al., 2023; Pinsky et al., 2010). Here, we test for similar patterns in *Acropora cf. tenuis* and its algal symbionts. Specifically, we examined whether (1) specific algal symbiont genotypes associated with specific *A. cf. tenuis* host genotypes and (2) host and symbionts showed similar or contrasting degree of genetic isolation by distance. Ultimately, we aimed to unpack the interacting relationships between genetic variation in corals, genetic variation in their algal symbionts, and physical location in space.

2.2 Materials and methods

2.2.1 Field sampling, field identification, and genomic library preparation

Field sampling was conducted from January to April 2016 across 47 sites in the Visayas region of the central Philippines, including areas surrounding the Camotes Sea and Cebu Strait. Sites were distributed across Cebu Province, including Cebu Island (n = 27 sites) and the Camotes Islands (n = 5), as well as Leyte Province (n = 15). Sites were selected to be approximately 10 km apart to capture ecologically relevant dispersal distances and enable testing for isolation by distance patterns in the study region (Fig. 2.1).

At each site, we characterized benthic cover using line point intercept transects. Three 15 m transects were deployed haphazardly parallel to shore, and the bottom type was recorded at 20 cm intervals along each transect. Following benthic surveys, we collected tissue samples from *Acropora cf. tenuis* colonies at each site. To locate colonies, we conducted a separate belt transect survey at each site by swimming parallel to shore within a 2 m wide belt for approximately one hour or until 20 samples were collected. During these surveys, we measured the maximum length, width, and depth of every *A. cf. tenuis* colony encountered and recorded the time of collection. We collected small tissue samples (approximately 2 cm × 2 cm) from 20 colonies per site, ensuring that sampled colonies were spaced at least 10 m apart to avoid resampling the same genet. A towed GPS unit was used to record the coordinates of each sampled colony. If fewer than 20 samples were obtained during the initial survey, an additional dive was conducted to complete the target sample size (depth information was not collected during these additional dives).

Acropora cf. tenuis specimens were identified in the field based on morphological characteristics described in Veron's "Corals of the World" (J. E. N. Veron, 2000). Key characteristics used for identification included: 1) colony growth form characterized by corymbose clumps, 2) long and tubular axial corallites, and 3) neatly arranged and slightly flaring radial corallites. Field identification focused on the combination of branching pattern, corallite structure, and overall colony architecture rather than relying on any single morphological trait. Detailed close-up photographs were taken of each collected specimen and are available at https://doi.org/10.5061/dryad.sf7m0cgnr.

In total, 258 samples were collected during initial surveys and 394 samples on additional dives. Tissue samples were preserved in 95% ethanol for genetic analysis. All samples were collected under Gratuitous Permit 0129-17 and transported to the United States under CITES export permit 4733. The Texas A&M Corpus Christi Genomics Core Laboratory performed all DNA extraction using silica column membrane kits, as well as double digest restriction-site associated DNA sequencing (ddRadSeq) library preparation (Peterson et al., 2012) , and sequencing. Library preparation for ddRadSeq used the enzymes SphI and EcoRI and targeted fragment sizes of 500-600 basepairs. All sample libraries were pooled and then sequenced across two Illumina HiSeq4000 2 x 150 bp lanes to mitigate the possibility of variation introduced by lane effects.

2.2.2 Sequence processing, alignment, and filtering

We did initial quality control and 3' read trimming with FastP version 0.23.4 (Chen et al., 2018), visualized the results with MultiQC (Ewels et al., 2016) , de-duplicated and compressed the read files with the Clumpify function from BBtools version 39.06, re-ran FastP for 5' read trimming, and re-paired unpaired reads with BBtools (Bushnell, 2014). We parallelized analysis with GNU Parallel version 20200122 (Tange, 2018). Full scripts with parameters are available on Github at https://github.com/pinskylab/Atenuis_Philippines (to be replaced with a Zenodo DOI upon manuscript acceptance). The pre-processing scripts were developed from Bird et al. (2024). We then mapped the trimmed reads to genomes from *Acropora tenuis* (Shinzato et al., 2021), *Cladocopium goreaui* (Martin-Cuadrado et al., 2024), *Durusdinium trenchii* (Dougan et al., 2024), and *Symbiodinium kawagutii* (Martin-Cuadrado et al., 2024), all downloaded from NCBI, using BWA version 0.7.17 (Li & Durbin, 2009). The *'Acropora tenuis'* genome assembly available on NCBI comes from Japan and is therefore unlikely to represent true *A. tenuis* (Bridge et al., 2024). Given the broad taxonomic uncertainty and extensive presence of cryptic species within *Acropora cf. tenuis*, this genome likely represents a congener to our samples, rather than a conspecific. Across individuals, a median of 41,236.5 reads, or 74% of total reads, mapped to the *Acropora tenuis* genome from NCBI. A median of 14,424.5 reads, or 15% of the total, successfully mapped to the *Cladocopium goreaui* genome, 2771 reads (2.4% of total) mapped to the *Symbiodinium kawagutii* genome, and 1447 reads (1.5% of total) mapped to the *Durusdinium trenchii* genome.

After sorting and indexing the resulting bamfiles with Samtools version 1.20 (Li et al., 2009) , we called SNPs using FreeBayes version 1.3.10 (Garrison & Marth, 2012), resulting in 2,491,826 *Acropora* SNPs across 652 individuals and 596,153 *Cladocopium* SNPs across 644 individuals. Nearly all individuals showed substantial missing data, with 184 (28%) of individuals showing more than 99.9% missing data after selecting only loci with a minimum quality score of >30 and a minimum depth of >3. More than half of individuals (359, 55%) were missing more than 90% of possible SNPs. We iteratively filtered SNPs and individuals using functions from vcftools and vcflib (Danecek et al., 2011; Garrison et al., 2022), in order to preserve the maximum number of each, as described in O'Leary et al. (2018). Ultimately, we retained all SNPs present in at least 85% of individuals and all individuals with at least 50% non-missing data. After quality filtering, we were left with 2,269 SNPs and 301 individuals in the *Acropora* assemblies, and 2,059 SNPs and 310 individuals in the *Cladopium* assemblies. We pruned SNPs for physical linkage using Plink2 by examining SNPs across a 50 bp window size and pruning those with $r^2>0.5$ (Chang et al., 2015). This process left us with 1,838 SNPs in *Acropora* and 873 SNPs in *Cladocopium*.

We calculated distance to shore for each sample using the global shorelines dataset from OpenStreetMap, downloaded on March 28, 2025 (OpenStreetMap contributors, 2025).

2.2.3 Identification of genetic clusters within *Acropora*

A. tenuis was traditionally believed to be a common coral species across shallow reefs in the western Pacific ocean and Red Sea. However, recent research has revealed it to comprise at least eleven morphologically similar but evolutionary distinct species (Bridge et al., 2024; J. E. N. Veron, 2000). Multiple species of *A. tenuis* lookalikes have been identified co-occurring on the same reefs in Australia, Okinawa, and the South Pacific (Bridge et al., 2024; Matias et al., 2023; Zayasu et al., 2021). While some of these *A. cf. tenuis* populations have been provisionally reassigned to new nominal species, those in Southeast Asia (including the Philippines) have so far only been defined as *Acropora sp(p).* The authors of a recent taxonomic revision note that this should be considered "an unresolved clade requiring further sampling and analysis" (Bridge et al., 2024). Here we refer to our samples as *Acropora cf. tenuis* to reflect both the species' traditional classification and current taxonomic uncertainty.

We determined the number of genetic clusters within the fully filtered *Acropora* SNP data using a Discriminant Analysis of Principal Components (DAPC) including the top 500 principal components, to capture the maximum amount of variation, as recommended by the package authors (Jombart & Collins, 2015). We determined the optimal solution by comparing Bayesian Information Criteria (BIC) for all solutions between one and sixteen clusters. We calculated principal components eigenvectors and eigenvalues using Plink2 version 2.00a5.10 in order to visualize these clusters in PCA space and quantify the percent of genetic variation accounted for by each principal component. We also examined the top three principal

components for linear correlation with latitude, longitude, distance to shore, and depth.

We quantified genetic distance between clusters by calculating FSTs between groups using the Hierfstat R package version 1.1.10 (Goudet, 2005). We then reshuffled all individuals between each pair of taxa and recalculated the FST 1000 times in order to simulate a null distribution of genetic distances. To assign statistical significance to the pairwise genetic distance between clusters, we compared each observed between-group FST to its simulated null distribution and calculated the percentile of the null distribution greater than the observed FST.

We also evaluated ancestry for each individual sample using ADMIXTURE version 1.3.0 and all possible numbers of ancestry groups between one and sixteen using a cross validation procedure (Alexander et al., 2009). This approach found ancestry groups that corresponded closely to the genetic groups found by the DAPC. Given these consistent differences and the substantial genetic differentiation between these groups despite their broadly overlapping ranges (see Results), we referred to these groupings as "taxa," which we numbered arbitrarily one through four with the most individuals assigned to cluster one and the fewest assigned to cluster four. We used the DAPC to assign each *Acropora* individual to a genetic cluster, and re-filtered SNP data separately within each cluster (Section 2.2). We used slightly different iterations of SNP and individual removal, but with the same final cutoffs as described above. After pruning, we ended with 116 individuals and 2308 SNPs in Taxon 1, 69 individuals and 1689 SNPs in Taxon 2, 57 individuals and 1221 SNPs in Taxon 3, and

53 individuals with 1213 SNPs in Taxon 4. We identified potential clones using the KING coefficient calculated in Plink2 using a cutoff of 0.354 (McMaster et al., 2025). We calculated heterozygosity and inbreeding coefficients (F_{IS}) for each individual sample and averaged across taxa using vcftools .

2.2.4 Genetic variation with environment and geography in *Acropora*

Non-parametric Kruskal-Wallis tests in R were used to test for differences in mean latitude, depth, and distance to shore between genetic clusters. We calculated isolation by distance (IBD) patterns for each genetic group individually in accordance with Sheets *et al.* (2018). We assessed isolation by distance in both one dimension (along the coast of Cebu) and two dimensions (all sites together). We did not analyze one dimensional patterns along the coast of Leyte because of insufficient coral samples along that coastline. We calculated pairwise linearized FST and the pairwise geographic distance between each pair of sampling sites. Only sites with at least two individuals were considered for FST calculations. For the two dimensional IBD assessment, we took the natural logarithm of these distances, following the equation for isolation by distance in two dimensions (Rousset, 1997). Mantel tests were conducted comparing the genetic and geographic distance matrices using the Vegan package version 2.6.8 (Dixon, 2003). In order to compare strength of IBD relationships between taxa, we calculated confidence intervals around regression slopes by using the standard error of the regression slope as the standard deviation for 1000 normally distributed slopes centered on the estimated regression coefficient. We

then quantified the percentage of these resampled regression slopes that were greater than zero, indicating a positive relationship between geographic and genetic distance. Finally, we identified putative parent/offspring pairs from *Acropora* SNP data using the GetMaybeRel() function of the Sequoia package version 3.0.3 in R with no age priors, assuming all individuals as hermaphrodites (Huisman, 2017).

2.2.5 Taxonomic variation within algal symbionts

To identify the taxonomic composition of the symbionts in our samples, we compared the percent of reads mapped to genomes from three common genera of algal symbionts (*Cladocopium goreaui, Durusdinium trenchii ,* and *Symbiodinium kawagutii*). To identify environmental correlates of symbiont composition, we used Kruskal-Wallis tests to compare the relative percentages of reads mapped from each individual to each genus to depth, distance to shore, latitude, island, and host coral genetic grouping. In nearly all individuals, by far the most reads mapped to the *Cladocopium goreaui* genome, leading us to proceed with further analysis for only these assemblies (see Fig. A2.2 for percent of reads mapping to each symbiont genome).

Similarly to *Acropora*, we used a DAPC and paired PCA to evaluate the number of genetic clusters and to visualize genetic groupings in PCA space. We found only one genetic cluster, and consequently did not subdivide our *Cladocopium* population for subsequent analyses.

We also ran an ADMIXTURE analysis for the *Cladocopium* genetypes, again evaluating all possible numbers of ancestry groups between one and sixteen using cross-validation. We assigned *Cladocopium* genomes to groups based on the taxon (1-4) of their *Acropora* host, calculated FSTs between those taxa, and calculated associated p-values using the same resampling procedure for simulated null distributions described in Section 2.4. After SNP filtering, more individual samples were found with >50% data present for the *Cladocopium* assemblies than for the *Acropora* assemblies, meaning that some (n=10) *Cladocopium* samples could not be assigned to *Acropora* taxa.

2.2.6 Isolation by distance and genetic variation with environment in *Cladocopium*

We used linear regression to compare the top three principal components of the *Cladocopium* genomes to latitude, longitude, distance to shore, and depth. We assessed isolation by distance in both one and two dimensions using a Mantel test from the Vegan package in R following the same methodology as described in Section 2.4. Confidence intervals around slopes were calculated similarly to the *Acropora* samples. To account for differences in sample size and geographic distribution of samples between the *Acropora* clusters and the full set of *Cladocopium* samples, we also evaluated isolation by distance patterns for *Cladocopium* within each genetic grouping of *Acropora* and reported distributions for those slopes as well. Finally, we used two partial Mantel tests to evaluate the influence of geographic

distance on genetic distance between *Cladocopium* populations while controlling for genetic distance between *Acropora* populations, as well as the influence of genetic distance between *Acropora* populations on the genetic distance between *Cladocopium* populations while controlling for geographic distance. We did not test for kin pairs within the *Cladocopium* samples, as they are haploid (Santos & Coffroth 2003). All analyses using R packages were performed using R version 4.4.1 and all Python analyses were performed in Python 3.9.25.

Results

2.3.1 Genetic groups in *Acropora cf. tenuis*

Our analysis revealed four distinct genetic clusters within the *Acropora cf. tenuis* genetic data. The four cluster solution resulted in the lowest BIC for the DAPC, closely followed by the five cluster solution (Table A2.2). These clusters appear distinct in PCA space, with more than 50% of the genetic variation loading on the first two principal components. However, some intermediate individuals may represent hybrids (Fig.2. 2A). Likewise, the ADMIXTURE analysis with four ancestry groups resulted in the lowest cross validation error, with the five ancestry groups in second place (Table A2.2). Most individuals showed a clearly dominant ancestry group, with 99% of individuals having more than half of their ancestry coming from a single group and 90% of individuals having at least 7/8th of their ancestry from a single group (Fig. 2.2B).

The ancestry groups found with the ADMIXTURE analysis corresponded well but imperfectly to the genetic clusters resolved by DAPC. The vast majority (298/301, 99%) of individuals assigned to a cluster by DAPC had greater than 1/2 ancestry fraction coming from that same cluster, and 90% (271/301) had at least 7/8th of their ancestry from that cluster.

Pairwise FST comparisons between these genetic clusters ranged from 0.10 to 0.16 (Table 2.1). For each pairwise comparison, the actual FST was higher than 100% of the simulated resamples with shuffled individuals.

These four genetic clusters were not separated in space. Each cluster occurred in at least 60% (26/43) of sampling sites and on both islands (Fig. 2.1). Taxa did appear somewhat structured by latitude (Kruskal-Wallis test, p-value=0.00026, n=301), with Taxon 2 having the highest median latitude (10.59 °N) and Taxon 3 having the lowest (10.00 °N). There was a marginally significant association between genetic grouping and average depth (Kruskal-Wallis test, p-value=0.07, n=97), with Taxon 1 having the greatest depth (13 ft) and Taxon 4 having the lowest median depth (9.5 ft). There was no association with distance to shore (Kruskal-Wallis test, p-value=0.22, n=301).

We found no association between the number of genetic reads mapped per sample and taxon (Kruskall-Wallis test p=0.22, n=301). Taxa did show significant differences in inbreeding coefficient (F) (Kruskall-Wallis test $p=3.1 \times 10^{-6}$, n=301). The median inbreeding coefficient for Taxon 4 was negative (F=-0.023) indicating observed homozygosity slightly lower than expected. Inbreeding coefficients were

positive but low (F=0.018 and F=0.0011) for Taxa 1 and 2, and higher in Taxon 3 (F=0.076). See Fig. A2.3 for boxplot of inbreeding coefficients.

2.3.2 Isolation by distance and dispersal in *Acropora cf. tenuis*

For two out of four taxa, there was on average a positive correlation between two-dimensional geographic distance between populations in log meters and genetic distance in pairwise linearized FST. However, the correlations for Taxa 1 and 2 were negative, and all confidence intervals from resampling slopes overlapped with zero (Fig. 2.3). Moreover, none of the relationships between genetic distance and geographic distance were statistically significant ($p<0.05$) when using a Mantel test (Tables A2.6 and A2.7). The strongest relationship, found in Taxon 4, was largely driven by three closely related individuals collected from sites at the north and south ends of Cebu, and excluding these individuals substantially reduced the percentage of positive IDB slopes in 1D for this taxon (Table 2.3). These individuals collectively account for the high FST values seen in some pairwise comparisons (Fig. 2.3G, H). Overall, a lack of strong IBD patterning suggests a high degree of genetic mixing within each cryptic *Acropora* taxon.

Pedigree analysis within the cryptic *Acropora* taxa found five putative parent/offspring pairs, or seven if both putatively clonal individuals at site CEB_01 were included (Table A2.8). All parent/offspring pairs were genotyped at a minimum of 1000 of the same SNPs and showed a minimum log likelihood ratio of 4, indicating that the paired individuals were 10^4 times more likely to represent parent/offspring

pairs than they were to represent unrelated individuals. Three of these pairs were defined as clones in the original clone scan with KING, and are marked in Fig. 2.4 with a letter C. Nearly all of the pairs occurred at widely spaced sites (Fig. 2.4). These results suggest that long (>50km) dispersal distances are possible across a single generation.

2.3.3 Identification of algal symbionts.

We identified the vast majority of algal symbionts as the genus *Cladocopium* across all four *Acropora* taxa and 43 sites. More than 98% (644/652) of individual samples had a higher number of reads successfully map to the *C. goreaui* genome than either the *D. trenchii* or *S. kawagutii* genomes. Three individuals, two of which belonged to Taxon 1 and one of which belonged to Taxon 4, had the highest number of reads map to *D. trenchii.* One *Acropora* individual, which belonged to Taxon 1, had the highest number of reads map to *S. kawagutii* (Tables A2.3 and A2.4). There was no significant relationship between percent of reads mapped to a given genus of symbiont, and host *Acropora* taxon (n=298, all p>0.5). Likewise, there was no significant association between relative number of reads mapping to different symbiont genera and either depth (Kruskal-Wallis test, p=0.71, n= 97) or distance to shore (Kruskal-Wallis test, p=0.13, n=295). Finally, linear regression models for each symbiont genus found no association between percentage of symbiont reads mapping to that genus and sample depth (n=97, all p>0.3). Since *Cladocopium* was by far the dominant symbiont genus for this dataset, we proceeded analyzing only symbiont

DNA mapped to the *C. goreaui* genome. Given the low probability of our samples belonging to *C. goreaui* specifically, we refer to reads mapped to the *C. goreaui* genome by the more general term *Cladocopium*.

2.3.4 Genetic variation within *Cladocopium* and its correspondence to coral host genotype

Cladocopium did not show the same genetic groupings as their *Acropora* hosts. Principal components and discriminant analysis of principal components did not reveal distinct genetic clusters within the *Cladocopium* SNP profiles (Fig. 2.5A). The BIC for the DAPC was minimized by finding a single cluster, and BIC increased monotonically with the number of clusters up to at least 16 clusters (Table A2.5). ADMIXTURE resolved three ancestry groups within the *Cladocopium*, but these ancestry groups did not obviously correspond to those found in their *Acropora* hosts (Fig. 2.5B). However, there was a noticeable structuring of ancestry with latitude (Fig. 2.5C).

Based on this PCA, *Cladocopium* populations do show evidence for genetic structuring in space across both regional and microhabitat scales. The second principal component of the *Cladocopium* genomes had a significant linear relationship to latitude (linear regression, $p=0.00027$, $n=310$). Similarly, there is a significant relationship between the first principal component of the *Cladocopium* genomes and host coral depth ($p=0.000013$, $n=107$).

Cladocopium populations associated with different *Acropora* cryptic taxa showed weak differentiation with extremely low FSTs. However, reshuffling individuals between taxa and recalculating FSTs of the associated *Cladocopium* populations reveals that while weak, some of these FSTs were significantly stronger than would be expected from random association (Table 2.2).

2.3.5 Isolation by distance in *Cladocopium*

Cladocopium showed more consistent patterns of genetic isolation by distance than did their coral hosts. Mantel tests found significant positive associations between pairwise linearized FST and geographic distance in one dimension along the coast of Cebu ($p=0.002$, $n=23$ sites) and between pairwise linearized FST and log geographic distance in two dimensions across the entire study area ($p=0.001$, $n=36$ sites). A higher percentage of the resampled slopes (99.7%) were positive than they were for any of the *Acropora* taxa, and the 95% confidence interval did not overlap with zero (Fig. 2.6).

When we analyzed IBD slopes for *Cladocopium* within each cryptic taxon separately to control for differences in sample size and geographic distribution of samples between *Cladocopium* and *Acropora* taxa, a higher percentage of IBD slopes were positive for the *Cladocopium* samples than for the *Acropora* samples in four out of four taxa for the one dimensional analysis, and in two out of four taxa for the two dimensional analysis (Table A2.3). In the two dimensional analysis, a higher percentage of IBD slopes were positive for three out of four *Cladocopium* samples than for the *Acropora* samples after excluding one potential clone. For Taxon 3, both

Cladocopium and *Acropora* resampled IBD slopes were positive for a large fraction of the draws, with a slightly higher percentage in *Cladocopium* for one dimensional analyses, and slightly higher for *Acropora* for two dimensional analyses (Table 2.3).

Geographic distance had a stronger influence on *Cladocopium* genetic similarity than did host *Acropora* genotype. A partial Mantel test assessing the relationship of FSTs between *Cladocopium* populations and FSTs between *Acropora* populations conditioned on geographic distance was not significant ($p=0.347$, $n=36$ sites). Conversely, a partial Mantel test of between-population *Cladocopium* FSTs and geographic distance conditioned on *Acropora* between-population FSTs was significant ($p=0.004$, $n=36$ sites).

2.4 Discussion

This study used dense genetic sampling across a seascape to infer patterns of dispersal and, more broadly, spatial genetic variation in *Acropora cf. tenuis* corals and their algal symbionts. Unexpectedly, we found four genetically distinct but sympatrically distributed groups of *Acropora* within our sample. All of the taxa exhibited genetic patterns across the study area consistent with long-distance dispersal, and we found putative parent/offspring pairs at widely spaced sites. However, all genetic clusters of *Acropora* hosted primarily a single type of algal symbiont belonging to the genus *Cladocopium*. *Cladocopium* genotypes were structured more strongly by geographic location rather than host genotype. When

comparing dispersal across hosts and symbionts, the algal symbionts showed greater genetic structure in space than did their *Acropora* hosts.

2.4.1 Sympatric cryptic diversity within *Acropora cf. tenuis*

Prior study of *Acropora cf. tenuis* suggests this species actually constitutes multiple morphologically similar species. In particular, the *Acropora cf. tenuis* group in Southeast Asia is poorly defined in terms of both genetics and morphology, and may constitute multiple lineages (Bridge et al., 2024). Our results strongly support the existence of at least four sympatric genetic groups within *Acropora cf. tenuis* in the Philippines, along with limited hybridization between those groups. Multiple analysis methods converged on four groups in our samples and assigned individual corals to groups with a high level of consistency, despite their lack of differentiation in space. Combining these lines of evidence, we consider these groups to be cryptic taxa, possibly constituting distinct members of a species complex. In particular, our ADMIXTURE results suggest limited interbreeding between the four ancestry groups, though the existence of mixed ancestry in some individuals implies that intermittent hybridization between these genetic clusters can occur.

Species definitions in *Acropora* are frequently ambiguous, with extensive hybridization between species (Ladner & Palumbi, 2012; Wu et al., 2024). Closely related *Acropora* species may be best defined as “syngameons,” or groups of two or more related species that are genetically distinct, yet regularly interbreed (Ladner & Palumbi, 2012). Given the apparently incomplete genetic separation of genetic groups within *A. cf. tenuis* individuals in our dataset, these populations may fit that

definition. While prior studies of *Acropora* species complexes have found microhabitat differences associated with different cryptic taxa (Ladner & Palumbi, 2012; Matias et al., 2023), we found only weak evidence of microhabitat differentiation between the cryptic taxa found here, defined in terms of depth and distance to shore. However, we had incomplete data on individual coral depths, which may have hindered our ability to observe such differentiation. Our results underscore the need for further study of *Acropora* taxonomy in the Philippines, which would allow us to uncover potentially differing distributions, ecological roles, and conservation needs of these previously conflated taxa.

2.4.2 Long-distance dispersal and weak spatial genetic variation in *Acropora*

Broadcast spawning corals, including *Acropora*, often show long distance connectivity through dispersal of their pelagic larvae. For example, a study of connectivity among *Acropora austera* populations in Mozambique found genetic near-panmixia across a 384 km stretch of coastline (Duvane et al., 2025). A genetic study of *A. hyacinthus* and *A. digitifera* in the south Pacific found isolation by distance patterns in both, but only on the spatial scale of thousands of kilometers (Davies et al., 2020). Research on *Pocillopora verrucosa*, a coral belonging to a different genus but with a similar reproductive mode to *Acropora*, on the Great Barrier Reef estimated dispersal distances anywhere between 21 and 52 kilometers using isolation by distance relationships to estimate dispersal kernel spread (Meziere et al., 2025).

Patterns of spatial genetic variation in each cryptic *Acropora* taxon studied here are consistent with long larval dispersal distances. We found no significant isolation by distance slopes in one or two dimensions despite dense sampling across 200 km. Confidence intervals for all slopes overlapped with zero, and resampling slopes resulted in substantial percentages with non-positive slopes. For one taxon (Taxon 2), the best-fit slope was less than zero. Taxon 4 also showed an average negative isolation by distance slope in the one dimensional analysis after excluding clones. All of this suggests minimal or no isolation by distance within the *Acropora* samples at 200 km scales. While still not significant, Taxon 3 had marginally stronger isolation by distance patterns than the other taxa, which may indicate shorter average dispersal in that taxon. However, this could also be due to lower effective population size, which would be consistent with the higher inbreeding coefficient in this taxon.

Unlike the results presented here, multiple studies of reef fishes in this same area of the Philippines have found clear isolation by distance patterns, which were then used to estimate dispersal kernel spreads. A 2010 study of anemonefish *Amphiprion clarkii* across Cebu and Leyte found a dispersal kernel spread of 11 km, with a confidence interval of 4 - 27 km (Pinsky et al., 2010), with additional research showing that dispersal varied both seasonally and interannually (Catalano et al., 2024). A study in the sister taxon *Amphiprion biaculeatus* found a similar dispersal kernel spread of 8.9 km, with a confidence interval of 2.3 - 18.4 km (Fitz et al., 2023).

The lack of any consistent isolation by distance pattern in *Acropora* across exactly the same geography as that used in the *Amphiprion* studies suggests longer,

and perhaps much longer, dispersal distances for *Acropora* corals than their co-occurring reef fishes. Rousset (1999) recommends a square sampling area for isolation by distance patterns of at least 10 times the dispersal distance of the study organism. In the case of this approximately 200 km by 100 km area, this guideline would suggest that clear isolation by distance patterns would have been apparent for dispersal distances of less than ten to twenty kilometers. The lack of such patterns suggests that *Acropora* dispersal may regularly exceed this threshold.

Kinship analysis added further evidence to this hypothesis, finding closely related individuals of *Acropora* separated by as much as 181 km. While these distances are mostly long, they are not implausible given the oceanography of the area and the life history of broadcast spawning corals. Some of the distances between close kin pairs found here fall within the calculated range of dispersal kernel spread for *Acropora* taxa on the Great Barrier Reefs calculated by Meziere *et al.* (2025). Larvae of many *Acropora* species experience precompetency periods of three to seven days before they are able to settle (Randall et al., 2024), and they may survive for 50 or even 100 days in the lab (Connolly & Baird, 2010; Miller et al., 2020; Nishikawa & Sakai, 2005). Dispersal models fit to genetic data suggest that dispersal times of more than 60 days are common in some *Acropora* species (Davies et al., 2015). Given that our study site exhibits mostly open coastlines, with surface current speeds that may exceed 0.5 meters per second during the seasonal monsoons, we can expect these competency times to result in long-distance larval transport (Catalano et al., 2024).

While three of these pairs were identified as possible clones by KING, this seems less plausible than close kin given known *Acropora* life history. *Acropora* do not produce asexual larvae and self-fertilize only rarely (Boutet & Schierwater, 2021; Willis et al., 1997). Clonal genotypes in other *Acropora* are most often found within a few meters of each other, as they are derived from physically fragmented adult corals (Howlett et al., 2024). However, some species of *Acropora* may be more prone to reproduction by fragmentation than others, and coral fragments have occasionally been documented to settle and grow after transportation by strong typhoons, such as those common in the Philippines (Anticamara & Tan, 2018; Pipithkul et al., 2021). It is possible though unlikely that these putative clone pairs result from fragmentation during strong storms and subsequent cross-island transportation.

Alternatively, coral polyps under acute stress occasionally detach themselves completely from the coral skeleton and form a "pseudo‑planula" in a process known as "polyp bailout". These detached polyps can later settle in a new location and grow into a new colony. Polyp bailout was originally documented in the 1940s (incidentally, in a species of *Acropora cf. tenuis*) , but remains an understudied process in coral ecology (Schweinsberg et al., 2021). Whether the related individuals in our dataset represent true clones or first degree relatives, our finding of closely related individuals at widely spaced sites provides strong evidence of long-distance gene flow across a single generation.

2.4.3 Algal symbionts structured more strongly by geography than host

Cladocopium taxonomy remains poorly resolved, with only a handful of formally recognized species out of potentially hundreds in nature (Butler et al., 2023; Davies et al., 2023). Some species of *Cladocopium* associate with specific coral hosts, especially but not exclusively hosts that transmit their symbionts vertically (Thornhill et al., 2014; Turnham et al., 2021). However, other named species of *Cladocopium* are generalists, found across thousands of kilometers and multiple hosts, including multiple species of *Acropora* (Butler et al., 2023). Extremely low FSTs between *Cladocopium* populations found in different coral taxa further imply that the taxonomic variation in our *Acropora* samples is not reflected in their algal symbionts. A study of co-occurring *Acropora cf. tenuis* cryptic taxa on the Great Barrier Reef also found a common pool of *Cladocopium* symbionts between cryptic taxa (Matias et al., 2023). Similarly in our study, we find a single genetic grouping of *Cladocopium* shared between all *Acropora* taxa. While ADMIXTURE resolved three ancestry groups, all groups were present in all *Acropora* taxa, showing structure with geography (latitude) rather than host. Our finding of weakly significant genetic differentiation between *Cladocopium* in different *Acropora* taxa could imply some symbiont selectivity by coral hosts, or it could result from common environmental factors structuring both host taxon occurrence and *Cladocopium* genotype. For example, we found that the *Acropora* taxa exhibited slight latitudinal differences in their distributions, and we found that latitude structured genetic variation in *Cladocopium* as well. This finding could result from neutral variation across the

seascape, or it could represent adaptive genetic differences relating to differences in temperature along the latitudinal gradient.

Studies of *Acropora* taxa on other reefs have also found genetic variation in symbionts that is structured by environmental factors separately from coral host genomes. Genetic variation of *Cladocopium* found in *Acropora cf. humilis* in the Coral Sea depends largely on environmental variables such as thermal stress, light attenuation, and latitude, and only very slightly on host genotype (Marzonie et al., 2024). *Acropora hyacinthus* in Palau host mostly *Cladocopium*, and the genomes of those *Cladocopium* vary both between reefs and with depth (Armstrong et al., 2024). However, studies in other *Acropora* taxa, including *A. hyacinthus* and *A. digitifera* in Micronesia, have found host specialization between different *Cladocopium* lineages (Davies et al., 2020). It is worth noting that all of the *Acropora* taxa in our study are likely closely related, as evidenced by the relatively low FSTs between the groups. Other co-occurring *Acropora* species in the central Philippines may selectively host different lineages of *Cladocopium*, or even other symbiont genera. However, within this *A. cf. tenuis* species complex, genetic variation in algal symbionts appears to be more driven by geography and environment than host genetic variation. This result is consistent with study of *Acropora* cryptic taxa on the Great Barrier Reefs, where a common pool of *Cladocopium* found across hosts nonetheless exhibited significant genetic variation with distance to shore (Matias et al., 2023).

In our study, *Cladocopium* exhibited significant isolation by distance patterning in both one and two dimensions. Resampled IBD slopes were more

consistently positive than those found in *Acropora*, even when controlling for sample size, for all of the taxa in one dimension and for three of four taxa in two dimensions. Our *Cladocopium* samples also exhibited spatial genetic variation at fine scales, as evidenced by the strong correlation between the second principle component of the algal genomes and depth. Partial Mantel tests also revealed that genetic distance between *Cladocopium* populations depended on geographic distance, when controlling for genetic distance between *Acropora* populations more strongly than the inverse. All of these lines of evidence indicate that within these *Acropora* populations, geography and environment structure symbiont genetic variation more strongly than does the genome of the host.

Despite these differences in genetic structure, the relative dispersal distances in the two taxa are difficult to measure directly. The slope of the relationship between geographic and genetic distance is inversely related to dispersal kernel spread, with steeper slopes implying shorter dispersal distances (Rousset, 1997). However, the slope is also inversely related to effective population size, with larger effective population sizes resulting in shallower slopes (Rousset, 1997). Without effective population size estimates for these taxa, dispersal cannot be estimated. In addition, differences in effective population size could explain some of the differences that we observed. For example, the weakly steeper slopes of some *Acropora* IBD relationships compared to the *Cladocopium* relationship could result from much higher effective population sizes in the latter. Microscopic *Cladocopium* can inhabit a variety of hosts and may also live freely in the water column or benthos (Bell &

Quigley, 2025; Lim et al., 2019). The inverse relationship, however, is highly unlikely, namely that *Acropora* corals have substantially higher effective population sizes than *Cladocopium* in our study region. Therefore, the generally stronger isolation by distance patterns in *Cladocopium,* along with the observed patterns of landscape genetic variation, most likely indicates that *Acropora* disperse much further than their algal symbionts.

2.4.5 Implications for gene flow and local adaptation

Corals are not the only marine animals that acquire photosymbionts from their settlement environment. Other examples include giant clams and jellyfish (Astorga et al., 2012; Butler et al., 2023; Fitt & Trench, 1981). In a very different marine environment, deep sea snails inhabiting hydrothermal vents also acquire their chemosynthetic bacterial partners horizontally (Breusing et al., 2022). Similarly to our finding that *Cladocopium* genotypes depend on geography and depth more strongly than host taxon, genetics of snail microsymbionts depend more strongly on site-specific environmental variables than on the genetics of their hosts. Environmental acquisition of shorter-dispersing symbionts can enable a far-dispersing host to acquire symbiont strains adapted to their specific local conditions (Breusing et al., 2022). Our results suggest the possibility of similar dynamics at play in *Acropora* in the Philippines. We found low genetic structuring in populations of four different *Acropora* taxa across a two hundred kilometer span on multiple islands, suggesting limited potential for genome-wide local adaptation. Conversely, we found genetic

variation in *Cladocopium* associated with latitude and depth, both of which determine the environmental conditions to which corals are exposed.

Our results revealed differing patterns of spatial genetic variation in *Cladocopium* and their *Acropora* hosts, despite their close symbiotic relationship. The contrast between extensive within-species connectivity in *Acropora*, contrasted with the spatial geographic structuring in *Cladocopium,* creates evolutionary advantages for the holobiont. Long dispersal distances enable genetic connectivity between far-flung populations, but can limit local adaptation when parents and offspring settle in very different conditions (Kawecki & Ebert, 2004). This may be a particular problem in the marine realm, where species tend to exhibit longer dispersal distances than do terrestrial taxa (Kinlan & Gaines, 2003). Here we see *Acropora cf. tenuis* larvae traversing potentially hundreds of kilometers of latitudinal span, as well as tens of meters of depth gradient, and ultimately settling in markedly different environments than their parents. Acquiring symbionts from the settlement environment may allow far-dispersing marine taxa to take advantage of locally adapted symbiont genotypes.

Given these differences, simulations of gene flow and evolution in corals should consider modeling coral hosts and their algal symbionts as distinct yet interacting components within a single framework . The close ecological relationship between *Acropora* and their *Cladocopium* symbionts does not require parallel patterns of landscape genetics, as the taxa exhibit contrasting patterns of speciation, gene flow, and possibly adaptation. Continued study of close symbiont pairs,

including corals, will be important for understanding how species interactions shape the co-evolution of dispersal.

Acknowledgements

This study was made possible by funding from a National Defense Science and Engineering Graduate Fellowship (JTB), the National Science Foundation under award OCE-2443233 (LCM), and the Paul M. Angell Foundation under award CON-F23-28 (MLP and JTB). The authors thank Isabel M. Silva and Peter T. Raimondi for comments on an earlier version of this project.

Data availability statement

Raw reads are downloadable from NCBI at https://www.ncbi.nlm.nih.gov/sra/PRJNA1445311.

All code, metadata, and selected intermediates are available on Github at https://github.com/pinskylab/Atenuis_Philippines.

Github repository will be replaced with Zenodo link upon acceptance.

Metadata is additionally published on GEOME at https://n2t.net/ark:/21547/HDm2 .

References

Alexander, D. H., Novembre, J., & Lange, K. (2009). Fast model-based estimation of ancestry in unrelated individuals. *Genome Research*, *19*(9), 1655–1664. https://doi.org/10.1101/gr.094052.109

Anticamara, J. A., & Tan, C. A. (2018). Survival and growth of re-attached storm-generated coral fragments post super-typhoon Haiyan (aka Yolanda). *Scince Diliman*, *30*, 5–31.

Arafeh-Dalmau, N., Munguia-Vega, A., Micheli, F., Vilalta-Navas, A., Villaseñor-Derbez, J. C., Précoma-de la Mora, M., Schoeman, D. S., Medellín-Ortíz, A., Cavanaugh, K. C., Sosa-Nishizaki, O., Burnham, T. L. U., Knight, C. J., Woodson, C. B., Abas, M., Abadía-Cardoso, A., Aburto-Oropeza, O., Esgro, M. W., Espinosa-Andrade, N., Beas-Luna, R., … Possingham, H. P. (2023). Integrating climate adaptation and transboundary management: Guidelines for designing climate-smart marine protected areas. *One Earth*, *6*(11), 1523–1541. https://doi.org/10.1016/j.oneear.2023.10.002

Armstrong, K. C., Lippert, M., Hanson, E., Nestor, V., Cornwell, B., Walker, N. S., Golbuu, Y., & Palumbi, S. R. (2024). Fine‐Scale Geographic Variation of *Cladocopium* in *Acropora hyacinthus* Across the Palauan Archipelago. *Ecology and Evolution*, *14*(12), e70650. https://doi.org/10.1002/ece3.70650

Astorga, D., Ruiz, J., & Prieto, L. (2012). Ecological aspects of early life stages of Cotylorhiza tuberculata (Scyphozoa: Rhizostomae) affecting its pelagic population success. In J. Purcell, H. Mianzan, & J. R. Frost (Eds.), *Jellyfish Blooms IV* (pp. 141–155). Springer Netherlands. https://doi.org/10.1007/978-94-007-5316-7_11

Bell, S. L., & Quigley, K. M. (2025). Global Free‐Living Symbiodiniaceae Biodiversity Mirrors Local Environments. *Journal of Biogeography*, *52*(7), e15137. https://doi.org/10.1111/jbi.15137

Bird, C. E. (2024). *Philippines PIRE FQ GZ Analysis Pipeline* (Version v1.0.0) [Computer software]. Zenodo. https://doi.org/10.5281/ZENODO.13988542

Boutet, A., & Schierwater, B. (2021). *Handbook of Marine Model Organisms in Experimental Biology: Established and Emerging* (1st ed.). CRC Press. https://doi.org/10.1201/9781003217503

Breusing, C., Genetti, M., Russell, S. L., Corbett-Detig, R. B., & Beinart, R. A. (2022). Horizontal transmission enables flexible associations with locally adapted symbiont strains in deep-sea hydrothermal vent symbioses. *Proceedings of the National Academy of Sciences*, *119*(14), e2115608119. https://doi.org/10.1073/pnas.2115608119

Bridge, T. C. L., Cowman, P. F., Quattrini, A. M., Bonito, V. E., Sinniger, F., Harii, S., Head, C. E. I., Hung, J. Y., Halafihi, T., Rongo, T., & Baird, A. H. (2024). A *tenuis* relationship: Traditional taxonomy obscures systematics and

biogeography of the ‘ *Acropora tenuis* ’ (Scleractinia: Acroporidae) species complex. *Zoological Journal of the Linnean Society*, *202*(1), zlad062. https://doi.org/10.1093/zoolinnean/zlad062

Bushnell, B. (2014). *BBTools* (Version 39.06) [Computer software]. https://bbmap.org

Butler, C. C., Turnham, K. E., Lewis, A. M., Nitschke, M. R., Warner, M. E., Kemp, D. W., Hoegh‐Guldberg, O., Fitt, W. K., Van Oppen, M. J. H., & LaJeunesse, T. C. (2023). Formal recognition of host‐generalist species of dinoflagellate (*Cladocopium* , Symbiodiniaceae) mutualistic with Indo‐Pacific reef corals. *Journal of Phycology*, *59*(4), 698–711. https://doi.org/10.1111/jpy.13340

Catalano, K. A., Dedrick, A. G., Stuart, M. R., Puritz, J. B., Montes, H. R., & Pinsky, M. L. (2021). Quantifying dispersal variability among nearshore marine populations. *Molecular Ecology*, *30*(10), 2366–2377. https://doi.org/10.1111/mec.15732

Catalano, K. A., Drenkard, E. J., Curchitser, E. N., Dedrick, A. G., Stuart, M. R., Montes, H. R., & Pinsky, M. L. (2024). The contribution of nearshore oceanography to temporal variation in larval dispersal. *Ecology*, *105*(10), e4412. https://doi.org/10.1002/ecy.4412

Chang, C. C., Chow, C. C., Tellier, L. C., Vattikuti, S., Purcell, S. M., & Lee, J. J. (2015). Second-generation PLINK: Rising to the challenge of larger and richer datasets. *Gigascience*, *4*(1), s13742-015-0047–0048. https://doi.org/10.1186/s13742-015-0047-8

Chen, S., Zhou, Y., Chen, Y., & Gu, J. (2018). fastp: An ultra-fast all-in-one FASTQ preprocessor. *Bioinformatics*, *34*(17), i884–i890. https://doi.org/10.1093/bioinformatics/bty560

Connolly, S. R., & Baird, A. H. (2010). Estimating dispersal potential for marine larvae: Dynamic models applied to scleractinian corals. *Ecology*, *91*(12), 3572–3583. https://doi.org/10.1890/10-0143.1

Cumbo, V. R., Baird, A. H., & Van Oppen, M. J. H. (2013). The promiscuous larvae: Flexibility in the establishment of symbiosis in corals. *Coral Reefs*, *32*(1), 111–120. https://doi.org/10.1007/s00338-012-0951-7

Danecek, P., Auton, A., Abecasis, G., Albers, C. A., Banks, E., DePristo, M. A., Handsaker, R. E., Lunter, G., Marth, G. T., Sherry, S. T., McVean, G., Durbin, R., & 1000 Genomes Project Analysis Group. (2011). The variant call format and VCFtools. *Bioinformatics*, *27*(15), 2156–2158. https://doi.org/10.1093/bioinformatics/btr330

Davies, S. W., Gamache, M. H., Howe-Kerr, L. I., Kriefall, N. G., Baker, A. C., Banaszak, A. T., Bay, L. K., Bellantuono, A. J., Bhattacharya, D., Chan, C. X., Claar, D. C., Coffroth, M. A., Cunning, R., Davy, S. K., Del Campo, J., Díaz-Almeyda, E. M., Frommlet, J. C., Fuess, L. E., González-Pech, R. A., … Parkinson, J. E. (2023). Building consensus around the assessment and interpretation of Symbiodiniaceae diversity. *PeerJ*, *11*, e15023. https://doi.org/10.7717/peerj.15023

Davies, S. W., Moreland, K. N., Wham, D. C., Kanke, M. R., & Matz, M. V. (2020). *Cladocopium* community divergence in two *Acropora* coral hosts across multiple spatial scales. *Molecular Ecology*, *29*(23), 4559–4572. https://doi.org/10.1111/mec.15668

Davies, S. W., Treml, E. A., Kenkel, C. D., & Matz, M. V. (2015). Exploring the role of Micronesian islands in the maintenance of coral genetic diversity in the Pacific Ocean. *Molecular Ecology*, *24*(1), 70–82. https://doi.org/10.1111/mec.13005

Dixon, P. (2003). VEGAN, a package of R functions for community ecology. *Journal of Vegetation Science*, *14*(6), 927–930. https://doi.org/10.1111/j.1654-1103.2003.tb02228.x

Dougan, K. E., Bellantuono, A. J., Kahlke, T., Abbriano, R. M., Chen, Y., Shah, S., Granados-Cifuentes, C., Van Oppen, M. J. H., Bhattacharya, D., Suggett, D. J., Rodriguez-Lanetty, M., & Chan, C. X. (2024). Whole-genome duplication in an algal symbiont bolsters coral heat tolerance. *Science Advances*, *10*(29), eadn2218. https://doi.org/10.1126/sciadv.adn2218

Duvane, J. A., Dupont, S., Sola, E., Ortega-Martinez, O., & Pereyra, R. T. (2025). Genetic diversity and structure among Acropora austera populations in Mozambique suggest low resilience potential of one of the world's most charismatic coral reefs. *Coral Reefs*, *44*(4), 1185–1195. https://doi.org/10.1007/s00338-025-02679-w

Ewald, P. W. (1987). Transmission Modes and Evolution of the Parasitism‐Mutualism Continuuma. *Annals of the New York Academy of Sciences*, *503*(1), 295–306. https://doi.org/10.1111/j.1749-6632.1987.tb40616.x

Ewels, P., Magnusson, M., Lundin, S., & Käller, M. (2016). MultiQC: Summarize analysis results for multiple tools and samples in a single report. *Bioinformatics*, *32*(19), 3047–3048. https://doi.org/10.1093/bioinformatics/btw354

Fisher, R., O'Leary, R. A., Low-Choy, S., Mengersen, K., Knowlton, N., Brainard, R. E., & Caley, M. J. (2015). Species Richness on Coral Reefs and the Pursuit of Convergent Global Estimates. *Current Biology*, *25*(4), 500–505. https://doi.org/10.1016/j.cub.2014.12.022

Fitt, W. K., & Trench, R. K. (1981). SPAWNING, DEVELOPMENT, AND ACQUISITION OF ZOOXANTHELLAE BY *TRIDACNA SQUAMOSA* (MOLLUSCA, BIVALVIA). *The Biological Bulletin*, *161*(2), 213–235. https://doi.org/10.2307/1540800

Fitz, K. S., Montes, H. R., Thompson, D. M., & Pinsky, M. L. (2023). Isolation‐by‐distance and isolation‐by‐oceanography in Maroon Anemonefish (*Amphiprion biaculeatus*). *Evolutionary Applications*, *16*(2), 379–392. https://doi.org/10.1111/eva.13448

Garrison, E., Kronenberg, Z. N., Dawson, E. T., Pedersen, B. S., & Prins, P. (2022). A spectrum of free software tools for processing the VCF variant call format: Vcflib, bio-vcf, cyvcf2, hts-nim and slivar. *PLOS Computational Biology*, *18*(5), e1009123. https://doi.org/10.1371/journal.pcbi.1009123

Garrison, E., & Marth, G. (2012). *Haplotype-based variant detection from short-read sequencing* (Version 2). arXiv. https://doi.org/10.48550/ARXIV.1207.3907

Goudet, J. (2005). HIERFSTAT , a package for R to compute and test hierarchical *F* ‐statistics. *Molecular Ecology Notes*, *5*(1), 184–186. https://doi.org/10.1111/j.1471-8286.2004.00828.x

Hand, B. K., Lowe, W. H., Kovach, R. P., Muhlfeld, C. C., & Luikart, G. (2015). Landscape community genomics: Understanding eco-evolutionary processes in complex environments. *Trends in Ecology & Evolution*, *30*(3), 161–168. https://doi.org/10.1016/j.tree.2015.01.005

Harii, S., Yasuda, N., Rodriguez-Lanetty, M., Irie, T., & Hidaka, M. (2009). Onset of symbiosis and distribution patterns of symbiotic dinoflagellates in the larvae of scleractinian corals. *Marine Biology*, *156*(6), 1203–1212. https://doi.org/10.1007/s00227-009-1162-9

Hartmann, A. C., Baird, A. H., Knowlton, N., & Huang, D. (2017). The Paradox of Environmental Symbiont Acquisition in Obligate Mutualisms. *Current Biology*, *27*(23), 3711-3716.e3. https://doi.org/10.1016/j.cub.2017.10.036

Howells, E. J., Beltran, V. H., Larsen, N. W., Bay, L. K., Willis, B. L., & Van Oppen, M. J. H. (2012). Coral thermal tolerance shaped by local adaptation of

photosymbionts. *Nature Climate Change*, *2*(2), 116–120. https://doi.org/10.1038/nclimate1330

Howlett, L., Camp, E. F., Locatelli, N. S., Baums, I. B., Strudwick, P., Rassmussen, S., & Suggett, D. J. (2024). Population and clonal structure of Acropora cf. Hyacinthus to inform coral restoration practices on the Great Barrier Reef. *Coral Reefs*, *43*(4), 1023–1035. https://doi.org/10.1007/s00338-024-02520-w

Huisman, J. (2017). Pedigree reconstruction from SNP data: Parentage assignment, sibship clustering and beyond. *Molecular Ecology Resources*, *17*(5), 1009–1024. https://doi.org/10.1111/1755-0998.12665

Johnston-Monje, D., Gutiérrez, J. P., & Lopez-Lavalle, L. A. B. (2021). Seed-Transmitted Bacteria and Fungi Dominate Juvenile Plant Microbiomes. *Frontiers in Microbiology*, *12*, 737616. https://doi.org/10.3389/fmicb.2021.737616

Jombart, T., & Collins, C. (2015, June 23). *A tutorial for Discriminant Analysis of Principal Components (DAPC) using adegenet 2.0.0*. Imperial College London MRC Centre for Outbreak Analysis and Modelling. https://adegenet.r-forge.r-project.org/files/tutorial-dapc.pdf

Kawecki, T. J., & Ebert, D. (2004). Conceptual issues in local adaptation. *Ecology Letters*, *7*(12), 1225–1241. https://doi.org/10.1111/j.1461-0248.2004.00684.x

Kinlan, B. P., & Gaines, S. D. (2003). PROPAGULE DISPERSAL IN MARINE AND TERRESTRIAL ENVIRONMENTS: A COMMUNITY PERSPECTIVE. *Ecology*, *84*(8), 2007–2020. https://doi.org/10.1890/01-0622

Ladner, J. T., & Palumbi, S. R. (2012). Extensive sympatry, cryptic diversity and introgression throughout the geographic distribution of two coral species complexes. *Molecular Ecology*, *21*(9), 2224–2238. https://doi.org/10.1111/j.1365-294X.2012.05528.x

Laurent‐Webb, L., Maurice, K., Perez‐Lamarque, B., Bourceret, A., Ducousso, M., & Selosse, M. (2024). Seed or soil: TRACING back the plant mycobiota primary sources. *Environmental Microbiology Reports*, *16*(3), e13301. https://doi.org/10.1111/1758-2229.13301

Li, H., & Durbin, R. (2009). Fast and accurate short read alignment with Burrows–Wheeler transform. *Bioinformatics*, *25*(14), 1754–1760. https://doi.org/10.1093/bioinformatics/btp324

Li, H., Handsaker, B., Wysoker, A., Fennell, T., Ruan, J., Homer, N., Marth, G., Abecasis, G., Durbin, R., & 1000 Genome Project Data Processing Subgroup. (2009). The Sequence Alignment/Map format and SAMtools. *Bioinformatics*, *25*(16), 2078–2079. https://doi.org/10.1093/bioinformatics/btp352

Lim, S. S. Q., Huang, D., Soong, K., & Neo, M. L. (2019). Diversity of endosymbiotic Symbiodiniaceae in giant clams at Dongsha Atoll, northern South China Sea. *Symbiosis*, *78*(3), 251–262. https://doi.org/10.1007/s13199-019-00615-5

Martin-Cuadrado, A.-B., Rubio-Portillo, E., Rosselló, F., & Antón, J. (2024). The coral Oculina patagonica holobiont and its response to confinement, temperature, and Vibrio infections. *Microbiome*, *12*(1), 222. https://doi.org/10.1186/s40168-024-01921-x

Marzonie, M. R., Nitschke, M. R., Bay, L. K., Bourne, D. G., & Harrison, H. B. (2024). Symbiodiniaceae diversity varies by host and environment across thermally distinct reefs. *Molecular Ecology*, *33*(9), e17342. https://doi.org/10.1111/mec.17342

Matias, A. M. A., Popovic, I., Thia, J. A., Cooke, I. R., Torda, G., Lukoschek, V., Bay, L. K., Kim, S. W., & Riginos, C. (2023). Cryptic diversity and spatial genetic variation in the coral *Acropora tenuis* and its endosymbionts across the Great Barrier Reef. *Evolutionary Applications*, *16*(2), 293–310. https://doi.org/10.1111/eva.13435

Matsuda, S. B., Chakravarti, L. J., Cunning, R., Huffmyer, A. S., Nelson, C. E., Gates, R. D., & Van Oppen, M. J. H. (2022). Temperature‐mediated acquisition of rare heterologous symbionts promotes survival of coral larvae under ocean warming. *Global Change Biology*, *28*(6), 2006–2025. https://doi.org/10.1111/gcb.16057

McClanahan, T. R., Maina, J. M., Darling, E. S., Guillaume, M. M. M., Muthiga, N. A., D'agata, S., Leblond, J., Arthur, R., Jupiter, S. D., Wilson, S. K., Mangubhai, S., Ussi, A. M., Humphries, A. T., Patankar, V., Shedrawi, G., Julius, P., Ndagala, J., & Grimsditch, G. (2020). Large geographic variability in the resistance of corals to thermal stress. *Global Ecology and Biogeography*, *29*(12), 2229–2247. https://doi.org/10.1111/geb.13191

McMaster, E. S., Lu‐Irving, P., Van Der Merwe, M. M., Ho, S. Y. W., & Rossetto, M. (2025). Evaluating Kinship Estimation Methods for Reduced‐Representation SNP Data in Non‐model Species. *Molecular Ecology Resources*, *25*(8), e70038. https://doi.org/10.1111/1755-0998.70038

Mellin, C., Hicks, C. C., Fordham, D. A., Golden, C. D., Kjellevold, M., MacNeil, M. A., Maire, E., Mangubhai, S., Mouillot, D., Nash, K. L., Omukoto, J. O., Robinson, J. P. W., Stuart-Smith, R. D., Zamborain-Mason, J., Edgar, G. J., & Graham, N. A. J. (2022). Safeguarding nutrients from coral reefs under climate change. *Nature Ecology & Evolution*, *6*(12), 1808–1817. https://doi.org/10.1038/s41559-022-01878-w

Meziere, Z., Prata, K., Lechene, M., Ferrari, R., Popovic, I., & Riginos, C. (2025). Connectivity differs by orders of magnitude among co-distributed corals, affecting spatial scales of eco-evolutionary processes. *Science Advances*, *11*(27), eadt2066. https://doi.org/10.1126/sciadv.adt2066

Miller, M. W., Bright, A. J., Pausch, R. E., & Williams, D. E. (2020). Larval longevity and competency patterns of Caribbean reef-building corals. *PeerJ*, *8*, e9705. https://doi.org/10.7717/peerj.9705

Moore, J. A., Miller, H. C., Daugherty, C. H., & Nelson, N. J. (2008). Fine‐scale genetic structure of a long‐lived reptile reflects recent habitat modification. *Molecular Ecology*, *17*(21), 4630–4641. https://doi.org/10.1111/j.1365-294X.2008.03951.x

Muscatine, L., & Cernichiari, E. (1969). ASSIMILATION OF PHOTOSYNTHETIC PRODUCTS OF ZOOXANTHELLAE BY A REEF CORAL. *The Biological Bulletin*, *137*(3), 506–523. https://doi.org/10.2307/1540172

Nishikawa, A., Katoh, M., & Sakai, K. (2003). Larval settlement rates and gene flow of broadcast-spawning (Acropora tenuis) and planula-brooding (Stylophora pistillata) corals. *Marine Ecology Progress Series*, *256*, 87–97. https://doi.org/10.3354/meps256087

Nishikawa, A., & Sakai, K. (2005). Settlement-competency Period of Planulae and Genetic Differentiation of the Scleractinian Coral Acropora digitifera. *Zoological Science*, *22*(4), 391–399. https://doi.org/10.2108/zsj.22.391

O'Leary, S. J., Puritz, J. B., Willis, S. C., Hollenbeck, C. M., & Portnoy, D. S. (2018). These aren't the loci you'e looking for: Principles of effective SNP filtering for molecular ecologists. *Molecular Ecology*, *27*(16), 3193–3206. https://doi.org/10.1111/mec.14792

OpenStreetMap contributors. (2025). *OpenStreetMap Coastlines* [Dataset]. https://www.openstreetmap.org/

Peterson, B. K., Weber, J. N., Kay, E. H., Fisher, H. S., & Hoekstra, H. E. (2012). Double Digest RADseq: An Inexpensive Method for De Novo SNP Discovery

and Genotyping in Model and Non-Model Species. *PLoS ONE*, *7*(5), e37135. https://doi.org/10.1371/journal.pone.0037135

Pinsky, M. L., Montes Jr., H. R., & Palumbi, S. R. (2010). USING ISOLATION BY DISTANCE AND EFFECTIVE DENSITY TO ESTIMATE DISPERSAL SCALES IN ANEMONEFISH: ISOLATION BY DISTANCE AND MARINE DISPERSAL. *Evolution*, *64*(9), 2688–2700. https://doi.org/10.1111/j.1558-5646.2010.01003.x

Pinsky, M. L., Saenz-Agudelo, P., Salles, O. C., Almany, G. R., Bode, M., Berumen, M. L., Andréfouët, S., Thorrold, S. R., Jones, G. P., & Planes, S. (2017). Marine Dispersal Scales Are Congruent over Evolutionary and Ecological Time. *Current Biology*, *27*(1), 149–154. https://doi.org/10.1016/j.cub.2016.10.053

Pipithkul, S., Ishizu, S., Shimura, A., Yokochi, H., Nagai, S., Fukami, H., & Yasuda, N. (2021). High Clonality and Geographically Separated Cryptic Lineages in the Threatened Temperate Coral, Acropora pruinosa. *Frontiers in Marine Science*, *8*, 668043. https://doi.org/10.3389/fmars.2021.668043

Pratchett, M. S., McCowan, D., Maynard, J. A., & Heron, S. F. (2013). Changes in Bleaching Susceptibility among Corals Subject to Ocean Warming and Recurrent Bleaching in Moorea, French Polynesia. *PLoS ONE*, *8*(7), e70443. https://doi.org/10.1371/journal.pone.0070443

Randall, C. J., Giuliano, C., Stephenson, B., Whitman, T. N., Page, C. A., Treml, E. A., Logan, M., & Negri, A. P. (2024). Larval precompetency and settlement behaviour in 25 Indo-Pacific coral species. *Communications Biology*, *7*(1), 142. https://doi.org/10.1038/s42003-024-05824-3

Rousset, F. (1997). 7. Genetic Differentiation and Estimation of Gene Flow from F-Statistics Under Isolation by Distance. *Genetics*, *145*(4), 1219–1228.

Russell, S. L. (2019). Transmission mode is associated with environment type and taxa across bacteria-eukaryote symbioses: A systematic review and meta-analysis. *FEMS Microbiology Letters*, *366*(3). https://doi.org/10.1093/femsle/fnz013

Schweinsberg, M., Gösser, F., & Tollrian, R. (2021). The history, biological relevance, and potential applications for polyp bailout in corals. *Ecology and Evolution*, *11*(13), 8424–8440. https://doi.org/10.1002/ece3.7740

Sheets, E. A., Warner, P. A., & Palumbi, S. R. (2018). Accurate population genetic measurements require cryptic species identification in corals. *Coral Reefs*, *37*(2), 549–563. https://doi.org/10.1007/s00338-018-1679-9

Shinzato, C., Khalturin, K., Inoue, J., Zayasu, Y., Kanda, M., Kawamitsu, M., Yoshioka, Y., Yamashita, H., Suzuki, G., & Satoh, N. (2021). Eighteen Coral Genomes Reveal the Evolutionary Origin of *Acropora* Strategies to Accommodate Environmental Changes. *Molecular Biology and Evolution*, *38*(1), 16–30. https://doi.org/10.1093/molbev/msaa216

Slatkin, M. (1987). Gene Flow and the Geographic Structure of Natural Populations. *Science*, *236*(4803), 787–792. https://doi.org/10.1126/science.3576198

Tange, O. (2018). *Gnu Parallel 2018*. Zenodo. https://doi.org/10.5281/ZENODO.1146014

Thomas, L., Rose, N. H., Bay, R. A., López, E. H., Morikawa, M. K., Ruiz-Jones, L., & Palumbi, S. R. (2018). Mechanisms of Thermal Tolerance in Reef-Building Corals across a Fine-Grained Environmental Mosaic: Lessons from Ofu, American Samoa. *Frontiers in Marine Science*, *4*, 434. https://doi.org/10.3389/fmars.2017.00434

Thornhill, D. J., Lewis, A. M., Wham, D. C., & LaJeunesse, T. C. (2014). HOST-SPECIALIST LINEAGES DOMINATE THE ADAPTIVE RADIATION OF REEF CORAL ENDOSYMBIONTS: ADAPTIVE RADIATION OF SYMBIOTIC DINOFLAGELLATES. *Evolution*, *68*(2), 352–367. https://doi.org/10.1111/evo.12270

Torres, A. F., Valino, D. A. M., & Ravago-Gotanco, R. (2021). Zooxanthellae Diversity and Coral-Symbiont Associations in the Philippine Archipelago: Specificity and Adaptability Across Thermal Gradients. *Frontiers in Marine Science*, *8*, 731023. https://doi.org/10.3389/fmars.2021.731023

Troast, D., Suhling, F., Jinguji, H., Sahlén, G., & Ware, J. (2016). A Global Population Genetic Study of Pantala flavescens. *PLOS ONE*, *11*(3), e0148949. https://doi.org/10.1371/journal.pone.0148949

Turnham, K. E., Wham, D. C., Sampayo, E., & LaJeunesse, T. C. (2021). Mutualistic microalgae co-diversify with reef corals that acquire symbionts during egg development. *The ISME Journal*, *15*(11), 3271–3285. https://doi.org/10.1038/s41396-021-01007-8

Veron, J. (Charlie) E. N., DeVantier, L. M., Turak, E., Green, A. L., Kininmonth, S., Stafford-Smith, M., & Peterson, N. (2011). The Coral Triangle. In Z.

Dubinsky & N. Stambler (Eds.), *Coral Reefs: An Ecosystem in Transition* (pp. 47–55). Springer Netherlands. https://doi.org/10.1007/978-94-007-0114-4_5

Veron, J. E. N. (2000). *Corals of the world. 3* (1. publ). Australian Institute of Marine Science.

Willis, B. L., Babcock, R. C., Harrison, P. L., & Wallace, C. C. (1997). Experimental hybridization and breeding incompatibilities within the mating systems of mass spawning reef corals. *Coral Reefs*, *16*(0), S53–S65. https://doi.org/10.1007/s003380050242

Wu, T., Xu, A. N., Lei, Y., & Song, H. (2024). Ancient Hybridisation Fuelled Diversification in *Acropora* Corals. *Molecular Ecology*, e17615. https://doi.org/10.1111/mec.17615

Zayasu, Y., Takeuchi, T., Nagata, T., Kanai, M., Fujie, M., Kawamitsu, M., Chinen, W., Shinzato, C., & Satoh, N. (2021). Genome‐wide SNP genotyping reveals hidden population structure of an acroporid species at a subtropical coral island: Implications for coral restoration. *Aquatic Conservation: Marine and Freshwater Ecosystems*, *31*(9), 2429–2439. https://doi.org/10.1002/aqc.3626

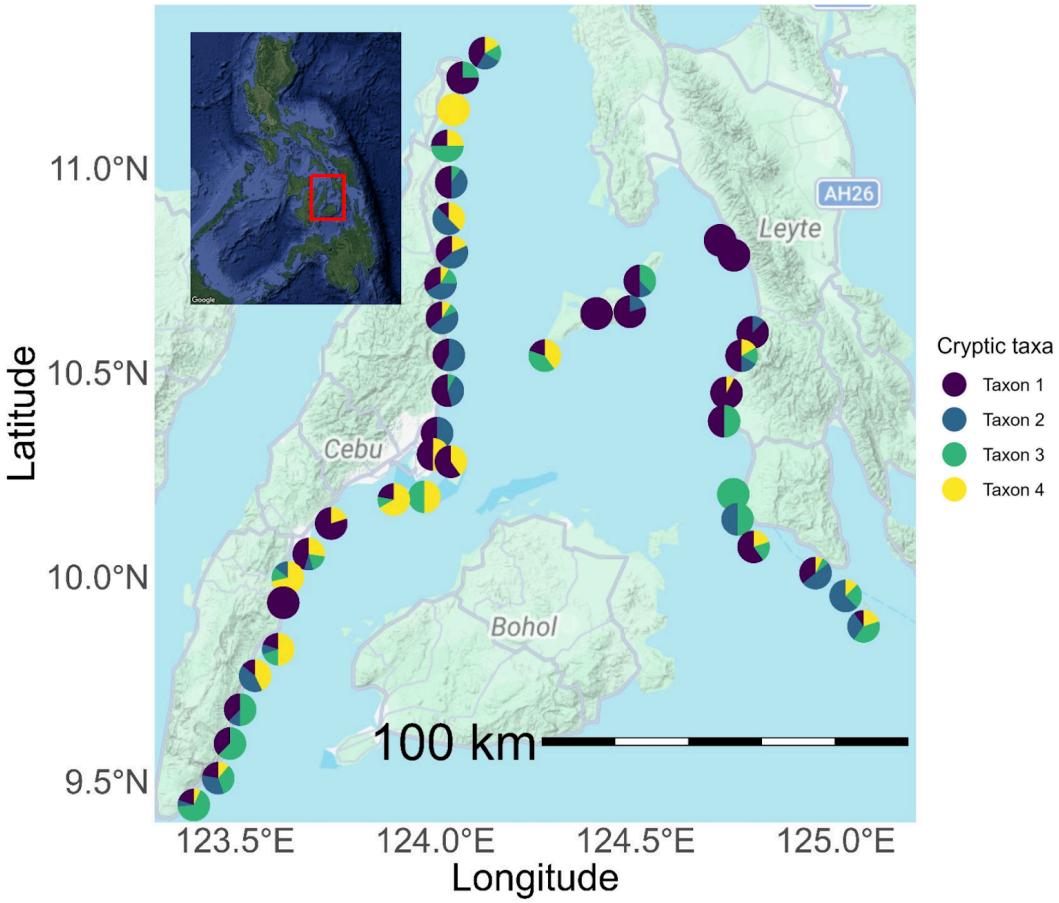

Fig. 2.1. Map of sampling sites in the central Philippines. The red rectangle in the inset map represents that area of the primary map. Each pie chart represents a separate sampling site. Pie charts show the percentage of *Acropora* samples collected at each site assigned to each cryptic taxon. Some sites with only one taxon present had only one or two total samples (see Table A2.1 for sample sizes). While taxa occurrence is weakly structured by latitude, all genetic groupings occurred at multiple sites on Cebu, Leyte, and the Camotes Islands.

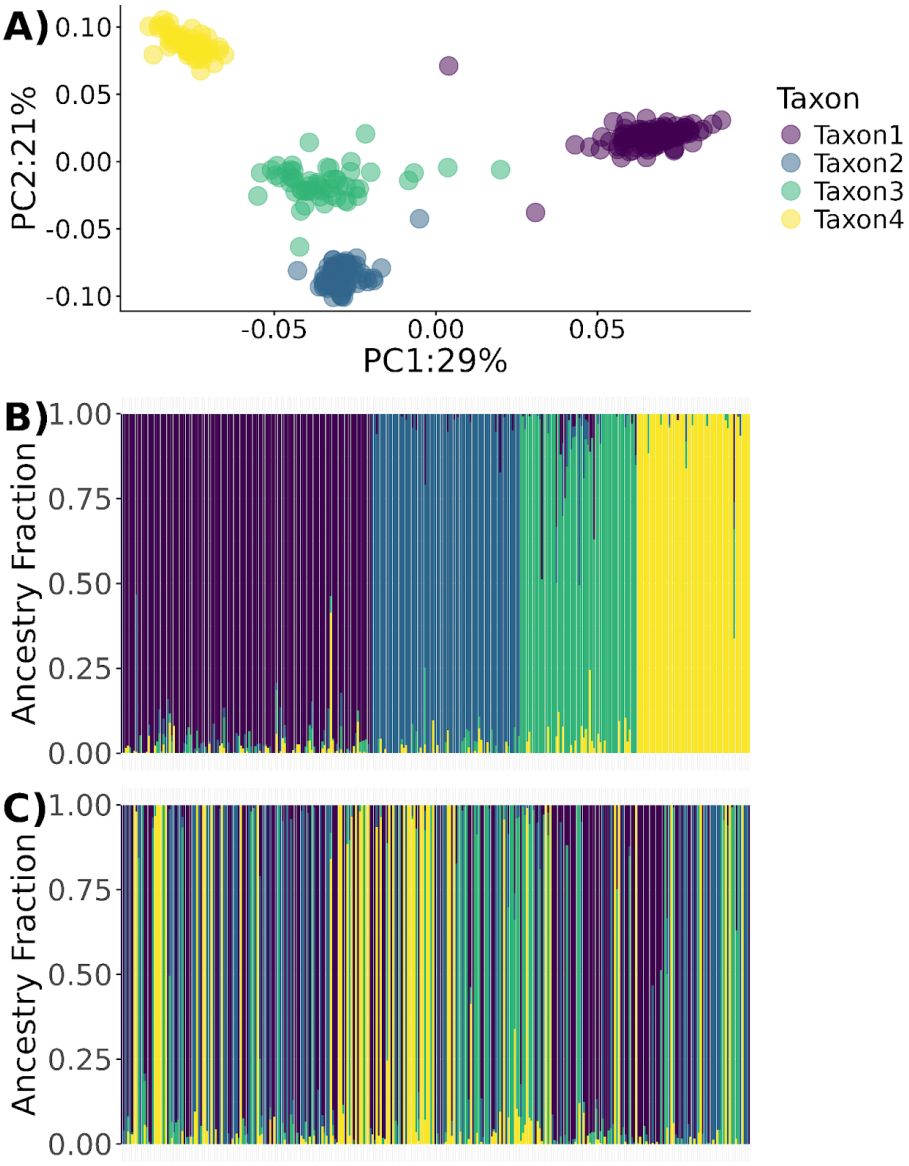

Fig. 2.2. *Acropora cf. tenuis* genetic samples belong to four distinct clusters. **A.** A Discriminant Analysis of Principal Components resolved four clusters, which we color and then plot on PCA axes one and two. PC1 accounted for 29% of the variation, and PC2 accounted for 21%. **B.** An ADMIXTURE analysis found four ancestry groups, and most individual samples had the majority of their ancestry derived from a single group. Individuals in this plot are grouped horizontally according to which ADMIXTURE group supplies the largest fraction of their ancestry. **C.** Sorting the ADMIXTURE plot by latitude shows intermixing of ancestry groups along a latitudinal gradient.

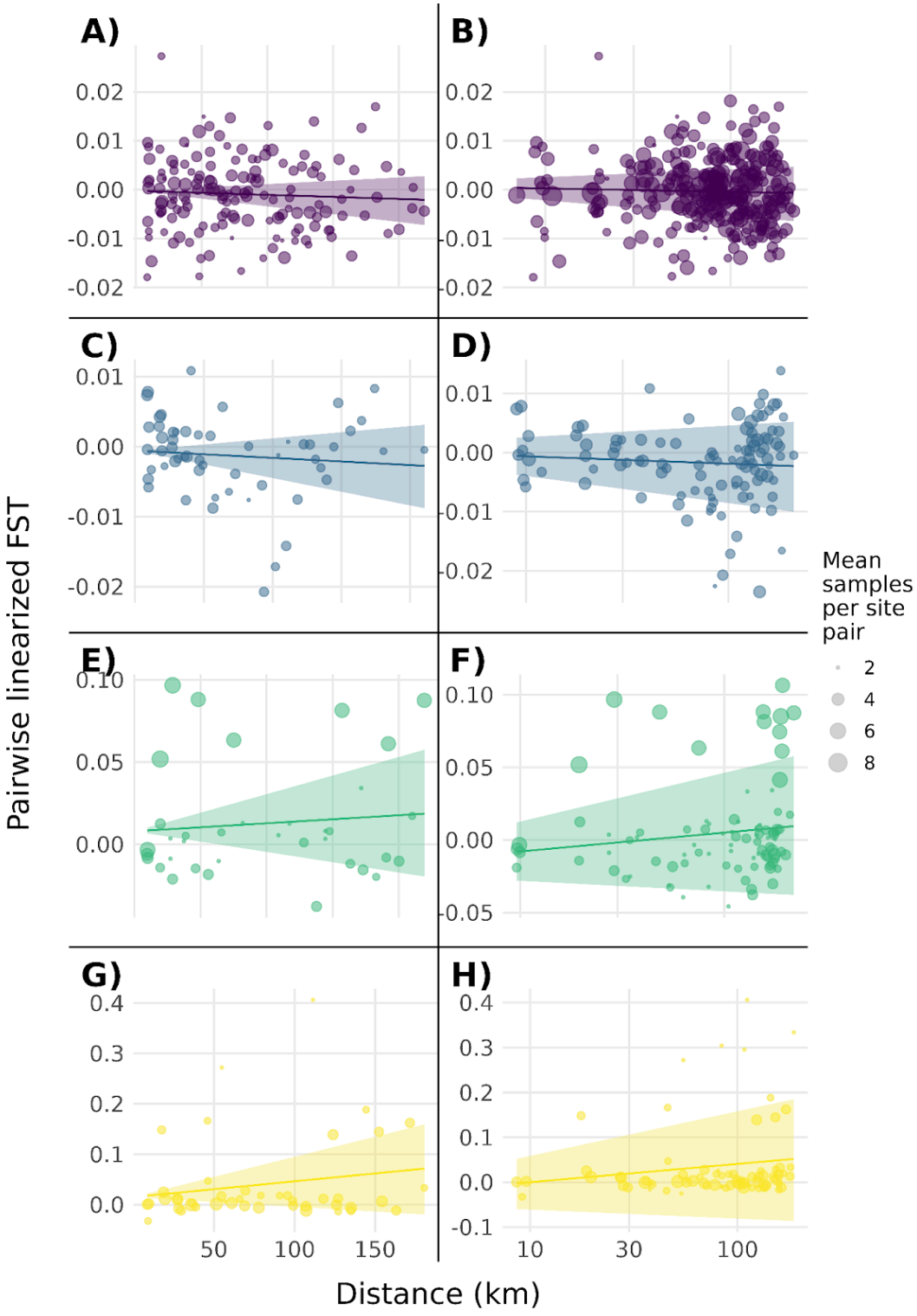
A)
B)
C)
D)
E)
F)
G)
H)
Pairwise linearized FST
Distance (km)
Mean samples per site pair
2
4
6
8

Fig. 2.3. No *Acropora cf. tenuis* taxon showed significant isolation by distance (IBD) patterns in either one or two dimensions. Each row shows one cryptic *Acropora* taxon (Taxon 1 - Taxon 4), plots on the left show one dimensional IBD comparisons using data from along the coast of Cebu only, and plots on the right show two dimensional IBD comparisons using data from all sites. Points correspond to pairwise comparisons of linearized FST and geographic distance (left panels) or log geographic distance (right panels) between sites. Shaded areas show the 95th percentile confidence intervals for the IBD slopes.

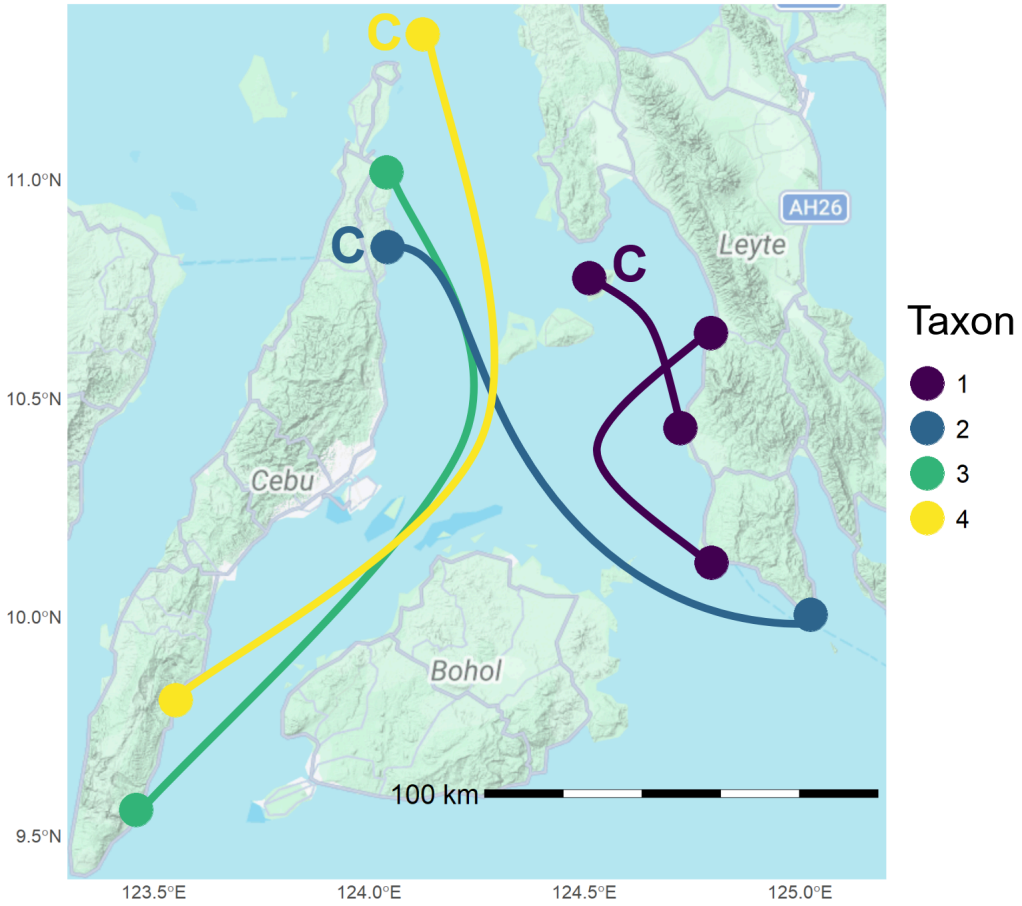

Fig. 2.4. Putative parent/offspring pairs found by Sequoia exist at widely spaced sites. Dots show sites with samples included in parent/offspring pairs,and curves show connections between sites. Closely related individuals that may constitute either first degree relatives or clonal genotypes are marked with a letter C.

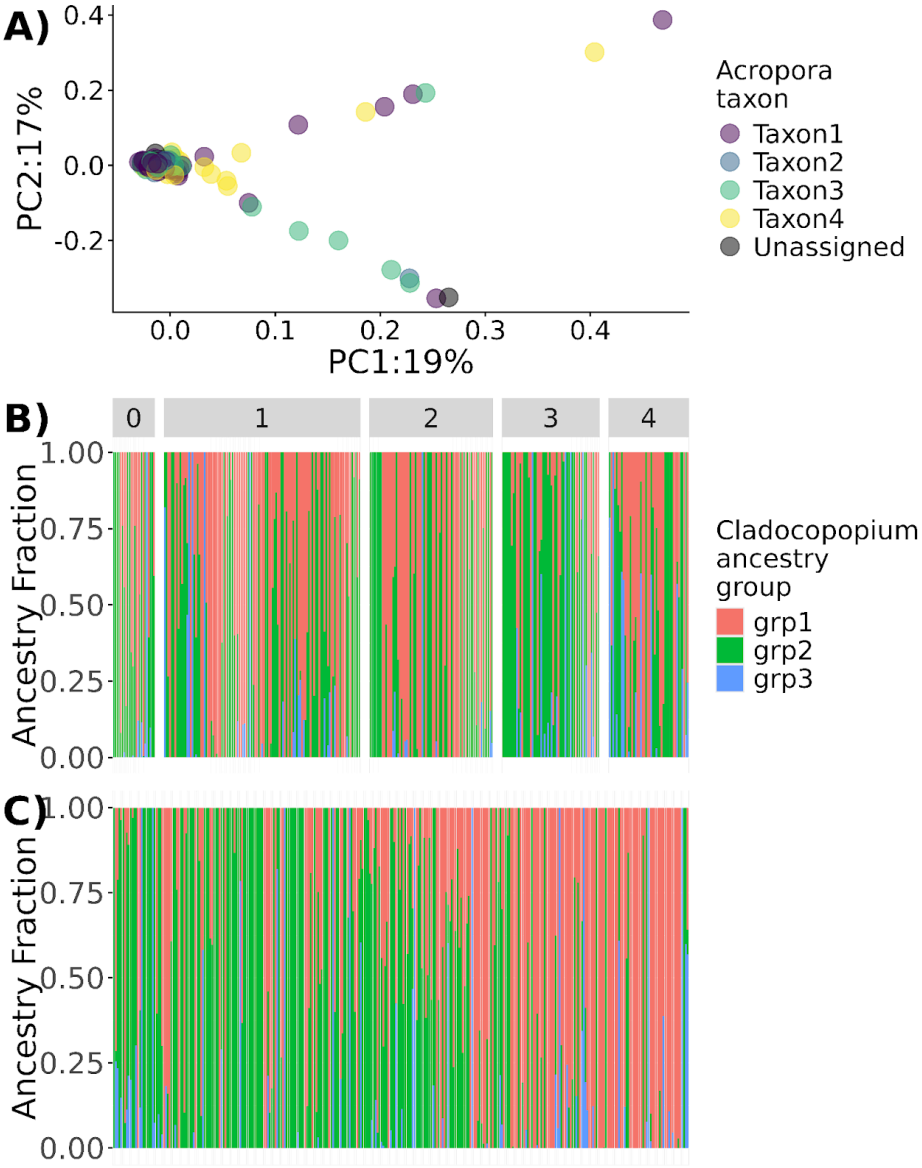

Fig. 2.5. *Cladocopium* genetic samples all belong to the same genetic cluster. **A.** A Discriminant Analysis of Principal Component analysis resolved only one cluster. We color *Cladocopium* samples by host *Acropora* cryptic taxon and then plot on PCA axes one and two. PC1 accounted for 19% of the variation, and PC2 accounted for 17%. **B.** An ADMIXTURE analysis found three ancestry groups, and many individuals had mixed ancestry from multiple groups. Individuals are organized by taxon of *Acropora* host, as shown by the numbered gray bars. Individuals labeled as '0' belong to hosts not assigned to a taxon due to insufficient reads of *Acropora* DNA. **C.** Sorting the ADMIXTURE plot by latitude revealed differences in *Cladocopium* ancestry with latitude.

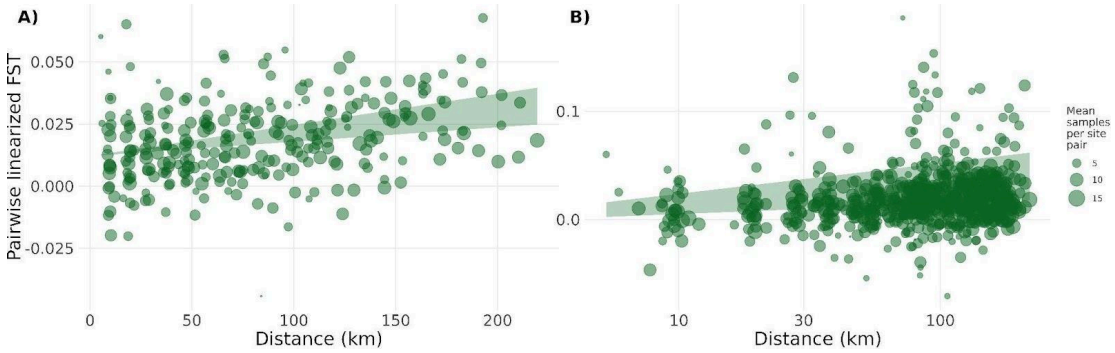

Fig. 2.6. Mantel tests reveal consistent positive relationships between genetic distance in pairwise linearized FST and geographic distance in both (A) one and (B) two dimensions for *Cladocopium*.

	Taxon 2	Taxon 3	Taxon 4
Taxon 1	FST=0.12 p=0.00	FST=0.11 p=0.00	FST=0.16 p=0.00
Taxon 2		FST=0.10 p=0.00	FST=0.15 p=0.00
Taxon 3			FST=0.12 p=0.00

Table 2.1. FSTs between cryptic taxa and associated p-values. All FSTs were higher than 100% of those on a null distribution calculated by reshuffling individuals between taxa.

	Taxon 2	Taxon 3	Taxon 4
Taxon 1	FST=0.00069 p=0.236	FST=0.0047 p=0.000	FST=0.00069 p=0.291
Taxon 2		FST=0.0034 p=0.026	FST=0.0040 p=0.013
Taxon 3			FST=0.0019 p=0.176

Table 2.2. FSTs between *Cladocopium* populations associated with different cryptic taxa of *Acropora* are extremely low, yet on average somewhat higher than would be expected by chance. The difference between those *Cladocopium* in Taxon 1 and those in Taxon 3 is particularly significant.

	Percent of resampled slopes >0, one dimension		Percent of resampled slopes >0, two dimensions	
	Acropora	*Cladocopium*	*Acropora*	*Cladocopium*
Taxon 1	0.235	0.760	0.279	0.822
Taxon 2	0.264	0.481	0.226	0.870
Taxon 3	0.718	0.908	0.899	0.765
Taxon 4	0.874 (0.050)	0.954	0.902 (0.684)	0.868

Table 2.3. A higher proportion of resampled slopes are positive in *Cladocopium* than in their *Acropora* hosts when accounting for sample size and geographic distribution. Rows correspond to individual corals assigned to each cryptic taxon. The left two columns show one dimensional analysis along the coast of Cebu for *Acropora* genotypes and their associated *Cladocopium*, and the right two columns show two dimensional analysis across all sites. For the final row, the values in parentheses show the proportion of positive slopes when excluding one of a pair of putative clones that occurred at the same site.

Appendix 2: Chapter 2 supplemental material

Site	Taxon 1 count	Taxon 2 count	Taxon 3 count	Taxon 4 count	*Cladocopium* count
CEB01	2	3	3	5	8
CEB02	2	0	1	0	1
CEB03	0	0	0	1	2
CEB04	1	0	4	1	9
CEB05	4	1	1	0	10
CEB06	5	1	0	5	11
CEB07	3	5	0	3	5
CEB08	4	5	2	6	9
CEB09	3	4	1	2	8
CEB10	7	2	0	0	5
CEB11	3	5	1	0	1
CEB12	4	1	0	0	7
CEB13	1	0	0	3	8
CEB14	4	0	0	2	2
CEB15	0	0	1	1	1
CEB16	4	0	2	3	10
CEB18	1	0	0	2	1
CEB19	1	2	2	2	1
CEB20	0	1	2	1	11
CEB21	1	0	0	0	0
CEB22	7	1	1	1	6
CEB23	3	1	0	1	4
CEB24	1	3	1	0	11
CEB25	4	0	4	0	6
CEB26	6	1	10	1	2
CEB27	3	1	1	1	8
CEB29	3	0	1	1	14

CEB30	0	0	0	0	3
CEB32	5	0	0	0	11
CEB33	1	7	0	0	7
CEB35	2	5	3	0	9
LEY01	1	0	0	0	11
LEY02	12	0	0	0	14
LEY04	2	3	0	0	16
LEY05	1	1	2	1	12
LEY06	1	0	0	1	12
LEY07	5	0	1	0	11
LEY09	0	0	2	0	8
LEY10	0	5	5	0	11
LEY11	1	0	1	1	4
LEY13	3	4	2	2	4
LEY14	0	4	1	4	4
LEY15	5	3	2	2	12

Table A2.1. Samples per site. Sites on each island are numbered from north to south. A full list of coordinates per site can be found at https://github.com/pinskylab/Atenuis_Philippines/tree/main/metadat in the 'all_Atenuis_sites.csv' file. Each row here corresponds to a site along the coast of Cebu ("CEB") or Leyte ("LEY"). Four columns show the number of *Acropora* samples assigned to each taxon at each site, and the final column shows the number of samples with usable *Cladocopium* genomes at each site.

Number of groups (K=)	BIC from DAPC clustering	ADMIXTURE cross-validation error
1	1573.9	0.38265
2	1553.9	0.34834
3	1542.8	0.33183
4	**1535.2**	**0.32198**
5	1535.3	0.32660
6	1539.2	0.32744
7	1543.5	0.33064
8	1546.8	0.33429
9	1550.9	0.33827
10	1554.9	0.34398
11	1558.8	0.34672
12	1562.6	0.35126
13	1566.5	0.35800
14	1570.7	0.36272
15	1574.6	0.36438
16	1578.9	0.36977

Table A2.2. Genetic clustering in *Acropora* with Discriminant Analysis of Principal Components and ADMIXTURE. The four genetic cluster solution minimizes the BIC for the DAPC, indicating the best model fit. Likewise, the lowest cross-validation error for the ADMIXTURE grouping occurs with four genetic ancestry groups.

Individual ID	Number of reads mapped to *Durusdinium*	% symbiont reads mapped to *Durusdinium*	*Acropora* taxon	Depth
CEB01_T14	**455033**	**92%**	**1**	**NA**
CEB04_T05	64	49%	NA	NA
CEB11_T08	28873	87%	NA	NA
CEB16_T04	260	59%	NA	NA
CEB18_T20	194	51%	NA	NA
CEB20_T08	**172902**	**82%**	**4**	**NA**
LEY02_T02	31833	58%	1	13 ft.

Table A2.3. Individual samples with the highest number of symbiont reads mapping to *Durusdinium*, rather than *Cladocopium* or *Symbiodium*. For three individuals, the total number of reads mapped was negligible (<1000), indicating poor sequencing, and two more individuals showed slightly higher but still low (<50,000) numbers of mapped reads. Two samples (CEB01_T14 and CEB20_T08) presented a high (>150,000) number of reads, with a substantial majority (>80%) mapping to *D. trenchii* rather than other symbiont genomes (bold). The *Acropora* taxon column shows the taxonomic group to which the host was assigned. Four of the hosts lacked sufficient SNPs to be confidently assigned to any taxon. The depth column shows the collection depth for the host coral in feet.

Individual ID	Number of reads mapped to *Symbiodinium*	% symbiont reads mapped to *Symbiodinium*	*Acropora* taxon	Depth
CEB11_T11	22467	64%	1	NA

Table A2.4. Individual samples with the highest number of symbiont reads mapping to *Symbiodium*, rather than *Cladocopium* or *Durusdinium*. One individual coral sample had a majority of symbiont reads mapping to the *S. kawagutii* genome.

Number of groups (K=)	BIC from DFA clustering	ADMIXTURE cross-validation error
1	**1520.3**	0.45678
2	1520.7	0.45692
3	1521.7	**0.45349**
4	1524.3	0.45647
5	1527.0	0.45629
6	1530.0	0.46088
7	1533.5	0.46570
8	1537.0	0.46804
9	1540.5	0.46868
10	1544.4	0.47380
11	1548.1	0.47189
12	1552.0	0.47404
13	1556.0	0.47852
14	1560.0	0.48440
15	1563.8	0.48839
16	1567.8	0.48202

Table A2.5. Genetic clustering in *Cladocopium* with Discriminant Analysis of Principal Components and ADMIXTURE. A single genetic cluster minimizes the BIC for the DAPC, indicating the best model fit. The lowest cross-validation error for the ADMIXTURE grouping occurs with three genetic ancestry groups.

Taxon	Slope	Standard error	Mantel test p-value
Acropora Taxon 1	-8.4×10^{-9}	1.2×10^{-8}	0.683
Acropora Taxon 2	-2.2×10^{-8}	1.5×10^{-8}	0.681
Acropora Taxon 3	4.9×10^{-8}	8.5×10^{-8}	0.273
Acropora Taxon 4	3.1×10^{-7}	2.6×10^{-7}	0.160
Cladocopium	9.2e-08	1.8×10^{-8}	0.001**

Table A2.6. One dimensional IBD slopes and Mantel tests along the coast of Cebu. P-values marked with ** are highly significant ($p<0.01$).

Taxon	Slope	Standard error	Mantel test p-value
Acropora Taxon 1	-0.00031	0.00053	0.679
Acropora Taxon 2	-0.00054	0.00074	0.710
Acropora Taxon 3	0.0056	0.0043	0.064*
Acropora Taxon 4	0.017	0.014	0.174
Cladocopium	0.0055	0.0014	0.004**

Table A2.7. Two dimensional IBD slopes and Mantel tests from across the entire study area, including Cebu, Leyte, and the Camotes islands. P-values marked with * are marginally significant ($p<0.1$) and p-values marked with ** are highly significant ($p<0.01$).

Individual 1	Individual 2	Taxon	Opposite homozygotes	SNPs in both	LLR	Geographic distance
LEY07_T02	**CEB35_T08**	**1**	**0**	**1245**	**16.12**	**58 km**
LEY11_T15	LEY04_T15	1	0	2284	13.88	45 km
LEY14_T09	**CEB07_T14**	**2**	**1**	**1649**	**26.00**	**142 km**
CEB26_T22	CEB05_T12	3	0	1200	14.94	174 km
CEB01_T12	**CEB23_T16**	**4**	**0**	**1075**	**5.46**	**181 km**
CEB01_T11	**CEB23_T16**	**4**	**0**	**1074**	**4.99**	**181 km**
CEB01_T11	**CEB01_T12**	**4**	**0**	**1159**	**4.79**	**0 km**

Table A2.8. Putative parent offspring pairs.

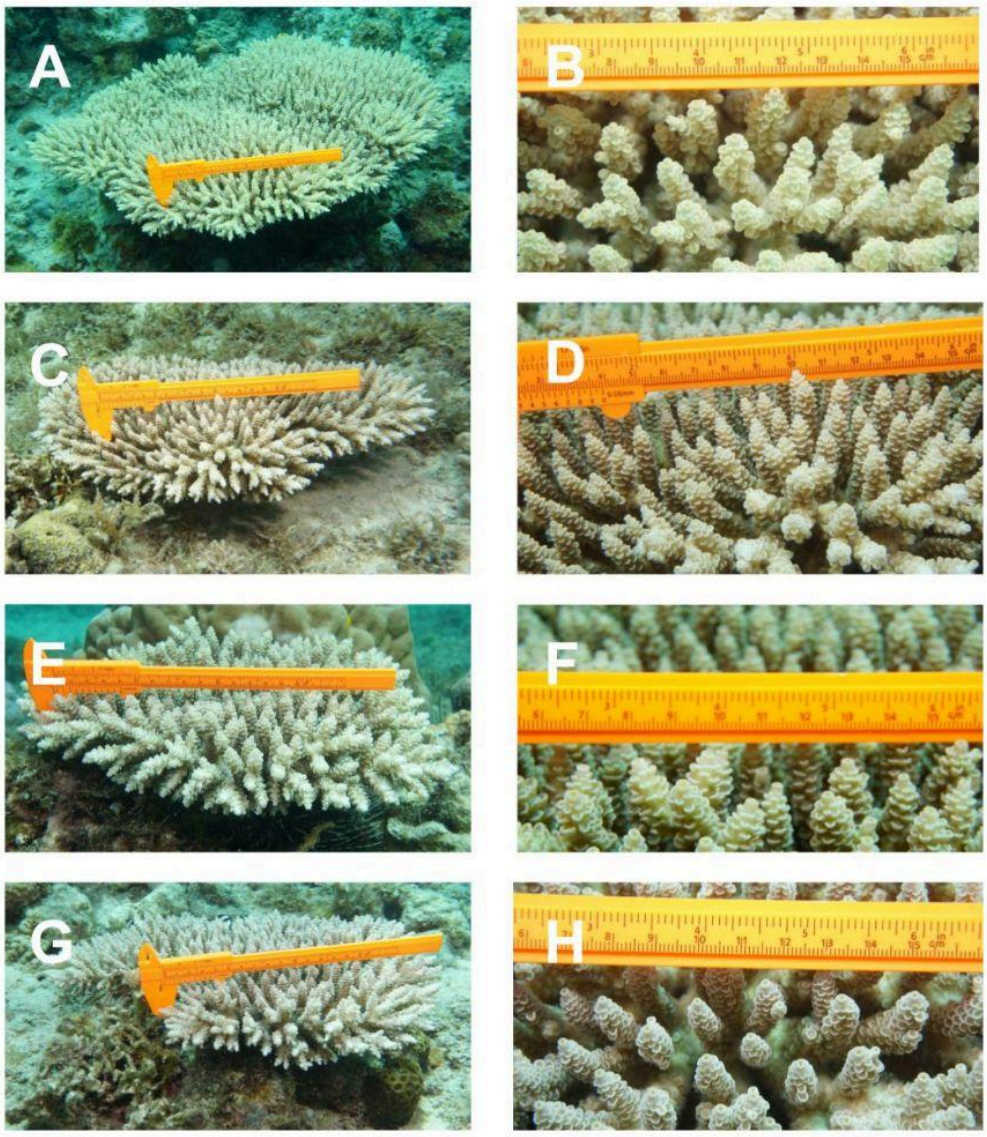

Fig. A2.1. Cryptic taxa in *Acropora cf. tenuis* are morphologically similar. Each row shows one representative sample from one cryptic taxon. The top row (**A** and **B**) shows Taxon 1, the second row shows Taxon 2, the third row shows Taxon 3, and the fourth row shows Taxon 4. The left column (**A**, **C**, **E, G)** shows overall growth form and the right column (**B**, **D**, **F**, **H**) shows close ups of corallite structure.

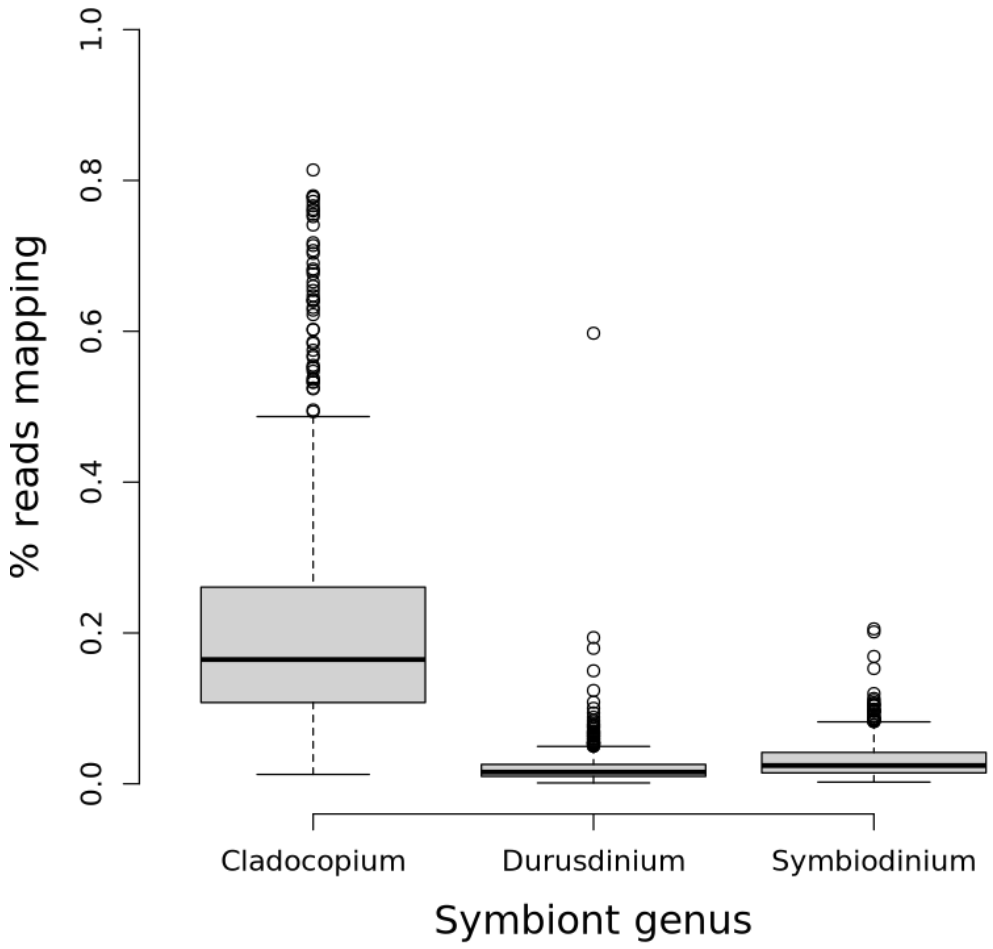

Fig. A2.2. Across samples, more reads mapped to the genome from the *Cladocopium* genus than genomes from the genera *Durusdinium* or *Symbiodinium*. A median of 14,424.5 reads, or 15% of the total, successfully mapped to the *Cladocopium goreaui* genome, 2771 reads (2.4% of total) mapped to the *Symbiodinium kawagutii* genome, and 1447 reads (1.5% of total) mapped to the *Durusdinium trenchii* genome.

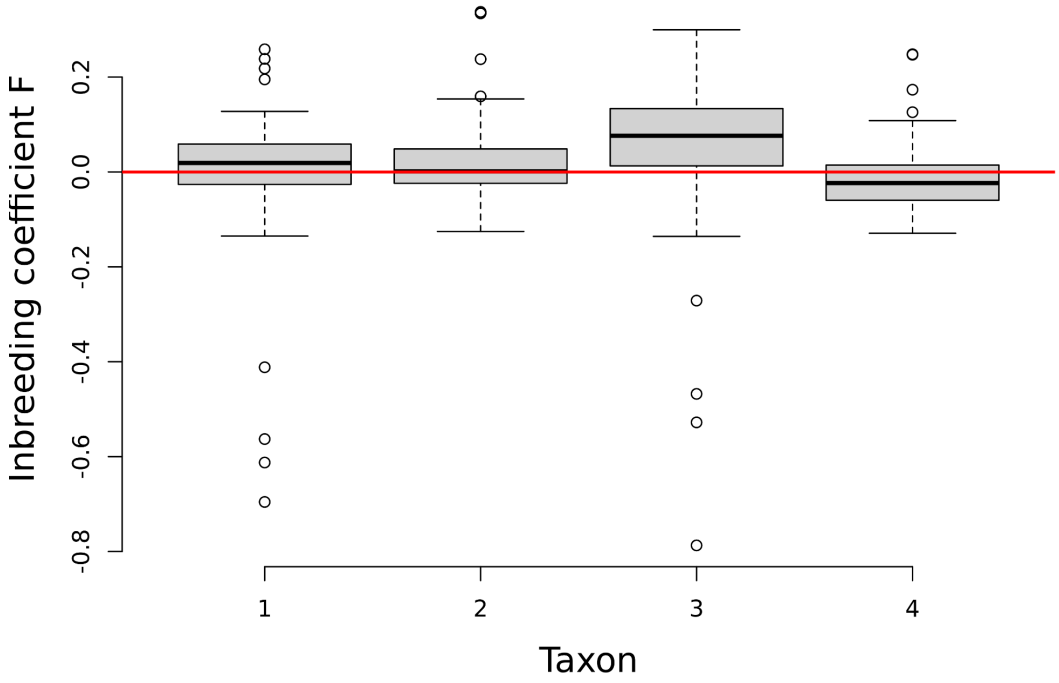

Fig. A2.3. Cryptic taxa in *Acropora* show different mean inbreeding coefficients (Kruskall-Wallis test $p=3.1 \times 10^{-6}$, n=295). The horizontal red line shows zero inbreeding (expected heterozygosity).

Chapter 3

Shared genetic variation genetic across ocean basins around a heat tolerance locus in *Acropora*

Bos, J.T.[1], Silva, I.M.[2], Pinsky, M.L.[1]

1. Department of Ecology & Evolutionary Biology, University of California Santa Cruz, 130 McAllister Way, Santa Cruz, California 95060, U.S.A.
2. Faculdade de Ciências Naturais, Lúrio University, Bairro Eduardo Mondlane, 3200, Pemba, Cabo Delgado, Mozambique.

Abstract

Corals face profound threats from climate change. However, genetic variation in heat tolerance means that some coral lineages are more vulnerable than others. This genetic variation can be unique to a coral species, or shared across lineages, and occurs at multiple spatial scales. Here, we conducted whole genome sequencing of a branching coral species, *Acropora aff. divaricata*, across multiple spatial scales in coastal Mozambique. We found that our samples represent two closely related species, one of which was only found in a hot microclimate inside a bay, and the other of which included genetically differentiated north and south populations. These species and populations differed most strongly at the 'HES-1 locus,' an area on chromosome 7 previously described in studies of *Acropora aff. hyacinthus* in American Samoa. The locus appears to have undergone positive selection in a species and population that occur in more heat-exposed areas . Strikingly, the species of *Acropora aff. divaricata* and *Acropora aff. hyacinthus* found in hot microclimates exhibited strong similarity at the HES-locus, indicating unexpected shared ancestry across species in this genomic region. Our results suggest that either incomplete lineage sorting or introgression from a third species have resulted in shared alleles related to heat tolerance in two widely geographically separated coral species, providing evidence for shared genetic variation as a novel source of climate adapted alleles.

3.1. Introduction

The history of life on earth is a history of constant evolution to novel environmental conditions. Multiple sources of genetic variation can enable populations to adapt to new environments, including *de novo* mutations, selection on standing genetic variation, and even hybridization between species (Stern, 2013). In the era of anthropogenic change, increasingly urgent research focuses on what genetic resources vulnerable species may be able to leverage to adapt to their swiftly changing world (Bitter et al., 2019; Hamilton & Miller, 2016).

Nowhere are questions of rapid adaptation more salient than in corals. Reef-building corals face growing threats from climate change, and populations will need to evolve in order survive the twenty-first century (Lachs, Bozec, et al., 2024). This is particularly true for corals of the branching genus *Acropora*, which provide critical habitat for fish but tend to be sensitive to heat-wave induced bleaching (Bonin, 2012; McClanahan et al., 2007). Despite the grim overall outlook, however, coral populations vary substantially in their ability to tolerate present and future climate change, thanks in part to differences in their available genetic resources (Adam et al., 2022; Kleypas et al., 2016).

Experimental and *in situ* bleaching studies reveal that heat tolerance in *Acropora* is a highly polygenic trait, with multiple genes significantly affecting bleaching thresholds and related mortality (Fifer et al., 2026; Fuller et al., 2020; Rose et al., 2018). Moreover, several genomic areas show consistent associations with hot

environments across multiple species of *Acropora.* A recent study of five different *Acropora* species, each sampled across at least five sites and 100 kilometers, identified 85 genomic regions associated with environmental heat stress in at least three different *Acropora* species. Moreover, a model using this data to predict frequency of heat-adapted *Acropora* genotypes across reefs significantly predicted *Acropora* decline measured from reef surveys (Selmoni et al., 2025).

The distribution of adaptive alleles varies across seascapes at multiple spatial scales. At broad spatial scales (100s of kms), bleaching risk depends strongly on baseline temperatures, and the absolute bleaching temperature of corals can differ by multiple degrees Celsius between regions (Riegl et al., 2012; Whitaker & DeCarlo, 2024). Moreover, temperature also varies within regions and within reefs, and coral populations from different areas of the same reef can exhibit differences in thermal tolerance of well over 1° C (Brown et al., 2024). In some cases, genetic differences in heat tolerance have been found in populations of *Acropora* from microhabitats separated by less than a kilometer (Thomas et al., 2018), including between cryptic species of *A. hyacinthus* on American Samoa (Rose et al., 2021).

The existence and extent of genetic adaptation to heat at fine spatial scales differs across species, even at the same sampling sites, and different species of *Acropora* can vary significantly in their heat tolerance across habitats (Lachs, Humanes, et al., 2024; Muir et al., 2017; Sakai et al., 2019). However, research on species-specific heat tolerance is complicated by the fact that *Acropora* are difficult to identify morphologically, and traditionally defined “common” species may constitute

multiple species with distinct evolutionary histories and environmental tolerances (Bridge et al., 2024; Grupstra et al., 2024). Even with adequate genetic data, species boundaries in *Acropora* may be porous, with substantial interspecific gene flow (Ladner & Palumbi, 2012; Van Oppen et al., 2002). Deep time introgression shaped the evolution of *Acropora* species, and may have contributed alleles that allowed specific lineages to adapt to novel habitats (Mao et al., 2018). However, the prevalence of hybridization in modern *Acropora* species remains a matter of debate, and may be lower than previously believed (Ramírez-Portilla et al., 2022; Rassmussen et al., 2025). The relatively recent diversification of *Acropora* in the Plio-Pleistocene may also contribute to allele sharing across species due to incomplete lineage sorting (Ramírez-Portilla et al., 2022; Wu et al., 2024).

Northern Mozambique constitutes a regional hotspot of coral biodiversity, including at least 32 species from the genus *Acropora* (McFadden et al., 2025; D. Obura, 2012; Sola et al., 2015). However, the true number of species may be even higher: recent genetic study in soft corals, a sister taxon, revealed that many individuals collected in Mozambique belong to previously undocumented species (Nassongole et al., 2026). Coral reefs in coastal Mozambique are mostly well-connected, but even *Acropora* species with long pelagic larval duration exhibit genetic structure along the length of the coast (Duvane et al., 2025). The country's reefs exhibit climate variation at multiple spatial scales, and are vulnerable to bleaching events provoked by heat waves (Schleyer et al., 1999; Silva et al., 2024).

Using two Mozambican reefs as a study system, we focus on a generalist species, *Acropora aff. divaricata*. Recent work in Taiwan and Japan suggests that this taxon includes multiple species, some of which overlap phylogenetically with lineages of *A. cf. solitaryensis* (Chow et al., 2025). Similarly, while *A. divaricata* is traditionally considered to exist in the Western Indian Ocean, individuals identified as *A. divaricata* in the Western Indian Ocean are morphologically distinct from *A. divaricata* in the Pacific and likely represent an undescribed species of *Acropora* (Veron, 2000; Tom Bridge, personal communication, October 2025).

In Mozambique, *A. aff. divaricata* is a commonly observed and apparently generalist taxon that can be found in a variety of microhabitats across multiple provinces. However, it has also been observed to bleach under heat stress. Consequently, *A. aff. divaricata* constitutes an ideal study system in which to examine genetic variation with environmental stress across multiple spatial scales. Here, we sample *A. aff. divaricata* at nested sampling sites in northern Mozambique to test for evolutionary adaptation to heat stress at both fine (<10 km) and broad (>100 km) spatial scales. Specifically, we ask 1) at what scale or scales is genetic variation associated with temperature differences, and 2) what is the evolutionary history of temperature-associated genetic variation?

Methods

3.2.1 Field sampling and genetic sequencing

Samples were collected in June of 2023 and from May to July of 2024. We collected samples at two broad-scale sites, in Pemba Bay in Cabo Delgado province and around Caldeira Island in Nampula province, and several smaller sampling areas within each of those sites (Fig. 3.1). The reefs in Caldeira are considerably cooler than those in Pemba, due to their position further from the equator and the presence of cool upwelling (Malauene et al., 2014; Sete et al., 2002). In Pemba, sampling areas were chosen based on areas of known coral cover in order to represent distinct microhabitats inside the bay, outside the bay to the north, and off the southern peninsula (Fig. 3.1B). On Caldeira, the two sampling areas represented reef crest and inshore habitat (Fig. 3.1C). At each sampling point, including two points inside Pemba Bay, we placed a HOBO Pro V2 temperature logger inside a PVC casing to provide shade and avoid biasing temperature readings (Rich et al., 2024). Six loggers were placed in 2023: four in Pemba, and two in Caldeira, and temperatures were recorded every 10 minutes. Three of the Pemba loggers and one of the Caldeira loggers were successfully recovered in 2024.

Within each sampling area, dive descent points were chosen haphazardly. Individuals of *Acropora aff. divaricata* were sampled in six meter by fifty meter belt transects. All sampled corals were separated by at least three meters from the nearest sampled coral to avoid sampling clones. At the end of the transect, we extended another transect in the direction of maximum coral cover at an angle of up to 90 degrees from the original transect. We photographed each sampled coral with an Olympus TG-7 underwater camera prior to sampling. Samples of *A. aff. divaricata*

were collected with steel clippers and kept in seawater until returning to shore, at which point they were immediately transferred to 96% ethanol and stored at -20°C, except for approximately six weeks of thawing during transport. For each sampled coral, we recorded depth, bleaching status, and both overall and closeup photos.

DNA extraction was conducted at the University of California, Santa Cruz using Qiagen Blood & Tissue 96 Well Plate kits, following the included protocol with small modifications as follows. Each coral fragment was removed from ethanol and patted dry with a Kimwipe. The entire skeletal fragment was then included intact in the incubation and cellular lysis phase of the extraction protocol. Sequence fragmentation and adapter ligation were performed using a transposase-based method using an Illumina Nextera library prep kit and an automatic workflow using a liquid handling robot (Illumina, Inc., 2018).

Paired end sequencing was conducted across three Illumina NovaSeq X+ 25B lanes, for a total of 16 billion reads. Library preparation and sequencing were conducted at the University of California Davis Genomics Core Lab.

3.2.2 Sequence processing, alignment, and filtering

We trimmed reads and conducted quality control with FastP version 0.23.4 and MultiQC, de-duplicated reads and compressed files using the Clumpify function from BBtools version 39.06, re-ran FastP for 5' read trimming, and re-paired unpaired reads with BBtools (Bushnell, 2014; Chen et al., 2018; Ewels et al., 2016). See https://github.com/jaelynbos/Mozambique_Acropora/ for scripts with

parameters. We used the BWA-mem function of BWA version 0.7.17 (Li & Durbin, 2009) to map reads to congener *Acropora millepora*, from NCBI, accession number GCF_013753865.1 (Fuller et al., 2020). After alignment, a mean of 92% of reads, with a standard deviation of 10%, successfully mapped to the reference genome across individual samples, for a median depth of 15.7x per individual ± 10.6x.

We sorted and indexed BAMfiles with SAMtools version 1.20 and called genotype likelihoods using the SAMtools method in ANGSD version 0.940 to produce Beagle files (Korneliussen et al., 2014; H. Li et al., 2009; H. Li, 2011). We retained only SNPs with a minimum map quality of 25, minimum quality score of 30, p-value of 10^{-6}, minimum depth corresponding to five times the number of individuals, maximum depth corresponding to 150 times the number of individuals, minimum individuals corresponding to 90% of the total sample size, and minimum minor allele frequency of 0.1, assigning major and minor alleles from observed base counts in the samples (Y. Li et al., 2010). We used NGSLD version 1.20 and PruneGraph version 0.4.0 to prune for linkage disequilibrium by removing SNPs with r^2 values of greater than 0.5 within 10 kb windows (Fox et al., 2019). After pruning, we were left with 8,547,065 SNPs for downstream analysis, with an average sequencing depth of 24x.

3.2.3 Identification of putative species and genome-wide patterns of diversity

We detected potential clones by calculating KING kinship coefficients using NGSrelate version 2.0 (Korneliussen & Moltke, 2015). Pairs of individuals with

KING coefficients greater than 0.354 were classified as clones (McMaster et al., 2025). Two pairs of individuals were classified as clones, and all clonal individuals occurred off the south peninsula of Pemba Bay. One pair was separated by 876 meters, and the other pair was separated by less than 50 meters. One member of each pair was removed from subsequent analysis.

We then evaluated genetic clusters and ADMIXTURE proportions on the unlinked SNPs using PCAngsd version 1.36.1 (Meisner & Albrechtsen, 2018). We assigned each individual to the ADMIXTURE ancestry group that contributed the largest fraction of its ancestry. We checked for evidence of cryptic speciation within our dataset by looking for significant sympatric variation not associated with geography, as well ADMIXTURE groups without evidence of hybridization. We named two non-hybridizing lineages as DA and DB. We calculated site allele frequencies for each ADMIXTURE group separately using the -doSAF function in ANGSD version 0.940 using the SNP list created in Section 2.2 (Nielsen et al., 2012). These allele frequencies were used to calculate FSTs between each population, as defined by dominant ancestry group, and species in ANGSD . We also calculated between-species and -population FSTs in 50 kb sliding windows with a 10 kb step along the genome.

We looked for evidence of selective sweeps around loci of interest using measures of genetic diversity and linkage disequilibrium in sliding windows. First, we calculated site allele frequencies and site frequency spectra in ANGSD after filtering SNPs by depth, map quality, and quality score, but not by p-value, in order to

include invariant sites. These latter SFSs were used as inputs for the saf2theta function in ANGSD. We subsequently calculated pi, Watterson's theta, and Tajima's D in 5 kb sliding windows along the genome using the thetaStat do_stat function in ANGSD (Korneliussen et al., 2013). We created an empirical cumulative distribution function for each of these statistics and calculated the percentile of each statistic for diverged loci of interest. We identified protein coding and regulatory areas using the annotation associated with the *A. millepora* genome from NCBI (Fuller et al., 2020).

We calculated the linkage percentile for loci of interest by using NGSLD to calculate linkage disequilibrium for all SNPs in each species across the entire genome in windows of up to 10kb. We then calculated average linkage at 5 kb in windows and used those to create a distribution of genome-wide linkage values. We then compared the mean 5 kb linkage around loci of interest to the distribution of genome-wide linkage values.

3.2.4 Comparison with *Acropora hyacinthus* species complex

We downloaded reads from the *Acropora aff. hyacinthus* species complex sequenced by Rose *et al.* (2021). The tabular corals defined in Rose *et al.* (2021) as *A. hyacinthus* species HC, HD, and HE have since been proposed as the species *A. tersa, A. bifurcata*, and *A. turbinata*, with *A. hyacinthus* HB remaining unnamed (Rassmussen et al., 2025). The names have yet to be accepted, and we here retain the original nomenclature from Rose *et al.* 2021 for the sake of clarity. HE is believed to occur in higher temperature areas, and demonstrate correspondingly elevated

bleaching resistance, compared to the other tabular corals in the study (Rose et al., 2021).

We ran these reads through the same alignment pipeline and aligned them to the same *A. millepora* genome as described in Section 2.2 . We used ANGSD to call genotype likelihoods, retaining SNPs with the same mapping quality, minor allele frequencies, and p-values as in Section 2.2. We retained SNPs with a minimum depth corresponding to two times the number of individuals, maximum depth corresponding to 120 times the number of individuals, and minimum individuals corresponding to 80% of the total sample size (Y. Li et al., 2010). The minimum and maximum depth cutoffs are lower than those used for the Mozambique samples alone, reflecting the lower sequencing depth of the *Acropora hyacinthus* samples. After pruning SNPs for linkage disequilibrium using the same procedure described in Section 2.2, we were left with 8,935,271 unlinked SNPs for further analysis.

We used PCAngsd to examine the set of *Acropora* genomes for genetic clustering and ancestry groupings. We examined the entire genome as well as individual areas of interest selecting by chromosome and position. To understand the background level of variation in clustering for single genes (rather than the whole genome), we also examined the first identified gene on each chromosome.

We created consensus FASTA files for each *Acropora hyacinthus* species, each population and species from Mozambique, using ANGSD -doFasta using the most common base at each position and filtering reads for map quality of 25 and quality score of 30. To create an outgroup for rooting trees, we downloaded reads

from *Isopora aff. cuneata* from NCBI (Wellcome Sanger Institute, 2026) ran it through the pipeline to align to the same *Acropora millepora* genome as the other samples, and created a consensus FASTA using the same procedure as above. We extracted genomic areas of interest from the consensus FASTA files by position using SAMtools faidx and aligned them with MAFFT version 7.526 (Katoh & Standley, 2013). We constructed phylogenetic trees using ape (Analysis of Phylogenetics and Evolution) package version 5.8 in R using the "balanced minimum evolution" method (Desper & Gascuel, 2002; Paradis & Schliep, 2019). For each tree, we created 1000 bootstrap replicates using the boot.phylo() function in APE, and counted the number of replicates containing each clade of the original tree using the prop.clades() function (Efron *et al* 1996).

We conducted two ABBA-BABA tests for introgression using -abbababa2 in ANGSD (Green et al., 2010; Korneliussen et al., 2014). For our outgroup, we used the same *Isopora aff. cuneata* consensus FASTA used in the previous section. We tested for introgression between *A. hyacinthus HE* and *A. aff. divaricata DB* using two different ABBA-BABA tests. The first run included DA, DB, HE, and the *Isopora* outgroup, to compare whether HE shares more derived alleles with DB than it does with DA. The second run included HD, HE, DB, and the *Isopora* outgroup, to compare whether DB shares more derived alleles with HE than it does with HD. We chose to include HD as the second lineage from American Samoa because it included the most samples out of the non-HE species. The ABBA-BABA tests allowed us to

evaluate whether DB showed signs of introgression with HE using both the *A. aff. divaricata* sister species and a *A. aff. hyacinthus* species for comparison.

3.2.5 Genetic associations with bleaching

Since our 2024 samples from the Pemba Bay area were collected during a mass bleaching event and several sampled corals showed signs of bleaching, we checked for association of specific genotypes with bleaching. We assessed bleaching and mortality based on field photos. Corals with any bleached areas or notable pallor were classified as showing signs of bleaching, whereas corals with partially dead areas, as evidenced by algal overgrowth, were defined as showing signs of mortality. All corals showing signs of mortality also showed signs of bleaching. We used a binary GLM in R to explain bleaching between our 2024 samples from Pemba Bay (n= 136). The dependent variable was "bleaching status" which was coded as either a zero (no bleaching) or one (some bleaching). We used a binary response variable rather than percent bleached because corals were photographed at different times during the bleaching event, meaning that some were still in the process of bleaching and some had begun to recover. Since we began sampling at the end of the bleaching season, after peak temperatures had already passed, we assume no corals began bleaching after they were sampled. We tested models using independent variables of latitude, depth, and *Acropora* species, as well as all full factorial combinations of those variables. We chose the best model by minimizing AIC.

We conducted three genome wide association tests using the ANGSD -doAssoc function, despite the fact that our sample size was well below the "thousands" of samples recommended (S. Y. Kim et al., 2011). Similarly to the binary GLM test, we used a dependent variable of "bleaching status". The first association test involved only samples from DA on the south peninsula. The second and third tests included individuals from the interior of the bay: test two included only individuals assigned to DB, and test three included individuals assigned to both DA and DB. Depth of sampled coral on the reef was included as a covariate. We adjusted the p-values for multiple comparisons using the p.adjust() function in R with the Benjamini and Hochberg method (Benjamini & Hochberg, 1995). All R analyses were performed in R version 4.3.3 (R Core Team, 2025).

Results

3.1 Spatial genetic structure within *Acropora aff. divaricata*

A MAP test in PCAngsd detected two significant PCs and revealed three corresponding genetic clusters (RMSE=8.9 x 10^{-6}) (Fig. 3.2). The first PC of the PCA accounted for 3.1% of the total variation and clearly divided 73 of the samples from the remaining 161, with no intermediate individuals (Fig.3. 2A). These 73 samples were all collected inside Pemba Bay. This corresponds to the sampling area with the hottest mean temperatures (Table A3.1, Fig A3.1) and is marked with a rectangle in Figure 3.1. The remaining 161 samples were spread across all locations, including

inside the bay. The second PC structured these remaining 161 samples and was strongly correlated with latitude (Pearson's correlation r=0.74).

ADMIXTURE analysis with PCAngsd showed three ancestry groups (Fig. 3.2B). The first group corresponded to the 73 individuals inside the bay and included little admixture with other groups. Individuals assigned to this group had a median of 96% of their ancestry, and a minimum of 88% of their ancestry, derived from this single group. Individuals from the other two groups exhibited substantially more ancestral mixing. The "north" ancestry group derived a median of 20% and maximum of 45% of their ancestry from the "south" group, and the "south" group derived a median of 6% and maximum of 38% of their ancestry from the north group.

Several lines of evidence point to the existence of two species. The first PC of our PCAngsd analysis described sympatric variation, a pattern that can indicate multi-species datasets (Riginos et al., 2024). We saw clear separation of two groups on this first PC, with no intermediate individuals. Moreover, an ADMIXTURE revealed little evidence of shared ancestry or hybridization between the groups, and no individuals that represented putative F1 or F2 hybrids. Consequently, we referred to groups structured on PC1 as *A. aff. divaricata A,* or "DA", and *A. aff. divaricata B, or* "DB", and treated them as different species. DA, with 161 individuals in our sample, was found across habitats at both sampling sites, and exhibited genetic structure with latitude. However, DA interbreeds readily across that latitudinal genetic structure, as evidenced by the presence of mixed ancestry within our dataset. The second species, represented by 73 samples, was collected only inside Pemba Bay

and does not readily hybridize with other genetic groups, even in the same location. We refer to this as DB.

While our ADMIXTURE analysis detected three ancestry groups, the two groups differentiated by PC2 appear unlikely to represent distinct species. This PC's strong correlation with latitude suggests isolation by distance more than sympatric differentiation. Likewise, we saw extensive mixed ancestry between these two putative groups, including several individuals that may represent F1 hybrids. Our PCAngsd analysis also revealed many intermediate individuals, and FST calculation between the groups differentiated on PC2 showed lower FST than that calculated between DA and DB.

Ancestry groups were structured in space. All individuals sampled at Caldeira Island corresponded to the "south" ancestry group detected in ADMIXTURE. Individuals of DA sampled in Pemba Bay corresponded mostly to the "north" ancestry group, but included individuals from the "south" ancestry group (Table A3.1). Within Pemba, there was no significant difference between the north and south ancestry groups in relative distribution of individuals per sampling area (chi-squared test n=93, p=0.19). Also within Pemba, the south genotypes were collected at slightly deeper depths than were north genotypes (mean 6.0± 0.7 meters, versus mean 4.9±0.3 meters for north genotypes), but the difference was not statistically significant (t-test n=93 , p=0.13). Restricting our sample to individuals sampled inside Pemba Bay, individuals of DB were on average sampled at higher latitude sampling points and

putatively warmer sampling points deeper inside the bay (Wilcoxon Rank Sum Test, n=95 , p=0.0004).

3.2 Genetic differentiation between *Acropora aff. divaricata* species

The weighted FST between DA and DB was 0.045, and the weighted FST between the north and south populations of DA was 0.012. However, this level of differentiation was inconsistent across the genome. Calculation of FST in sliding windows across the genome revealed an area of excess differentiation between DA and DB on chromosome 7, with FST>0.3 between approximately 20.44 and 20.55 Mb (Fig. 3.3A). This region contained no fixed differences between the two species. We found a similar spike in differentiation at roughly the same location between the north and south populations of DA (Fig. 3.3B). This spike persisted when comparing DB separately to the north and south populations of DA, and DB was slightly more similar to the south population than the north population at this locus (Supplemental Figure 3.2). Given its colocation with the HES-1 locus described by Rose *et al.* 2021, we refer to this area as the HES-1 locus.

The HES-1 genomic region showed lower genetic diversity than the genome-wide average. This lack of diversity was especially pronounced in DB and the north population of DA: the median pi and Wattersons' theta of the HES-1 region were in the bottom 3rd percentile of pi and Watterson's theta values for all windows across the genome. The same pattern did not hold in the south population of DA. Tajima's D was also below the genome-wide average for these taxa, suggesting that

this area may have been subject to a selective sweep in some of these populations. However, the pattern in Tajima's D is weaker than the pattern seen in pi and Watterson's theta (Table 3.2).

Tajima's D also varied within the HES-1 region, with lower values in putatively coding regions (Fig. 3.4). This genomic area includes four putative protein-coding genes: one short 3.8kb gene beginning at 20.mb, and three longer genes with lengths greater than 15kb. These genes begin at 20.45mb (gene 114955281), 20.50mb (gene 114955285), and 20.53mb. For the first long coding gene of the region, Tajima's D was below the genome wide 5th percentile for all three taxa. For the second gene, Tajima's D was at the 5th percentile for DB but above the 50th percentile for both of the DA populations. None of the genes in this region have known functions or associated gene ontogeny terms based on the annotation accompanying the *A. millepora* alignment.

3.3.3 Comparison with *Acropora aff. hyacinthus*

When analyzed jointly, *Acropora* populations from our Mozambican (*A. aff. divaricata*) samples were strongly differentiated from the *A. aff. hyacinthus* collected by Rose *et al.* (2021) in American Samoa. Differences between the *A. aff. divaricata* and *A. aff. hyacinthus* samples comprised the first PC of a PCA and accounted for 19% of total genetic variation (Fig. 3.5A). The second PC accounted for 2.9% of the variation and divided *A. aff. divaricata A* from *A. aff. divaricata B*. The third PC accounted for 1.8% of variation and separated the four *A. aff. hyacinthus* species from

each other. A phylogenetic tree confirmed that all samples from Mozambique belonged to a single monophyletic clade (Fig. 3.5B).

Trimming the genome to the broad definition of the HES-1 locus described in Rose *et al.* (chromosome 7, 20.35 - 20.53 Mb) revealed increased differentiation between the heat-tolerant '*A. hyacinthus* HE' species and the rest of the *A. hyacinthus* species complex (Fig. 3.5C). A minimum evolution tree constructed from this locus classified *A. hyacinthus HE* as the closest relative to *A. aff. divaricata* among the *A. hyacinthus* taxa (Fig. 3.5D).

Narrowing the genetic window under consideration to the two genes near the peak of the HES-1 differentiation described above, as well as a putatively non-coding region between them, showed closer association between DB and HE, the two species disproportionately found in hot microclimates. Analysis of gene 114955281 grouped DB and HE on the minimum evolution tree (Fig. 3.5F) while also grouping the *A. aff. divaricata* species together on the PCA (Fig. 3.5E). A PCA of part of the non-coding region adjacent to gene 114955285, chosen to exclude areas coding for either mRNA or lncRNA, closely resembled the PCA of the adjacent gene, rather than the full genome (Fig. 3.5G), and the tree matched the adjacent genes (Fig. 3.5H). Analysis at gene 114955285 clearly showed DB and HE grouped together in both the PCA and phylogenetic tree (Fig 3.5I and 3.5J). Clades containing DB and HE showed a high degree of statistical support (>90% of bootstrap replicates) for the second analyzed gene, as well as the locus as a whole.

We also tested whether this pattern of clustering was observed for other single genes across the *Acropora* genome. PCAs and phylogenetic trees constructed from the first alignable gene of each chromosome show patterns similar to those seen in the whole genome PCA, with *A. aff. divaricata* taxa grouped together and *A. hyacinthus* taxa grouped together, reflecting the substantial geographic and evolutionary separation between these species complexes across nearly the whole genome (Fig. A3.3).

ABBA-BABA testing failed to reveal evidence of introgression between HE and DB. We observed statistically strong evidence of weak introgression between HE and DA, rather than DB, in a comparison involving (DA, DB), HE) and the *Isopora* outgroup (D= -0.018, p=3.2 x 10^{-67}). We saw no significant evidence of introgression between any *A. aff. hyacinthus* species and DB in the test involving (HD, HE), DB) and the *Isopora* outgroup (D=0.001, p=0.31). However, ABBA-BABA testing of (DA, HE), DB) and (HD, DB), HE) in 50 kb windows revealed incongruence with this pattern at the HES-1 locus. For the block between 20.45 and 20.50 Mb, DB shared more derived alleles with HE than it did with sister species DA (n=27034 SNPs). For the same window, HE shared more derived alleles with DB than it did with its sister species HD (n=24922 SNPs, D=0.85).

3.3.4 Genetic variation with bleaching

Bleaching varied at both broad and fine spatial scales. We observed no bleaching at the more southern site on Caldeira Island, among either our samples or in

other *Acropora* taxa. However, we did observe bleaching at the northern site in Pemba, and bleaching rates varied with sampling area around the bay. None of the individual corals (0/8) at the coolest, most exposed, area of the northern peninsula bleached. Off the moderately exposed southern peninsula, 6% of individuals (3/50) showed at least partial bleaching, and one of those (1/50) was at least partially dead. Inside the bay, at the warmest and least-exposed sampling area, 38% of individuals (28/73) showed some signs of bleaching, and 15% (11/73) showed at least partial mortality. Sampling points inside the bay could be further characterized by their distance to the mouth of the bay. Sampling points deeper inside the bay, further from the mouth, receive less water circulation from the ocean and experienced the highest levels of bleaching. At the sampling point furthest from the mouth of the bay, 76% of individuals (16/21) showed at least partial bleaching, including 100% (3/3) of the individuals from species DA.

The best model for explaining bleaching inside Pemba Bay included only latitude, which is a proxy for distance from the mouth of the bay. The model suggested more bleaching at sites further from the mouth of the bay. Adding either depth or *Acropora* species as independent or interaction terms worsened model performance as defined by AIC. However, this was partly because the differences in latitude already account for most of the differences in species. There was a significant difference in average latitude between DA and DB. After adjusting p-values for multiple comparisons, we found no SNPs significantly associated with bleaching.

3.4. Discussion

Branching corals face profound threats from rising temperatures, yet vary in their heat tolerance both between and within regions. Here we sampled a Mozambican *Acropora* species at multiple spatial scales to look for genetic variation associated with heat tolerance. We found two putative species within our sample, one of which (DB) was only found in the hottest microclimate inside the bay. These two species were most strongly differentiated at the HES-1 locus, a genetic region previously described in *A. aff. hyacinthus* and speculated to be related to heat tolerance. The north and south populations of the other species (DA) also differed at this locus. Low diversity, low Tajima's D values, and high linkage disequilibrium suggested that this locus experienced a selective sweep in both of the *A. aff. divaricata* populations that are subject to higher heat stress. Surprisingly, we found strong evidence of shared evolutionary history at the HES-1 locus between putatively heat tolerant *A. aff. divaricata* species in Mozambique and *A. aff. hyacinthus* species in American Samoa. This evidence points to incomplete lineage sorting or introgression from an additional unsampled lineage as a potential source of important adaptive alleles across oceans.

3.4.1 *Acropora aff. divaricata* in Mozambique represents two cryptic species with distinct environmental niches

The increasing accessibility of SNP-based genetics to researchers has enabled a revolution in *Acropora* taxonomy, and revealed dozens of independently evolving lineages within traditionally-defined *Acropora* "species." These newly discovered sister species have broadly overlapping ranges, yet hybridize only infrequently (Cowman et al., 2026).

Genetic differentiation despite broad-scale range overlap may enable specialization on the microgeographic scale below the range of larval dispersal. In corals, cryptic species frequently occur in different depth niches and may exhibit significantly different responses to heat stress (Grupstra et al., 2024; Riginos et al., 2024). For example, three species of *Acropora* previously defined as *A. tenuis* on the Great Barrier Reef exhibit structuring by not only latitude, but also inshore vs. offshore position (Matias et al., 2023). Similarly, species of tabular corals previously identified as *A. hyacinthus* vary significantly in both their ranges and microhabitat association (Rassmussen et al., 2025). Microhabit differentiation between tabular coral species has been most extensively studied in American Samoa. One apparently heat-tolerant species, *A. hyacinthus HE*, was collected in a high temperature lagoon and displayed elevated bleaching tolerance in experimental settings as compared to four other tabular species (Gold & Palumbi, 2018; Rose et al., 2018). Across the entire genome, the area that most strongly differentiated the heat-tolerant species, *A. hyacinthus HE*, from the three other species in the complex was found on chromosome 7 between 20.35 and 20.53 Mb, an area subsequently named the HES-1 locus (Rose et al., 2021).

Our analysis of *A. aff. divaricata* from Mozambique strongly supports the existence of two cryptic species within our sample, with overlapping ranges at the regional scale, but different habitats at the sub-reef scale. DA was present at every sampling site and represented 100% of the individuals collected at Caldeira Island. Points inside Pemba Bay, which are warmer and more sheltered from wave action compared to other sampling points, were apparently dominated by DB, though with some individuals of DA. This may point to higher heat tolerance, lower tolerance for wave action, or other differing environmental tolerance for DB as compared to DA. However, our sampling does not necessarily capture stable climax communities. The reef on Pemba Bay's south peninsula was heavily damaged by Cyclone Kenneth in 2019 and had not fully recovered as of our sampling in 2023 and 2024 (Silva et al., 2024). Given this, it is possible that DB may have previously existed in less-sheltered areas around the bay.

Given the strong overall north to south directional current along Mozambique's coast (Ullgren et al., 2016), we would expect north genotypes moving south, rather than southern genotypes moving north. The unexpected pattern seen here may arise because we did not capture either one of our samples' entire geographic range. The Quirimbas archipelago to the north of Pemba hosts extensive coral reefs and exceptional *Acropora* biodiversity (Sola et al., 2016), possibly including both our DB and one or more genotypes of DA. Rather than revealing south-to-north transport of "southern" genotypes of DA from Caldeira to Pemba, our dataset may show northern genotypes from the Quirimbas settling as far as Pemba but

not reaching Caldeira Island. This is consistent with previous observations of population-level genetic differentiation between *Acropora* in the Primeiras and Segundas Islands, including Caldeira, and populations further north (Duvane et al., 2025).

The presence of multiple species with overlapping ranges and morphologies within this study points to a need for further investigation of the taxonomy and evolutionary history of *A. aff. divaricata*. Populations with morphological similarities to *A. divaricata* constitute a highly polyphyletic group, and *A. aff. divaricata* in Mozambique may not correspond to any extant type specimens (Cowman et al., 2020). *A. "divaricata"* would likely benefit from a taxonomic revision such as those recently seen in *A. tenuis* and *A. hyacinthus* (Bridge et al., 2024; Rassmussen et al., 2025). Moreover, taxonomic specificity is especially lacking on the East African coral reef tract, despite the region's status as a center of marine invertebrate biodiversity (McFadden et al., 2025; D. O. Obura, 2016). Even multi-region efforts to sample *Acropora* across the Indo-Pacific frequently exclude the entirety of the African mainland (Cowman et al., 2020; Rassmussen et al., 2025; Richards et al., 2016). All of this suggests that Mozambique, and East Africa more broadly, may host many more species of *Acropora* than are currently documented.

In a striking similarity to Rose *et al.* (2021), the closely related *A. aff. divaricata* species seen in this study also differ mostly strongly at the HES-1 locus on chromosome 7. The HES-1 locus represents the area of highest differentiation between DA and DB, and also between the north and south populations of DA. Both

species and populations inhabit overlapping ranges, but do experience different environmental conditions on average, especially with regards to temperature. This raises the question of whether the HES-1 locus contains adaptive variation for specific environmental conditions.

3.4.4 The HES-1 locus shows patterns of genetic variation consistent with a selective sweep

Selective sweeps play a key role species adaptation to novel environments, and they leave behind characteristic genetic signatures including decreased allelic diversity, decreased Tajima's D, and increased linkage disequilibrium around the locus under selection (Charlesworth & Jensen, 2021; Y. Kim & Nielsen, 2004; Messer & Petrov, 2013; Tajima, 1989). Some of these signatures have been detected around specific genes in coral genomes. Post-glacial expansion of *Acropora tenuis* on the Great Barrier Reef likely involved selective sweeps on genes involved in skeletal development, osmotic regulation, and establishment of symbiosis, identified in part by genomic regions of low Tajima's D (Cooke et al., 2020). Similarly, genome-wide analysis of linkage disequilibrium in *A. millepora* populations on the Great Barrier Reef revealed evidence of a hard selective sweep around the Δ9-desaturase gene, which the researchers linked to increased cold tolerance (Black et al., 2025).

The HES-1 locus showed patterns of genetic variation consistent with a selective sweep in both DB and the north genotype of DA. In both taxa, the HES-1 locus showed low diversity, high linkage, and low Tajima's D. While none of these metrics showed their most extreme values around the HES-1 locus, these patterns are

consistent with a selective sweep. Tajima's D also varied within the HES-1 region but showed different patterns between DB and the DA north type. Both taxa showed signs of positive selection on the first gene of the region (gene 114955281) as measured by Tajima's D, and this pattern was especially strong in the north type of DA. By contrast, only DB showed signs of positive selection on the second gene (gene 114955285). In both taxa, selection appeared relaxed in the intragenic region. Previous research has hypothesized that genes within the HES-1 region may constitute a "supergene" containing multiple genes that interact to influence heat tolerance (Rose et al., 2021), but our work suggests that not all genes within this region experience equal selective pressure. However, these results are consistent with HES-1 playing a role in heat tolerance. The locus as a whole showed signs of selection in the two populations expected to experience higher temperatures: DB, exclusively found in the hottest habitats inside Pemba Bay, and the north type of DA, also found exclusively in Pemba rather than the cooler sites around Caldeira Island.

3.4.5 Shared genetic architecture between *A. aff. divaricata* and *A. aff. hyacinthus*

Multiple evolutionary events may lead to non-sister lineages sharing specific haplotypes. Both incomplete lineage sorting (ILS) and introgression can lead to shared genetic sequences in different lineages and result in incongruent phylogenetic trees for some parts of the genome (Stern, 2013). Likewise, both processes can transmit important forms of adaptive variation, and can act in tandem in clades undergoing rapid adaptive radiations (Combrink et al., 2025). Examples of early ILS

contributing critical variation for downstream speciation have been documented in adaptive radiations as diverse as cichlid fish, wild tomatoes, and primates (Olave & Meyer, 2020; Pease et al., 2016; Rivas-González et al., 2023). ILS may be pervasive within *Acropora*, owing to the genus's evolutionarily recent radiation (Ramírez-Portilla et al., 2022). However, distinguishing ILS from either ancient introgression or modern hybridization from genetic evidence remains difficult (Combrink et al., 2025).

Introgression is also a mechanism by which taxa, including *Acropora*, may acquire genes to adapt to novel environments. Ancient hybridization between now distantly-related clades likely played a role in the adaptive radiation of *Acropora* in the Miocene (Wu et al., 2024). Repeated introgression across evolutionary time may have spread adaptive variation, as evidenced by genomic regions introgressed from other species that evolve faster than the rest of the genome (Mao et al., 2018). Present day corals may still acquire adaptive alleles from other species. A study of *Acropora* in Okinawa following the 1998 mass bleaching event found several hybrid individuals and identified candidate loci putatively subject to introgression and selective sweeps (Furukawa et al., 2025). On the Great Barrier Reef, three species of tabular *Acropora* were found to hybridize at the southern end of their range and showed consistent patterns of introgression at specific genetic regions. Genetic areas of increased minor-parent ancestry were disproportionately likely to contain stress response genes and to be under positive selection. Intriguingly, the HES-1 locus was

found to be disproportionately likely to be a site of introgression among tabular *Acropora* species on the Great Barrier Reef (Popovic et al., 2026).

Our results strongly suggest a common evolutionary origin for the HES-1 locus in both *A. aff. divarciata DB* and *A. hyacinthus HE*. We see clear phylogenetic incongruence between the whole genome and the center of the HES-1 locus, especially around gene 114955285. The clear clustering of DB with HE, including in a non-coding area of the genome, is strongly suggestive of some kind of shared genetic ancestry at this locus. While amino acid level similarities may indicate convergent evolution, shared nucleotide sequences such as seen here are much more likely to indicate either ILS or introgression (Stern 2013). This is striking, given the vast geographic separation between the two species, as well as their high genome-wide levels of differentiation.

Our ABBA-BABA testing results suggested ILS, rather than introgression, as a plausible explanation for these patterns, though with some important caveats. ABBA-BABA testing found no significant support for direct introgression between *A. aff. divaricata DB* and *A. aff. hyacinthus HE.* This is unsurprising, given the distance between the species' presumed geographic ranges. *A. turbinata*, a proposed synonym of *A. hyacinthus HE*, has only been documented in the Central Pacific, more than 10,000 kilometers from *A. aff. divaricata*'s known range in the Western Indian Ocean (Rassmussen et al., 2025). Given the prevalence of ILS in rapidly-radiated species, it may be plausible that a common ancestral population of both *A. aff. divaricata* and *A. aff. hyacinthus* contained the version of HES-1 now present in both *A. aff. divaricata*

DB and *A. aff. hyacinthus HE.* This version may be particularly advantageous in hot microclimates, or possibly deleterious outside them.

However, our results also cannot exclude the possibility of introgression playing a role in transmitting the alleles on HES-1 between species. HES-1 introgression involving a third, or even fourth, species, may also be plausible given our results here. ABBA-BABA testing can give misleading results in cases of introgression from "ghost" lineages, which may be extinct species or simply taxa unsampled in the present study (Tricou et al., 2022). In fact, one of our ABBA-BABA tests does suggest introgression between *A. hyacinthus HE* and *A. aff. divaricata A*, though not at the HES-1 locus. While this does not account for the patterns we observe at the HES-1 locus, it may support the idea of pervasive introgression in *Acropora* lineages. Given that a single historical introgression is a key assumption of ABBA-BABA testing, this may also cause inaccurate results (Frankel & Ané, 2023).

Rose *et al.* hypothesized that the HES-1 locus may have introgressed into *A. hyacinthus HE* from *A. millepora.* Popovic *et al.* note the HES-1 locus is disproportionately likely to be a site of introgression for tabular *Acropora* on the Great Barrier Reef (Popovic et al., 2026). While *Acropora turbinata* and *Acropora millepora* are not known to exist in northern Mozambique, dozens of other *Acropora* species do, including many tabular species (Sola et al., 2015). Examination of the HES-1 locus in other species would clarify the evolutionary history of this gene group.

Regardless of the exact mechanism by which it arose, an area of shared genetic material between two *Acropora* species inhabiting hot microclimates, but not their immediate sister lineages, suggests that variation on HES-1 may contribute to heat tolerance. Despite the association between HES-1 variation and environmental heat stress, the HES-1 locus has never been definitively linked to coral bleaching or survival during heat waves. A study of 231 *A. millepora* samples from the Great Barrier Reef found no strong association between SNPs on the HES-1 locus and bleaching (Fuller et al., 2020). Similarly, a comprehensive study of genomic regions associated with heat tolerance across *Acropora* species uncovered 85 loci associated with heat tolerance in at least two species, none of which corresponded to the HES-1 locus (Selmoni et al., 2025). Neither our analysis nor Rose *et al.* (2021) found clear associations between HES-1 variation and bleaching. In fact, Rose *et al.* (2021) reported that *A. hyacinthus* from non-HE lineages with "HE-like" genotypes at the HES-1 locus were slightly more likely to bleach than their non "HES-like" conspecifics. In our own study, our ability to find associations between either species or specific SNPs and bleaching resistance was severely limited by the confounding of genotype and environment at every spatial scale. It is also possible that the HES-1 links to some other heat tolerance function besides bleaching resistance, such as bleaching survival and recovery (Thomas et al., 2019). However, the absence of the HES-1 locus in other studies of genetic variation and bleaching means that this locus cannot be definitively treated as adaptive with regards to bleaching or other forms of heat tolerance.

3.4.6 Multiple sources of genetic variation but limited evidence of evolutionary rescue.

The persistence of coral reefs depends on their ability of corals to evolve increased heat tolerance, which depends in turn on the natural genetic variability present in coral populations (Humanes et al., 2022; McManus et al., 2021). Mechanistically, this adaptive capacity stems largely from the ability of heat-tolerant coral genotypes to colonize cooler areas (Matz et al., 2020). While our results showed some evidence for genetic variability in heat tolerance among closely-related *Acropora* species in Mozambique, we found no evidence of the putatively more heat tolerance lineage colonizing surrounding areas.

We saw strong spatial variation in a locus putatively associated with heat tolerance at both broad and fine spatial scales. Despite existing at the same locus in closely related species, there are two different variants of HES-1, one of which arose from incomplete lineage sorting or introgression with another part of the *Acropora* species tree. In addition to hosting genetic variation likely associated with heat tolerance, the DB *Acropora* species is previously unrecognized, and possibly spatially restricted. Further genetic study and protection of corals inside Pemba Bay, including DB, should be a conservation priority.

The presence of heat-adapted *Acropora* genotypes within a hot microclimate hints at the possibility of broader ecosystem-level adaptation to climate change (Bay et al., 2017). However, we see little evidence of *A. aff. divaricata* having broad reaching effects on coral resilience in Mozambique. Despite the sympatric presence

of a close sister species, we also do not observe recent hybridization between DA and DB in Mozambique. The HES-1 locus in particular constitutes a genetic area of high differentiation, not similarity, between these taxa. As observed in Rose *et al.* (2021), this could be because some gene or genes on the HES-1 locus may have different phenotypic effects in different species, and may be maladaptive in sister taxa. Similarly, we do not observe any individuals of DB colonizing the cooler microhabitats immediately outside Pemba Bay, or cooler habitats further south, despite warming ocean temperatures across habitats in the last thirty years in northern Mozambique (Fennessy et al., 2024). There are several potential explanations for this apparent failure of DB to spread.

First, the oceanography of mostly closed bays, including Pemba, can increase larval retention (Gouezo et al., 2025). Current flow in and around Pemba Bay may limit the number of coral larvae from inside the bay available to colonize areas outside the bay. Similarly, lack of DB outside the bay could be due to limits in other environmental tolerances such as cold or wave action, or competitive disadvantage outside the hottest microclimates. In American Samoa, HE exhibited significantly lower growth rates compared to the three less heat tolerant species *A. aff. hyacinthus* species (Gold & Palumbi, 2018). It is possible that DB similarly grows slower than its sister species in Mozambique. Finally, DB may have previously existed at nearby sites outside Pemba Bay, especially off the southern peninsula, but have failed to recover after the passage of Cyclone Kenneth in 2019 for any of the above-mentioned reasons (Silva et al., 2024).

Assisted migration of heat-tolerant coral genotypes has gained popularity as an intervention for buffering reefs against climate change, though its effectiveness remains a matter of debate (Bay et al., 2017; DeFilippo et al., 2022; Humanes et al., 2026). Given their geographic proximity and genetic similarly, sister species of *A. aff. divaricata* in Mozambique may prove to be good candidates for this type of intervention. Ongoing restoration experiments in Pemba, involving outplanting *A. aff. divaricata* from sites inside the bay to sites on the south peninsula, may clarify whether DB is able to survive outside of Pemba Bay, and whether it actually shows an advantage over DA at extreme high temperatures. Similarly, more extensive genetic sampling of corals in northern Mozambique as well as surrounding countries could give us critical information about the biogeography of *A. aff. divaricata,* as well as other local *Acropora* species. Our work here reveals multiple potential sources of adaptive variation in branching corals. Time will tell whether they persist into the future.

Acknowledgements

Samples were collected under Administração Nacional das Áreas de Conservação de Moçambique credential number 01/07/2023 in collaboration with the Universidade do Lúrio Faculdade de Ciências Naturais, and exported under CITES permit number 24MZ000873. This work was made possible by funding from the Rutgers Ecology and Evolution Small Grant program (JTB), the American Philosophical Society Lewis and Clark Fund for Exploration and Field Research (JTB), the Phillip

Stephenson Exploration Advancement Program (JTB), the UCSC Committee on Research Large Grant program (JTB and MLP) and the Paul M. Angell Foundation under award CON-F23-28 (MLP and JTB). We would like to thank Pete Raimondi and Lisa McManus for feedback on an earlier version of this project, and Tom Bridge and Erwan Sola for valuable comments on *Acropora* taxonomy. We would also like to thank Chafim Turabe Califa, Fernando Joaquim Mutipa, and Pieter Jacobs for field work support in Pemba, Jack Truter and Enock Madzure for graciously offering accommodation and support for field work on Caldeira Island, and Bibiana Nassongole for additional field assistance and invaluable advice and support. Thank you to Sidonio Machaieie and Cristóvão Nanvonamuquitxo for your support at UniLurio, especially with permitting and administration. Thank you to Joshua Fortmann, for generously sharing your apartment in Maputo, and Dawndra Wilburn, for sharing your quintal in Pemba. Thank you to the staff of the Maputo Natural History Museum Biobank, especially Iara Gomes-Jaintilal, for generous assistance with sample storage and transportation. Finally, sincere thanks to Antumane Árabe for many hours underwater.

References

Adam, A. A. S., Thomas, L., Underwood, J., Gilmour, J., & Richards, Z. T. (2022). Population connectivity and genetic offset in the spawning coral *Acropora digitifera* in Western Australia. *Molecular Ecology*, *31*(13), 3533–3547. https://doi.org/10.1111/mec.16498

Bay, R. A., Rose, N. H., Logan, C. A., & Palumbi, S. R. (2017). Genomic models predict successful coral adaptation if future ocean warming rates are reduced. *Science Advances*, *3*(11), e1701413. https://doi.org/10.1126/sciadv.1701413

Benjamini, Y., & Hochberg, Y. (1995). Controlling the False Discovery Rate: A Practical and Powerful Approach to Multiple Testing. *Journal of the Royal Statistical Society Series B: Statistical Methodology*, *57*(1), 289–300. https://doi.org/10.1111/j.2517-6161.1995.tb02031.x

Bitter, M. C., Kapsenberg, L., Gattuso, J.-P., & Pfister, C. A. (2019). Standing genetic variation fuels rapid adaptation to ocean acidification. *Nature Communications*, *10*(1), 5821. https://doi.org/10.1038/s41467-019-13767-1

Black, K. L., Bay, L. K., & Matz, M. V. (2025). A Genetic Variant of Delta‐9 Desaturase Is Associated With Latitudinal Adaptation in a Coral from the Great Barrier Reef. *Molecular Ecology*, *34*(3), e17634. https://doi.org/10.1111/mec.17634

Bonin, M. C. (2012). Specializing on vulnerable habitat: Acropora selectivity among damselfish recruits and the risk of bleaching-induced habitat loss. *Coral Reefs*, *31*(1), 287–297. https://doi.org/10.1007/s00338-011-0843-2

Bridge, T. C. L., Cowman, P. F., Quattrini, A. M., Bonito, V. E., Sinniger, F., Harii, S., Head, C. E. I., Hung, J. Y., Halafihi, T., Rongo, T., & Baird, A. H. (2024). A *tenuis* relationship: Traditional taxonomy obscures systematics and biogeography of the ‘ *Acropora tenuis* ’ (Scleractinia: Acroporidae) species complex. *Zoological Journal of the Linnean Society*, *202*(1), zlad062. https://doi.org/10.1093/zoolinnean/zlad062

Brown, K. T., Martynek, M. P., & Barott, K. L. (2024). Local habitat heterogeneity rivals regional differences in coral thermal tolerance. *Coral Reefs*, *43*(3), 571–585. https://doi.org/10.1007/s00338-024-02484-x

Bushnell, B. (2014). *BBTools* (Version 39.06) [Computer software]. https://bbmap.org

Charlesworth, B., & Jensen, J. D. (2021). Effects of Selection at Linked Sites on Patterns of Genetic Variability. *Annual Review of Ecology, Evolution, and*

Systematics, *52*(1), 177–197. https://doi.org/10.1146/annurev-ecolsys-010621-044528

Chen, S., Zhou, Y., Chen, Y., & Gu, J. (2018). fastp: An ultra-fast all-in-one FASTQ preprocessor. *Bioinformatics*, *34*(17), i884–i890. https://doi.org/10.1093/bioinformatics/bty560

Chow, S. W., Chen, C.-H., Tsai, D.-Y., Mezaki, T., Kubota, S., Hsieh, H. J., Keshavmurthy, S., & Chen, C. A. (2025). A clear distinction and presence of Acropora aff. Divaricata within Acropora cf. Solitaryensis species complex along their biogeographic distribution in East Asia. *Scientific Reports*, *15*(1), 9739. https://doi.org/10.1038/s41598-025-90051-x

Combrink, L. L., Golcher‐Benavides, J., Lewanski, A. L., Rick, J. A., Rosenthal, W. C., & Wagner, C. E. (2025). Population Genomics of Adaptive Radiation. *Molecular Ecology*, *34*(2), e17574. https://doi.org/10.1111/mec.17574

Cooke, I., Ying, H., Forêt, S., Bongaerts, P., Strugnell, J. M., Simakov, O., Zhang, J., Field, M. A., Rodriguez-Lanetty, M., Bell, S. C., Bourne, D. G., Van Oppen, M. J., Ragan, M. A., & Miller, D. J. (2020). Genomic signatures in the coral holobiont reveal host adaptations driven by Holocene climate change and reef specific symbionts. *Science Advances*, *6*(48), eabc6318. https://doi.org/10.1126/sciadv.abc6318

Cowman, P. F., Bridge, T. C. L., Ainsworth, T. D., Benzoni, F., Bonito, V., Budd, A., Cabaitan, P., Camp, E. F., Chen, C. A., Connolly, S. R., Crosbie, A. J., Figueiredo, J., Fenner, D., Forsman, Z., Fukami, H., Head, C. E. I., Hoeksema, B. W., Huang, D., Kitahara, M. V., … Baird, A. H. (2026). Modern Coral Taxonomy Requires Reproducible Data Alongside Field Observations—Comments on Veron et al. (2025). *Diversity*, *18*(2), 60. https://doi.org/10.3390/d18020060

Cowman, P. F., Quattrini, A. M., Bridge, T. C. L., Watkins-Colwell, G. J., Fadli, N., Grinblat, M., Roberts, T. E., McFadden, C. S., Miller, D. J., & Baird, A. H. (2020). An enhanced target-enrichment bait set for Hexacorallia provides phylogenomic resolution of the staghorn corals (Acroporidae) and close relatives. *Molecular Phylogenetics and Evolution*, *153*, 106944. https://doi.org/10.1016/j.ympev.2020.106944

DeFilippo, L. B., McManus, L. C., Schindler, D. E., Pinsky, M. L., Colton, M. A., Fox, H. E., Tekwa, E. W., Palumbi, S. R., Essington, T. E., & Webster, M. M. (2022). Assessing the potential for demographic restoration and assisted evolution to build climate resilience in coral reefs. *Ecological Applications*, *32*(7), e2650. https://doi.org/10.1002/eap.2650

Desper, R., & Gascuel, O. (2002). Fast and Accurate Phylogeny Reconstruction Algorithms Based on the Minimum-Evolution Principle. *Journal of Computational Biology*, *9*(5), 687–705. https://doi.org/10.1089/106652702761034136

Duvane, J. A., Dupont, S., Sola, E., Ortega-Martinez, O., & Pereyra, R. T. (2025). Genetic diversity and structure among Acropora austera populations in Mozambique suggest low resilience potential of one of the world's most charismatic coral reefs. *Coral Reefs*, *44*(4), 1185–1195. https://doi.org/10.1007/s00338-025-02679-w

Efron, B., Halloran, E., & Holmes, S. (1996). Bootstrap confidence levels for phylogenetic trees. *Proceedings of the National Academy of Sciences*, *93*(23), 13429–13429. https://doi.org/10.1073/pnas.93.23.13429

Ewels, P., Magnusson, M., Lundin, S., & Käller, M. (2016). MultiQC: Summarize analysis results for multiple tools and samples in a single report. *Bioinformatics*, *32*(19), 3047–3048. https://doi.org/10.1093/bioinformatics/btw354

Fennessy, S. T., Quick, A. J. R., Mutombene, R. J., Abdula, S., Leong, E. R., Dias, N., Filipe, O., Chacate, O., Malauene, B. S., Fernando, S., Mualeque, D. O., Vianello, P., & Roberts, M. J. (2024). A rapid approach to assessing the vulnerability of Mozambican fisheries' species to climate change. *PLOS Climate*, *3*(5), e0000372. https://doi.org/10.1371/journal.pclm.0000372

Fifer, J. E., Speare, K. E., Leinbach, S. E., Hendricks, S. F., Davies, S. W., Rose, N. H., Burkepile, D. E., Adam, T. C., Hofmann, G. E., & Strader, M. E. (2026). Rapid Evolution in a Coral Population Following a Mass Mortality Event. *Evolutionary Applications*, *19*(2), e70198. https://doi.org/10.1111/eva.70198

Fox, E. A., Wright, A. E., Fumagalli, M., & Vieira, F. G. (2019). *ngsLD*: Evaluating linkage disequilibrium using genotype likelihoods. *Bioinformatics*, *35*(19), 3855–3856. https://doi.org/10.1093/bioinformatics/btz200

Frankel, L. E., & Ané, C. (2023). Summary Tests of Introgression Are Highly Sensitive to Rate Variation Across Lineages. *Systematic Biology*, *72*(6), 1357–1369. https://doi.org/10.1093/sysbio/syad056

Fuller, Z. L., Mocellin, V. J. L., Morris, L. A., Cantin, N., Shepherd, J., Sarre, L., Peng, J., Liao, Y., Pickrell, J., Andolfatto, P., Matz, M., Bay, L. K., & Przeworski, M. (2020). Population genetics of the coral *Acropora millepora*: Toward genomic prediction of bleaching. *Science*, *369*(6501), eaba4674. https://doi.org/10.1126/science.aba4674

Furukawa, M., Tarigan, A. I., Kitanobo, S., Hanahara, N., Ohki, S., & Morita, M. (2025). Introgression and adaptive potential following heavy bleaching events in Acropora corals. *Current Biology*, *35*(13), 3064-3075.e5. https://doi.org/10.1016/j.cub.2025.05.038

Gold, Z., & Palumbi, S. R. (2018). Long-term growth rates and effects of bleaching in Acropora hyacinthus. *Coral Reefs*, *37*(1), 267–277. https://doi.org/10.1007/s00338-018-1656-3

Google Maps. (2026, June). maps.google.com

Gouezo, M., Langlais, C., Beardsley, J., Roff, G., Harrison, P. L., Thomson, D. P., & Doropoulos, C. (2025). Going with the flow: Leveraging reef‐scale hydrodynamics for upscaling larval‐based restoration. *Ecological Applications*, *35*(3), e70020. https://doi.org/10.1002/eap.70020

Green, R. E., Krause, J., Briggs, A. W., Maricic, T., Stenzel, U., Kircher, M., Patterson, N., Li, H., Zhai, W., Fritz, M. H.-Y., Hansen, N. F., Durand, E. Y., Malaspinas, A.-S., Jensen, J. D., Marques-Bonet, T., Alkan, C., Prüfer, K., Meyer, M., Burbano, H. A., … Pääbo, S. (2010). A Draft Sequence of the Neandertal Genome. *Science*, *328*(5979), 710–722. https://doi.org/10.1126/science.1188021

Grupstra, C. G. B., Gómez-Corrales, M., Fifer, J. E., Aichelman, H. E., Meyer-Kaiser, K. S., Prada, C., & Davies, S. W. (2024). Integrating cryptic diversity into coral evolution, symbiosis and conservation. *Nature Ecology & Evolution*, *8*(4), 622–636. https://doi.org/10.1038/s41559-023-02319-y

Hamilton, J. A., & Miller, J. M. (2016). Adaptive introgression as a resource for management and genetic conservation in a changing climate. *Conservation Biology*, *30*(1), 33–41. https://doi.org/10.1111/cobi.12574

Humanes, A., Bay, L., Riginos, C., Aguirre, J. D., Angilletta, M. J., Aranda, M., Baker, A. C., Baria-Rodriguez, M. V., Baums, I. B., Bhagooli, R., Duarte, C. M., Guest, J. R., Hendry, A. P., Kenkel, C. D., Lasky, J. R., Mead, D., Van Oppen, M. J. H., Peixoto, R. S., Le Port, A., … Ortiz, J. C. (2026). Accelerating coral assisted evolution to keep pace with climate change. *Nature Reviews Biodiversity*, *2*(5), 306–321. https://doi.org/10.1038/s44358-026-00147-z

Humanes, A., Lachs, L., Beauchamp, E. A., Bythell, J. C., Edwards, A. J., Golbuu, Y., Martinez, H. M., Palmowski, P., Treumann, A., Van Der Steeg, E., Van Hooidonk, R., & Guest, J. R. (2022). Within-population variability in coral heat tolerance indicates climate adaptation potential. *Proceedings of the Royal Society B: Biological Sciences*, *289*(1981), 20220872. https://doi.org/10.1098/rspb.2022.0872

Katoh, K., & Standley, D. M. (2013). MAFFT Multiple Sequence Alignment Software Version 7: Improvements in Performance and Usability. *Molecular Biology and Evolution*, *30*(4), 772–780. https://doi.org/10.1093/molbev/mst010

Kim, S. Y., Lohmueller, K. E., Albrechtsen, A., Li, Y., Korneliussen, T., Tian, G., Grarup, N., Jiang, T., Andersen, G., Witte, D., Jorgensen, T., Hansen, T., Pedersen, O., Wang, J., & Nielsen, R. (2011). Estimation of allele frequency and association mapping using next-generation sequencing data. *BMC Bioinformatics*, *12*(1), 231. https://doi.org/10.1186/1471-2105-12-231

Kim, Y., & Nielsen, R. (2004). Linkage Disequilibrium as a Signature of Selective Sweeps. *Genetics*, *167*(3), 1513–1524. https://doi.org/10.1534/genetics.103.025387

Kleypas, J. A., Thompson, D. M., Castruccio, F. S., Curchitser, E. N., Pinsky, M., & Watson, J. R. (2016). Larval connectivity across temperature gradients and its potential effect on heat tolerance in coral populations. *Global Change Biology*, *22*(11), 3539–3549. https://doi.org/10.1111/gcb.13347

Korneliussen, T. S., Albrechtsen, A., & Nielsen, R. (2014). ANGSD: Analysis of Next Generation Sequencing Data. *BMC Bioinformatics*, *15*(1), 356. https://doi.org/10.1186/s12859-014-0356-4

Korneliussen, T. S., & Moltke, I. (2015). NgsRelate: A software tool for estimating pairwise relatedness from next-generation sequencing data. *Bioinformatics*, *31*(24), 4009–4011. https://doi.org/10.1093/bioinformatics/btv509

Korneliussen, T. S., Moltke, I., Albrechtsen, A., & Nielsen, R. (2013). Calculation of Tajima's D and other neutrality test statistics from low depth next-generation sequencing data. *BMC Bioinformatics*, *14*(1), 289. https://doi.org/10.1186/1471-2105-14-289

Lachs, L., Bozec, Y.-M., Bythell, J. C., Donner, S. D., East, H. K., Edwards, A. J., Golbuu, Y., Gouezo, M., Guest, J. R., Humanes, A., Riginos, C., & Mumby, P. J. (2024). Natural selection could determine whether *Acropora* corals persist under expected climate change. *Science*, *386*(6727), 1289–1294. https://doi.org/10.1126/science.adl6480

Lachs, L., Humanes, A., Mumby, P. J., Donner, S. D., Bythell, J., Beauchamp, E., Bukurou, L., Buzzoni, D., De La Torre Cerro, R., East, H. K., Edwards, A. J., Golbuu, Y., Martinez, H. M., Van Der Steeg, E., Ward, A., & Guest, J. R. (2024). High coral heat tolerance at local-scale thermal refugia. *PLOS Climate*, *3*(7), e0000453. https://doi.org/10.1371/journal.pclm.0000453

Ladner, J. T., & Palumbi, S. R. (2012). Extensive sympatry, cryptic diversity and introgression throughout the geographic distribution of two coral species complexes. *Molecular Ecology*, *21*(9), 2224–2238. https://doi.org/10.1111/j.1365-294X.2012.05528.x

Li, H. (2011). A statistical framework for SNP calling, mutation discovery, association mapping and population genetical parameter estimation from

sequencing data. *Bioinformatics*, *27*(21), 2987–2993. https://doi.org/10.1093/bioinformatics/btr509

Li, H., Handsaker, B., Wysoker, A., Fennell, T., Ruan, J., Homer, N., Marth, G., Abecasis, G., Durbin, R., & 1000 Genome Project Data Processing Subgroup. (2009). The Sequence Alignment/Map format and SAMtools. *Bioinformatics*, *25*(16), 2078–2079. https://doi.org/10.1093/bioinformatics/btp352

Li, Y., Vinckenbosch, N., Tian, G., Huerta-Sanchez, E., Jiang, T., Jiang, H., Albrechtsen, A., Andersen, G., Cao, H., Korneliussen, T., Grarup, N., Guo, Y., Hellman, I., Jin, X., Li, Q., Liu, J., Liu, X., Sparsø, T., Tang, M., … Wang, J. (2010). Resequencing of 200 human exomes identifies an excess of low-frequency non-synonymous coding variants. *Nature Genetics*, *42*(11), 969–972. https://doi.org/10.1038/ng.680

Malauene, B. S., Shillington, F. A., Roberts, M. J., & Moloney, C. L. (2014). Cool, elevated chlorophyll-a waters off northern Mozambique. *Deep Sea Research Part II: Topical Studies in Oceanography*, *100*, 68–78. https://doi.org/10.1016/j.dsr2.2013.10.017

Mao, Y., Economo, E. P., & Satoh, N. (2018). The Roles of Introgression and Climate Change in the Rise to Dominance of Acropora Corals. *Current Biology*, *28*(21), 3373-3382.e5. https://doi.org/10.1016/j.cub.2018.08.061

Matias, A. M. A., Popovic, I., Thia, J. A., Cooke, I. R., Torda, G., Lukoschek, V., Bay, L. K., Kim, S. W., & Riginos, C. (2023). Cryptic diversity and spatial genetic variation in the coral *Acropora tenuis* and its endosymbionts across the Great Barrier Reef. *Evolutionary Applications*, *16*(2), 293–310. https://doi.org/10.1111/eva.13435

Matz, M. V., Treml, E. A., & Haller, B. C. (2020). Estimating the potential for coral adaptation to global warming across the Indo‐West Pacific. *Global Change Biology*, *26*(6), 3473–3481. https://doi.org/10.1111/gcb.15060

McClanahan, T., Ateweberhan, M., Graham, N., Wilson, S., Sebastián, C., Guillaume, M., & Bruggemann, J. (2007). Western Indian Ocean coral communities: Bleaching responses and susceptibility to extinction. *Marine Ecology Progress Series*, *337*, 1–13. https://doi.org/10.3354/meps337001

McFadden, C. S., Erickson, K. L., Lane, A., Nassongole, B., Aguilar, S., Dunakey, S. K., Durkin, K. M., Lalas, J. A. A., Kushida, Y., Macrina, L., Minor, N. P., Morales-Paredes, M., Nelson, J., Peddada, A., Poole, S., Porto, R., Purow-Ruderman, R., Snyder, K. E., Wismar, T., … Benayahu, Y. (2025). Biodiversity and biogeography of zooxanthellate soft corals across the Indo-Pacific. *Scientific Reports*, *15*(1), 15461. https://doi.org/10.1038/s41598-025-98790-7

McManus, L. C., Forrest, D. L., Tekwa, E. W., Schindler, D. E., Colton, M. A., Webster, M. M., Essington, T. E., Palumbi, S. R., Mumby, P. J., & Pinsky, M. L. (2021). Evolution and connectivity influence the persistence and recovery of coral reefs under climate change in the Caribbean, Southwest Pacific, and Coral Triangle. *Global Change Biology*, *27*(18), 4307–4321. https://doi.org/10.1111/gcb.15725

McMaster, E. S., Lu‐Irving, P., Van Der Merwe, M. M., Ho, S. Y. W., & Rossetto, M. (2025). Evaluating Kinship Estimation Methods for Reduced‐Representation SNP Data in Non‐model Species. *Molecular Ecology Resources*, *25*(8), e70038. https://doi.org/10.1111/1755-0998.70038

Meisner, J., & Albrechtsen, A. (2018). Inferring Population Structure and Admixture Proportions in Low-Depth NGS Data. *Genetics*, *210*(2), 719–731. https://doi.org/10.1534/genetics.118.301336

Messer, P. W., & Petrov, D. A. (2013). Population genomics of rapid adaptation by soft selective sweeps. *Trends in Ecology & Evolution*, *28*(11), 659–669. https://doi.org/10.1016/j.tree.2013.08.003

Muir, P. R., Marshall, P. A., Abdulla, A., & Aguirre, J. D. (2017). Species identity and depth predict bleaching severity in reef-building corals: Shall the deep inherit the reef? *Proceedings of the Royal Society B: Biological Sciences*, *284*(1864), 20171551. https://doi.org/10.1098/rspb.2017.1551

Nassongole, B. A. F., Buhl-Mortensen, L., Da Silva, I. M., Hilário, A., & McFadden, C. S. (2026). Exploring the diversity and distribution of Mozambique's soft corals (Octocorallia) through an integrative approach. *Marine Biodiversity*, *56*(2), 23. https://doi.org/10.1007/s12526-026-01628-2

Nextera XT DNA Library Prep Kit Reference Guide. (2018, February).

Nielsen, R., Korneliussen, T., Albrechtsen, A., Li, Y., & Wang, J. (2012). SNP Calling, Genotype Calling, and Sample Allele Frequency Estimation from New-Generation Sequencing Data. *PLoS ONE*, *7*(7), e37558. https://doi.org/10.1371/journal.pone.0037558

Obura, D. (2012). The Diversity and Biogeography of Western Indian Ocean Reef-Building Corals. *PLoS ONE*, *7*(9), e45013. https://doi.org/10.1371/journal.pone.0045013

Obura, D. O. (2016). An Indian Ocean centre of origin revisited: Palaeogene and Neogene influences defining a biogeographic realm. *Journal of Biogeography*, *43*(2), 229–242. https://doi.org/10.1111/jbi.12656

Olave, M., & Meyer, A. (2020). Implementing Large Genomic Single Nucleotide Polymorphism Data Sets in Phylogenetic Network Reconstructions: A Case Study of Particularly Rapid Radiations of Cichlid Fish. *Systematic Biology*, *69*(5), 848–862. https://doi.org/10.1093/sysbio/syaa005

Paradis, E., & Schliep, K. (2019). ape 5.0: An environment for modern phylogenetics and evolutionary analyses in R. *Bioinformatics*, *35*(3), 526–528. https://doi.org/10.1093/bioinformatics/bty633

Pease, J. B., Haak, D. C., Hahn, M. W., & Moyle, L. C. (2016). Phylogenomics Reveals Three Sources of Adaptive Variation during a Rapid Radiation. *PLOS Biology*, *14*(2), e1002379. https://doi.org/10.1371/journal.pbio.1002379

Popovic, I., Prata, K. E., Naugle, M. S., Byrne, I., Howitt, S. M., Meziere, Z., Bridge, T. C. L., Mocellin, V. J. L., Howells, E. J., Bay, L. K., Bierne, N., & Riginos, C. (2026). *Localised admixture triggers parallel adaptation in a coral species trio on the Great Barrier Reef*. Evolutionary Biology. https://doi.org/10.64898/2026.02.07.704610

R Core Team. (2025). *R: A Language and Environment for Statistical Computing* [Dataset]. R Foundation for Statistical Computing.

Ramírez-Portilla, C., Baird, A. H., Cowman, P. F., Quattrini, A. M., Harii, S., Sinniger, F., & Flot, J.-F. (2022). Solving the Coral Species Delimitation Conundrum. *Systematic Biology*, *71*(2), 461–475. https://doi.org/10.1093/sysbio/syab077

Rassmussen, S. H., Cowman, P. F., Baird, A. H., Crosbie, A. J., Quattrini, A. M., Bonito, V., Sinniger, F., Harii, S., Cabaitan, P. C., Fadli, N., Tan, C.-H., Hung, J. Y.-H., Rongo, T., Huang, D., Halafihi, T., & Bridge, T. C. L. (2025). The tables have turned: Taxonomy, systematics and biogeography of the Acropora hyacinthus (Scleractinia: Acroporidae) complex. *Invertebrate Systematics*, *39*(8), IS24049. https://doi.org/10.1071/IS24049

Rich, W. A., Glanz, J. S., Mele, G., Burt, N. J., Carvalho, S., Doo, S. S., Goergen, E. A., Krieger, E. C., Li, L., Osman, E. O., Suggett, D. J., Johnson, M. D., & Fox, Michael. D. (2024). Widespread inconsistency in logger deployment methods in coral reef studies may bias perceptions of thermal regimes. *PLOS Climate*, *3*(12), e0000517. https://doi.org/10.1371/journal.pclm.0000517

Richards, Z. T., Berry, O., & Van Oppen, M. J. H. (2016). Cryptic genetic divergence within threatened species of Acropora coral from the Indian and Pacific Oceans. *Conservation Genetics*, *17*(3), 577–591. https://doi.org/10.1007/s10592-015-0807-0

Riegl, B. M., Purkis, S. J., Al-Cibahy, A. S., Al-Harthi, S., Grandcourt, E., Al-Sulaiti, K., Baldwin, J., & Abdel-Moati, A. M. (2012). Coral Bleaching and Mortality Thresholds in the SE Gulf: Highest in the World. In B. M. Riegl & S. J. Purkis (Eds.), *Coral Reefs of the Gulf* (Vol. 3, pp. 95–105). Springer Netherlands. https://doi.org/10.1007/978-94-007-3008-3_6

Riginos, C., Popovic, I., Meziere, Z., Garcia, V., Byrne, I., Howitt, S. M., Ishida, H., Bairos-Novak, K., Humanes, A., Scharfenstein, H., Richards, T., Briggs, E., Clark, V., Lei, C., Khan, M., & Prata, K. E. (2024). Cryptic species and hybridisation in corals: Challenges and opportunities for conservation and restoration. *Peer Community Journal*, *4*, e106. https://doi.org/10.24072/pcjournal.492

Rivas-González, I., Rousselle, M., Li, F., Zhou, L., Dutheil, J. Y., Munch, K., Shao, Y., Wu, D., Schierup, M. H., & Zhang, G. (2023). Pervasive incomplete

lineage sorting illuminates speciation and selection in primates. *Science*, *380*(6648), eabn4409. https://doi.org/10.1126/science.abn4409

Rose, N. H., Bay, R. A., Morikawa, M. K., & Palumbi, S. R. (2018). Polygenic evolution drives species divergence and climate adaptation in corals. *Evolution*, *72*(1), 82–94. https://doi.org/10.1111/evo.13385

Rose, N. H., Bay, R. A., Morikawa, M. K., Thomas, L., Sheets, E. A., & Palumbi, S. R. (2021). 3. Genomic analysis of distinct bleaching tolerances among cryptic coral species. *Proceedings of the Royal Society B: Biological Sciences*, *288*(1960), 20210678. https://doi.org/10.1098/rspb.2021.0678

Sakai, K., Singh, T., & Iguchi, A. (2019). Bleaching and post-bleaching mortality of *Acropora* corals on a heat-susceptible reef in 2016. *PeerJ*, *7*, e8138. https://doi.org/10.7717/peerj.8138

Schleyer, M., Obura, D., Motta, H., & Rodrigues, M. (1999). *A PRELIMINARY ASSESSMENT OF CORAL BLEACHING IN MOZAMBIQUE* (Unpublished Report No. 168). South African Association for Marine Biological Research.

Selmoni, O., Cleves, P. A., & Exposito-Alonso, M. (2025). Global coral genomic vulnerability explains recent reef losses. *Nature Communications*, *17*(1), 896. https://doi.org/10.1038/s41467-025-67616-5

Sete, C., Ruby, J., & Dove, V. (2002). *Seasonal variation of tides, currents, salinity and temperature along the coast of Mozambique.* Centro Nacional de Dados Oceanográficos.

Silva, I. M. D., Lobo, M., Muipela, A., Rocha, R. J. M., & Quintino, V. (2024). Coral Reefs Community Structure in Pemba, Northern Mozambique: 2012 vs 2016. *Journal of Coastal Research*, *113*(sp1). https://doi.org/10.2112/JCR-SI113-182.1

Sola, E., Glassom, D., & Silva, I. (2015). An annotated and illustrated checklist of species of the coral genus Acropora (Cnidaria: Scleractinia) from Vamizi Island, Mozambique. *African Invertebrates*, *56*(3), 807–844.

Sola, E., Marques Da Silva, I., & Glassom, D. (2016). Reproductive synchrony in a diverse *Acropora* assemblage, Vamizi Island, Mozambique. *Marine Ecology*, *37*(6), 1373–1385. https://doi.org/10.1111/maec.12348

Stern, D. L. (2013). The genetic causes of convergent evolution. *Nature Reviews Genetics*, *14*(11), 751–764. https://doi.org/10.1038/nrg3483

Tajima, F. (1989). The effect of change in population size on DNA polymorphism. *Genetics*, *123*(3), 597–601. https://doi.org/10.1093/genetics/123.3.597

Thomas, L., López, E. H., Morikawa, M. K., & Palumbi, S. R. (2019). Transcriptomic resilience, symbiont shuffling, and vulnerability to recurrent bleaching in reef‐building corals. *Molecular Ecology*, *28*(14), 3371–3382. https://doi.org/10.1111/mec.15143

Thomas, L., Rose, N. H., Bay, R. A., López, E. H., Morikawa, M. K., Ruiz-Jones, L., & Palumbi, S. R. (2018). Mechanisms of Thermal Tolerance in Reef-Building Corals across a Fine-Grained Environmental Mosaic: Lessons from Ofu, American Samoa. *Frontiers in Marine Science*, *4*, 434. https://doi.org/10.3389/fmars.2017.00434

Tricou, T., Tannier, E., & De Vienne, D. M. (2022). Ghost Lineages Highly Influence the Interpretation of Introgression Tests. *Systematic Biology*, *71*(5), 1147–1158. https://doi.org/10.1093/sysbio/syac011

Ullgren, J. E., André, E., Gammelsrød, T., & Hoguane, A. M. (2016). Observations of strong ocean current events offshore Pemba, Northern Mozambique. *Journal of Operational Oceanography*, *9*(1), 55–66. https://doi.org/10.1080/1755876X.2016.1204172

Van Oppen, M. J. H., Willis, B. L., Van Rheede, T., & Miller, D. J. (2002). Spawning times, reproductive compatibilities and genetic structuring in the *Acropora aspera* group: Evidence for natural hybridization and semi‐permeable species boundaries in corals. *Molecular Ecology*, *11*(8), 1363–1376. https://doi.org/10.1046/j.1365-294X.2002.01527.x

Veron, J. E. N. (2000). *Corals of the world. 3* (1. publ). Australian Institute of Marine Science.

Wellcome Sanger Institute. (2026). *Isopora aff. Cuneata* (ERX16119961: Illumina NovaSeq 6000 paired end sequencing) [Dataset]. https://www.ncbi.nlm.nih.gov/sra/ERX16119961[accn]

Whitaker, H., & DeCarlo, T. (2024). Re(de)fining degree-heating week: Coral bleaching variability necessitates regional and temporal optimization of global forecast model stress metrics. *Coral Reefs*, *43*(4), 969–984. https://doi.org/10.1007/s00338-024-02512-w

Wu, T., Xu, A. N., Lei, Y., & Song, H. (2024). Ancient Hybridisation Fuelled Diversification in *Acropora* Corals. *Molecular Ecology*, e17615. https://doi.org/10.1111/mec.17615

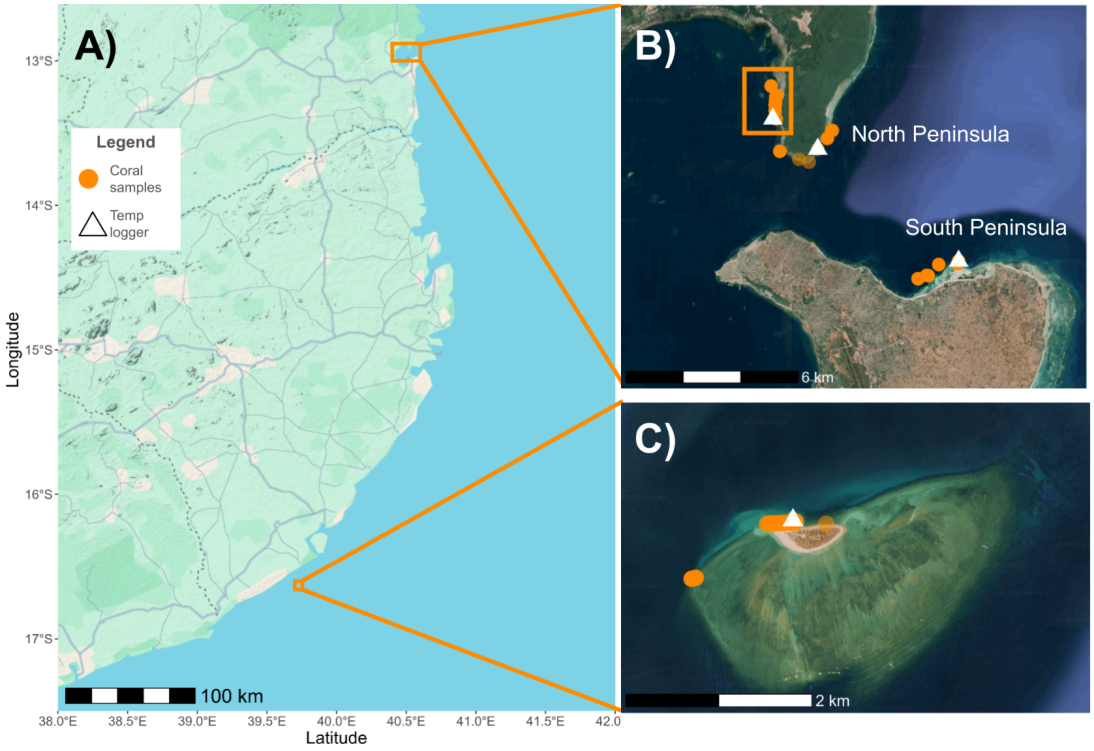

Fig. 3.1. Sampling location in Mozambique showing coral samples and HOBO submerged temperature loggers (*Google Maps*, June 2026). (A) We collected samples at two regions in northern Mozambique separated by approximately 500 km. (B) The northern region, Pemba Bay was sampled in 2023 and 2024. We collected and successfully sequenced 168 samples from a variety of microhabitats. The orange rectangle indicates the sampling areas inside the bay with the highest average temperatures. (C) The more southern site, Caldeira Island, was sampled in 2024. We successfully collected and sequenced 68 samples from the reef crest and inshore area.

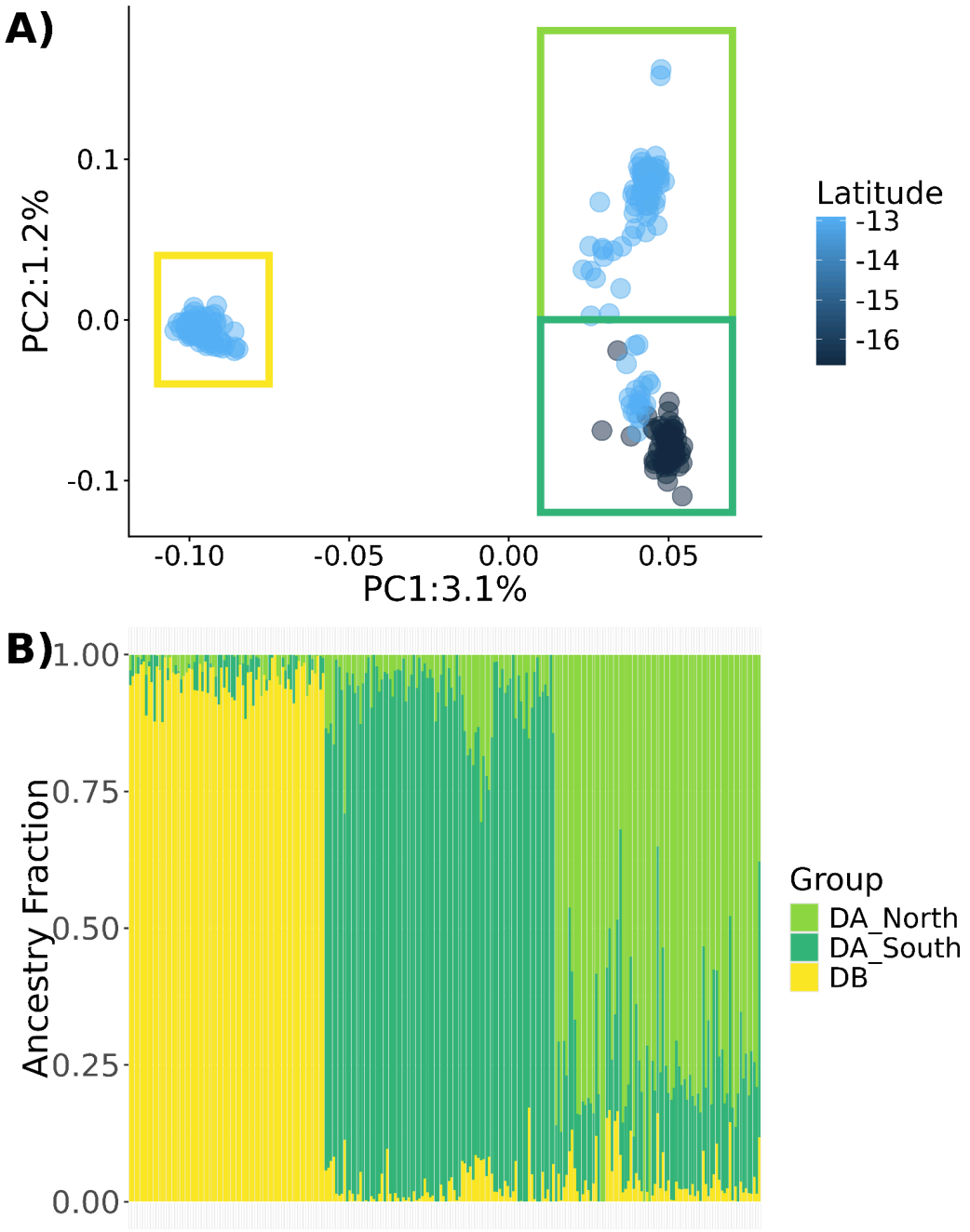

Fig. 3.2. *A. aff. divaricata* from northern Mozambique formed three genetic groups, two of which showed evidence of recent hybridization. (A) The first PC accounted for 2.9% of variation and separated one cluster of 73 individuals from the remaining samples. The second PC sorted the remaining samples and was correlated with latitude. (B) ADMIXTURE found three genetic ancestry groups. Colored boxes on the PCA plot correspond to the colors used in the ADMIXTURE plot.

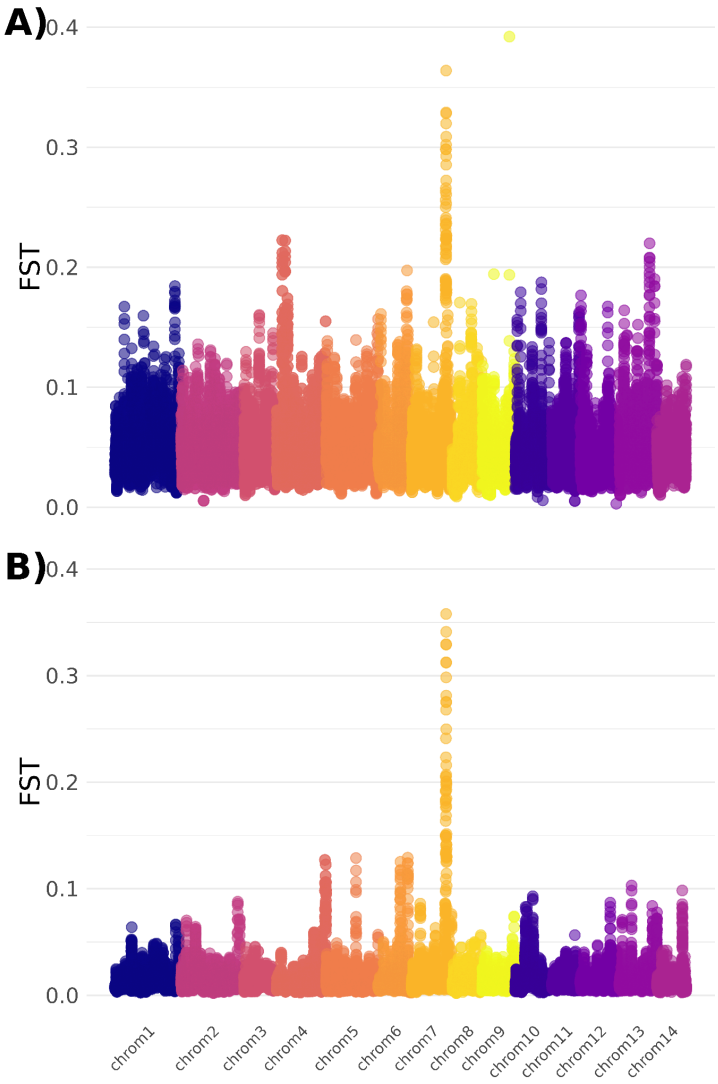

Figure 3.3: Relative differentiation between populations varied across the genome. Windowed FST comparisons are arranged by genomic position and colored by chromosome. (A) Genome-wide FST between DA and DB is 0.045 with a clear spike in FST on chromosome 7. (B) This approximately 100 kb area also differentiates the "north" and "south" genotypes of DA, which had an overall FST of 0.012.

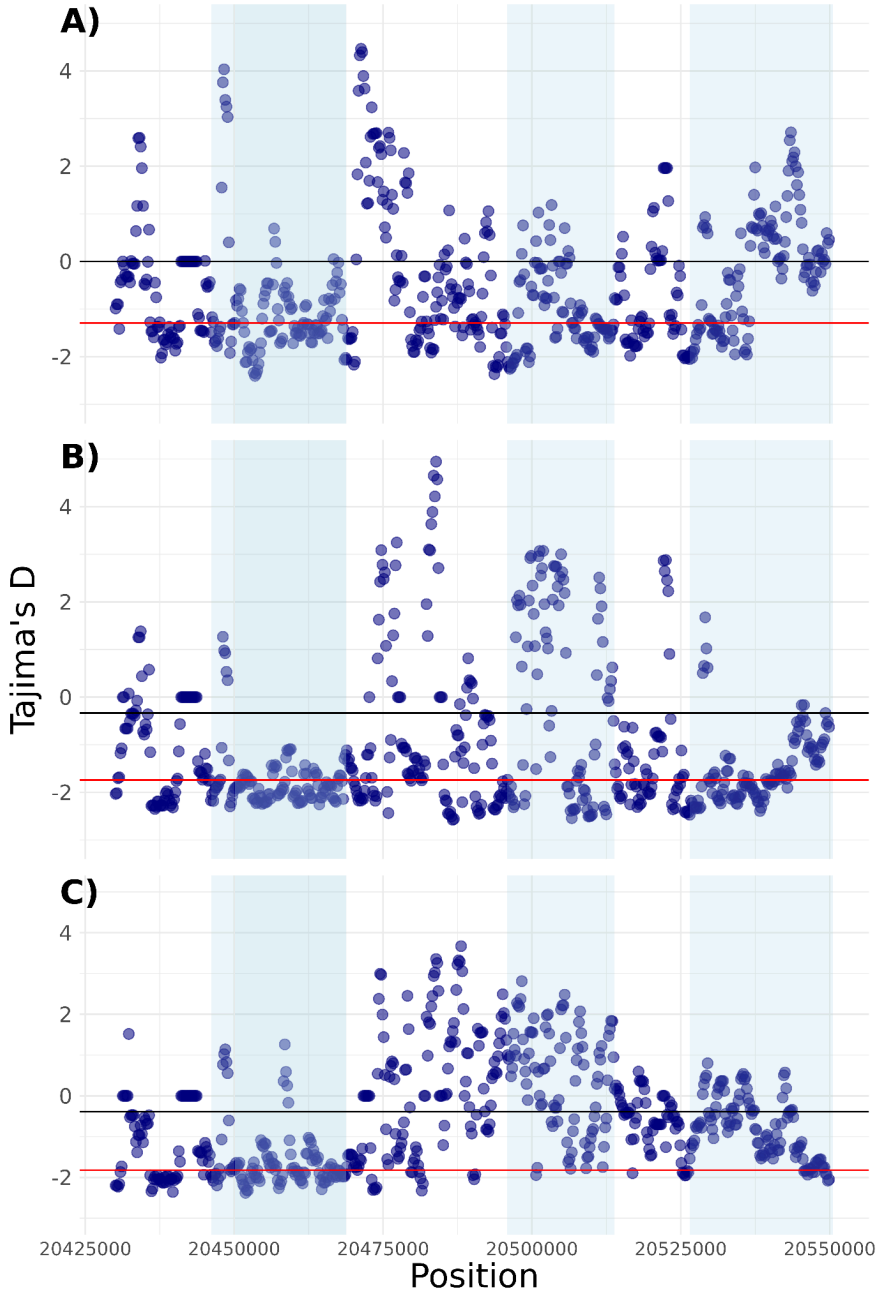

Figure 3.4: Tajima's D at the HES-1 locus is lower than the genome-wide average, but varies between coding and non-coding regions and between populations. The X axis is the genomic position on chromosome 7 from the *A. millepora* assembly. For each population, the black horizontal line represents the genome wide median Tajima's D, and the red line represents the genome wide 5th percentile Tajima's D.

Blue bars show areas corresponding to coding regions, some of which overlap. (A) In DB, Tajima's D was below the genome wide 5th percentile in two different coding regions. (B) In the north population of DA, Tajima's D was below the genome-wide 5th percentile in the first major coding region, but not the second. (C) In the south population of DA, Tajima's D was near the genome-wide average.

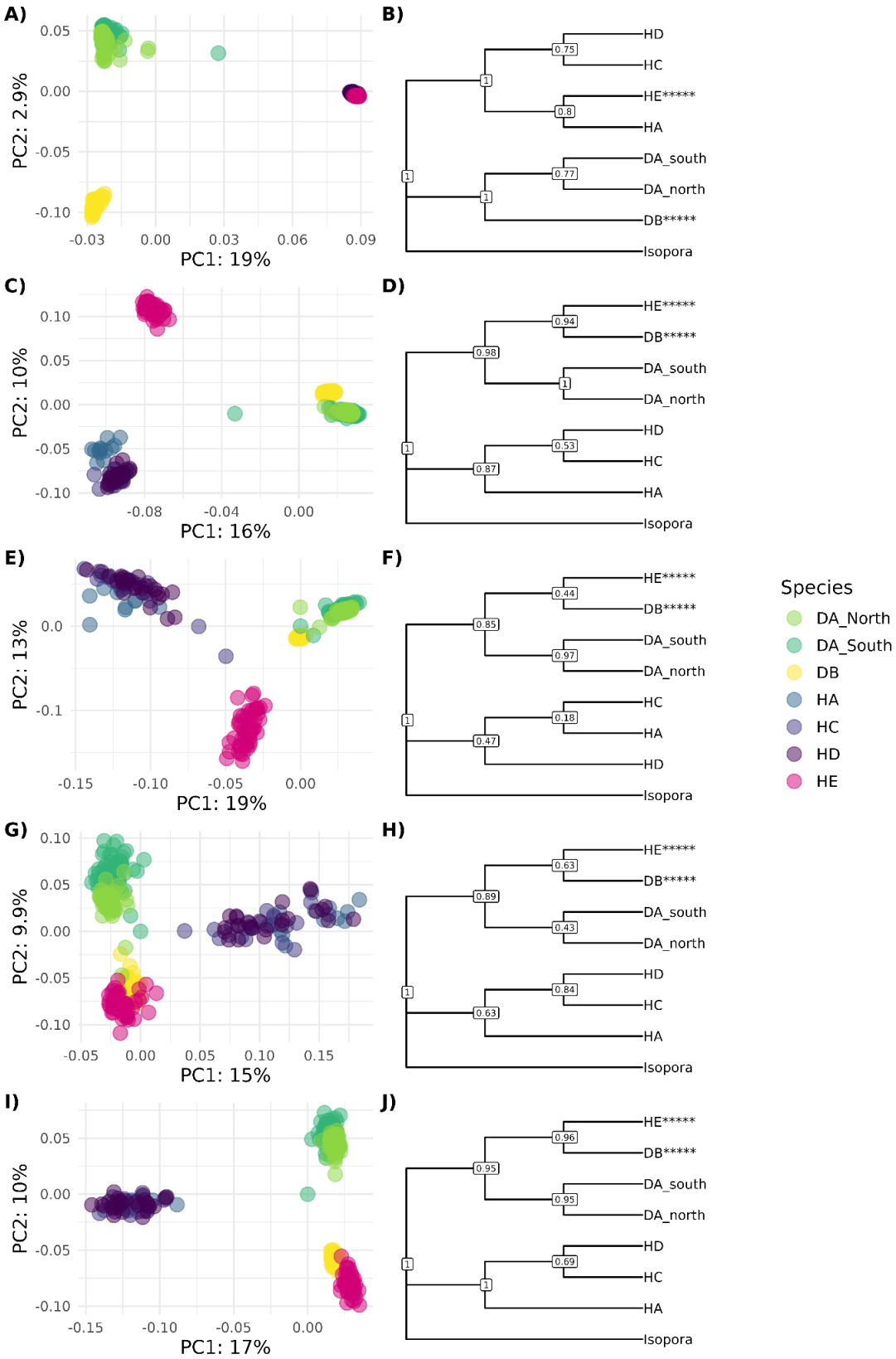
A)
B)
C)
D)
E)
F)
G)
H)
I)
J)
PC1: 19%
PC2: 2.9%
PC1: 16%
PC2: 10%
PC1: 19%
PC2: 13%
PC1: 15%
PC2: 9.9%
PC1: 17%
PC2: 10%
HD
HC
HE*****
HA
DA_south
DA_north
DB*****
Isopora
Species
DA_North
DA_South
DB
HA
HC
HD
HE

Fig. 3.5. Patterns of differentiation between *A. aff. divaricata* and *A. aff. hyacinthus* vary across the genome. Boxed numbers on nodes of trees show the number of bootstrap replicates (out of 1000) containing that node. Asterisks on tree tips indicate species collected primarily in hot microclimates. Branch lengths were omitted for ease of display. (A) and (B) At the whole genome level, the first PC clearly divided all *A. aff. divaricata* species from all *A. aff. hyacinthus*. The second and third PCs divided species within each group, but accounted for much less overall variation. (C) and (D) Analysis of the HES-locus as defined by Rose *et al.* (2021) clustered HE more closely with the *A. aff. divaricata* samples. (E) and (F) We saw increased distance between HE and the other *A. hyacinthus* taxa in the first major coding area (gene 114955281) of HES-1, as well as monophyletic grouping of *DB* and *HE* on a phylogenetic tree. (G) and (H) PCA clustering of the non-coding region of HES-1 also clustered DB and HE in both the PCA and the phylogenetic tree. (I) and (J) In the second coding area (gene 114955285) of HES-1, DB and HE clustered together in both the PCA and in the phylogenetic tree.

Sampling area	Samples of DA "north" type	Samples of DA "south" type	Samples of DB
Pemba Bay, inside bay	16	4	73
Pemba Bay, north peninsula	7	5	0
Pemba Bay, south peninsula	47	12	0
Caldeira Island	0	68	0

Table 3.1. Sampling areas and sites vary in which taxa they host. The inside of Pemba Bay hosted all of the individuals of DB, as well as some of DA from both north and south lineages. The two outer peninsulas of Pemba Bay hosted a mix of north and south lineages of DA. Caldeira Island hosted only the south lineage of DA.

	Percentile pi	Percentile Wattersons' theta	5 kb linkage percentile	Percentile Tajima's D
DB	2.2	2.7	91	12
DA north	1.3	2.3	93	6.9
DA south	20	14	94	37

Table 3.2. DB and DA north had low diversity, high linkage, and low Tajima's D at the HES-1 locus.

Appendix 3: Chapter 3 supplemental material

Logger location	Latitude	Longitude	Depth	Jan-May 2024 mean temperature	Jan-May 2024 mean daily temp range
Inner Bay Pemba	-12.916°	40.499°	7.5m	29.7° C	0.7° C
North Peninsula Pemba	-12.925°	40.514°	5.0m	29.5° C	0.8° C
South Peninsula Pemba	-12.960°	40.559°	9.0m	29.4° C	0.9° C
Caldeira Island Dock	-16.641°	39.723°	2.0m	27.6° C	1.4° C

Table A3.1. Temperature logger data by sampling area. Each row corresponds to one successfully recovered temperature logger. Logger deployment timeframes overlapped from January through May of 2024, so we report statistics for that period. All loggers were deployed with shading from white PVC pipe housings. Shallow deployment depth of the recovered logger on Caldeira Island likely resulted in substantially hotter and more variable temperatures than would otherwise have been observed at depths equivalent to Pemba deployments.

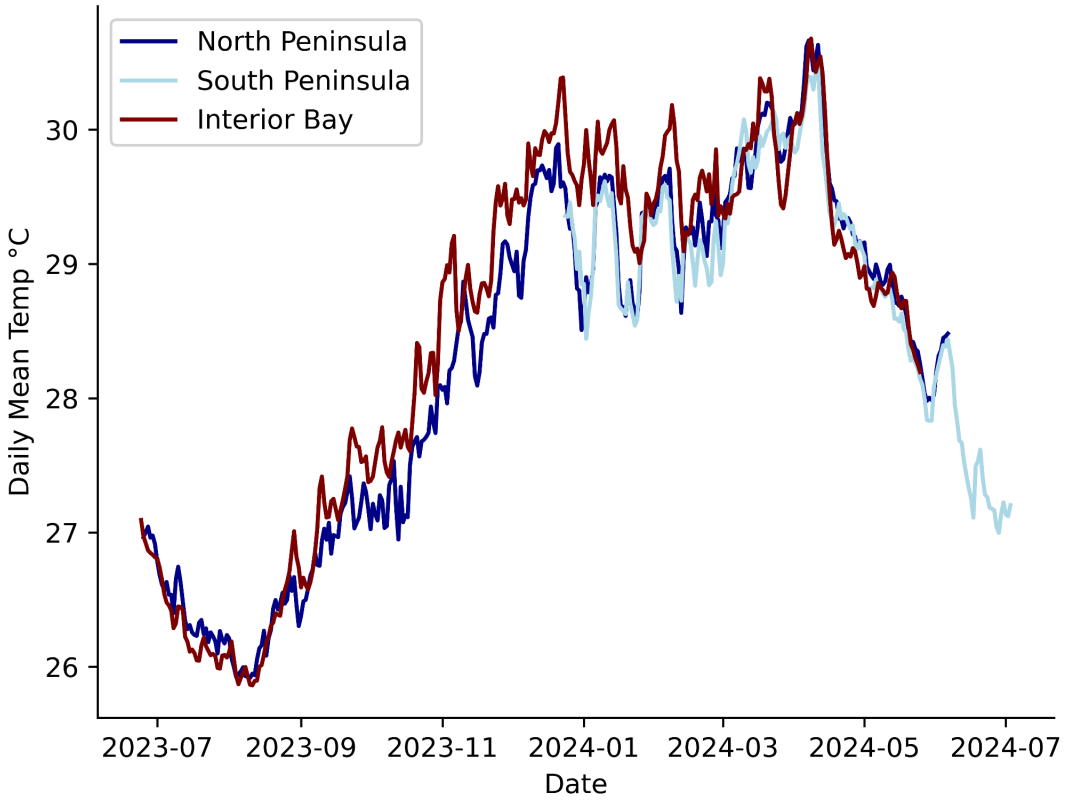

Fig A3.1. Daily mean temperatures vary with sampling area across the sites at Pemba Bay. Overall, the logger in the interior of Pemba Bay recorded the highest temperatures. Notes that differences in deployment depths between loggers (Table A3.1) may minimize the true temperature differences between areas.

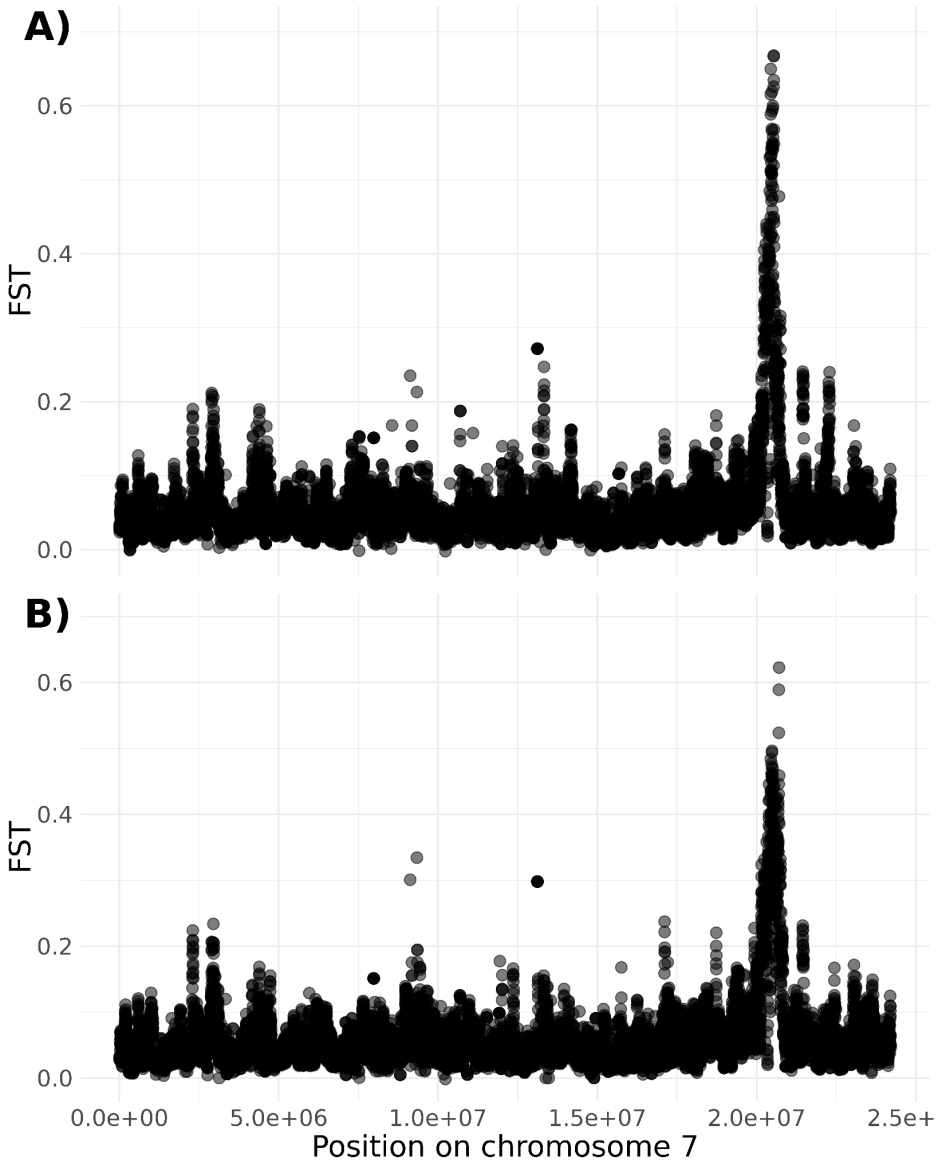

Fig. A3.2. *Acropora* species DB differentiates from both the north and south lineages of *Acropora* species DA at the HES-locus on Chromosome 7. (A) Windowed FST between DB and the north lineages of DA across chromosome 7 shows a spike in differentiation around the HES-1 locus. (B) Windowed FST between DB and the south lineages of DA across chromosome 7 shows a slightly weaker spike in differentiation around the HES-1 locus than that seen between DB and the north lineage of DA.

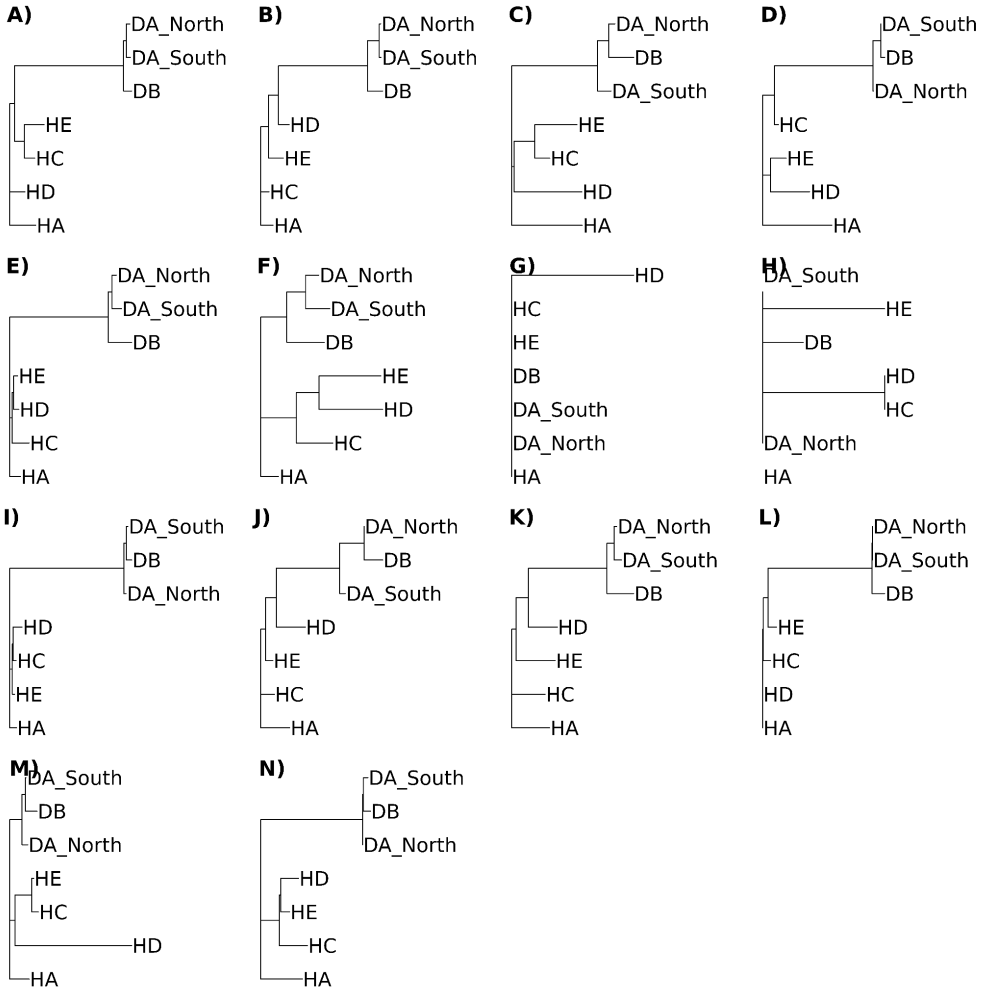

1.

Fig. A3.3. Single gene phylogenies for *Acropora* species in American Samoa and Mozambique. Each panel (A-N) corresponds to the first gene on a chromosome (Chromosome 1 - Chromosome 14). Tip names beginning with H correspond to corals collected in American Samoa, and tip names beginning with D correspond to corals collected in Mozambique. While exact tree configurations vary between genes, twelve of the trees show all Mozambique lineages in a monophyletic group, and no trees include clades with an American Samoa lineage and some but not all Mozambique lineages.

CONCLUSION

Corals face profound challenges from global change, yet continue to adapt to varying environments at multiple spatial scales. Here, I examine the spatial scale of variation in both climate and coral genetics to assess potential and evidence for local adaptation.

Chapters one and two consider spatial scale in climate variation and coral genetic variation, respectively. The contrast between the fine spatial scales of climate variation shown in Chapter 1 and the broad spatial scales of genetic variation in Chapter 2 would seem to preclude local adaptation at the sub-reef scale. However, additional results from Chapter 2 and Chapter 3 hint at how corals may adapt despite this mismatch. While my analysis for Chapter 2 does not show significant isolation by distance patterns in coral animals, all sampled coral host symbionts from a single genetic group, which do show significant isolation by distance patterns. These results suggest that hosting locally adapted symbionts may be one mechanism by which broadcast spawning corals adapt to local environmental conditions below their scale of dispersal.

Further study of these symbionts, especially using SNP-based methods such as RADSeq and whole genome sequencing, will be critical to understanding climate adaptation in corals. Algal symbiont genotype plays an important role in determining heat tolerance of a coral holobiont (Howells et al., 2016; Strader & Quigley, 2022). Historically, however, many studies of algal symbionts have been limited in their taxonomic specificity, only resolving lineages to the genus level (LaJeunesse et al.,

2018). Genomic marker-based methods offer finer taxonomic precision, while still missing important variation (Davies et al., 2023; González-Pech et al., 2021). A growing body of research suggests that SNP-based methods may reveal additional ecologically relevant variation within *Symbiodiniaceae* lineages (Eriksson et al., 2025). More studies in examining SNP-level genetic variation in *Symiodiniaceae* could illuminate the extent to which spatial variation in symbiont genetics contributes to fine scale climate adaptation, especially in corals with long larval dispersal distances.

Chapter 3 reveals that coral hosts can also show evidence for local adaptation, including at sub-10-kilometer spatial scales. *Acropora* found exclusively in the hottest microclimate of my sampling sites in Mozambique and morphologically similar *Acropora* found across all sampling sites constitute different, albeit closely related, species. The lack of hybridization between these groups may minimize outbreeding depression and allele swamping for two species that are geographically co-located but adapted to different microenvironments. The presence of closely related non-interbreeding species in distinct microclimates suggests that speciation may be another mechanism by which corals maintain genetic adaptations at spatial scales below their range of dispersal. Moreover, striking genetic similarity at the HES-1 locus between hot microclimate species found in Mozambique and American Samoa indicates an evolutionary mechanism for heat adaptation beyond *de novo* mutation. Either inherited variation from deep evolutionary time in the form of incomplete lineage sorting or cross-species genetic transfer via introgression could have resulted

in two widely geographically separated and genetically diverged species carrying the same adaptive allele. My results demonstrate that even closely related *Acropora* species may vary substantially at key adaptive loci.

Our inability to consistently delimit coral species using classical morphology complicates our ability to identify, much less conserve, species hosting potentially important adaptive variation. The last decade of genetic sequencing work has revealed that the genus *Acropora* contains many more species than previously believed (Bridge et al., 2024; Rassmussen et al., 2025). For example, two of my chapters reveal multiple *Acropora* species with overlapping distributions within putatively single species samples. This problem of ambiguous species identities is particularly severe in under sampled environments such as Mozambique. Moreover, the lack of study of Mozambican *Acropora* compared to other regions did not arise by chance. Rather, African universities often "lack investment in research and researchers" (Nganhane & Farooq, 2024). Field sampling and genetic sequencing play an increasingly central role in defining coral diversity, including in Mozambique (Duvane et al., 2025; Nassongole et al., 2026). Increased investment in Mozambican coral research, especially genetic sampling, could reveal unexpected taxonomic diversity. Some of this diversity, if managed and conserved, may play a role in buffering Indian Ocean coral reefs against climate change. Finally, such sampling can also contribute to better understanding of *Acropora* evolutionary history, including introgression events, and reveal additional sources of adaptive variation.

Taken together, these chapters suggest that while most genetic variation in broadcast spawning corals such as *Acropora* occurs at broad spatial scales, fine scale variation may also play a role in fostering local adaptation. In a best-case future scenario, heat tolerant coral genotypes found in hot microclimates may spread into nearby cooler microclimates, allowing coral communities to persist in spite of dangerously rising temperatures. However, much research remains to be done in order to determine if this scenario is plausible, let alone occurring.

Experimental studies of corals often focus on heat stress, but wild corals vary in their environmental tolerances across multiple axes (Fox et al., 2021; Higuchi et al., 2015; Kahng et al., 2019). Different microclimates vary in terms of not only average temperature but also temperature variability, depth, UV light exposure, and water quality. Increased genetic sampling of corals with respect to multiple environmental gradients, as well as experimental study of non-heat stressors, can inform our understanding of coral niches and how they vary across seascapes.

Global monitoring of coral bleaching has already led to major discoveries about risk factors for bleaching, as well as evidence for community-level evolution (McClanahan et al., 2019; Sully et al., 2019). Moving forward, incorporating genetic sampling into both baseline reef monitoring and monitoring of bleaching recovery can show if and how coral and symbiont lineages shift their ranges over time. Genotypes proliferating in the aftermath of heat stress could reveal pockets of adaptive potential.

Assisted migration of heat tolerant coral lineages across latitudinal gradients, or even ocean basins, remains mostly hypothetical and deeply controversial (Barreto et al., 2023; Camacho et al., 2026; Quigley et al., 2019). However, assisted migration of potentially heat tolerant coral genotypes from hot microclimates to nearby cooler microclimates is already occurring in the form of some coral restoration projects (Pausch et al., 2018).Coral outplanting more likely to be effective when created with explicit goals around genetic adaptation (Baums et al., 2019; Morikawa & Palumbi, 2019). Carefully monitored restoration projects that source coral fragments from warm areas and outplant to cooler areas could provide key information on when and whether hot microclimate corals actually thrive in cooler areas. Coupling such efforts with genetic sequencing could determine whether corals and symbionts in hot microclimates really do contain distinct alleles, and whether any of these alleles are adaptive.

No method of coral conservation provides a substitute for mitigating climate change and other anthropogenic impacts. However, research on corals continues to reveal an intriguing array of evolutionary innovations that allow these organisms to adapt to environmental differences across ocean basins and even within reefs. Hopefully, some combination of human action and corals' natural adaptive capacity will prove sufficient for coral reefs to survive and thrive far into the future.

References

Barreto, M. M., Schmidt-Roach, S., Zhong, H., & Aranda, M. (2023). Assessing the feasibility of assisted migration of corals in the Red Sea. *Frontiers in Marine Science*, *10*, 1181456. https://doi.org/10.3389/fmars.2023.1181456

Baums, I. B., Baker, A. C., Davies, S. W., Grottoli, A. G., Kenkel, C. D., Kitchen, S. A., Kuffner, I. B., LaJeunesse, T. C., Matz, M. V., Miller, M. W., Parkinson, J. E., & Shantz, A. A. (2019). Considerations for maximizing the adaptive potential of restored coral populations in the western Atlantic. *Ecological Applications*, *29*(8), e01978. https://doi.org/10.1002/eap.1978

Bridge, T. C. L., Cowman, P. F., Quattrini, A. M., Bonito, V. E., Sinniger, F., Harii, S., Head, C. E. I., Hung, J. Y., Halafihi, T., Rongo, T., & Baird, A. H. (2024). A *tenuis* relationship: Traditional taxonomy obscures systematics and biogeography of the ' *Acropora tenuis* ' (Scleractinia: Acroporidae) species complex. *Zoological Journal of the Linnean Society*, *202*(1), zlad062. https://doi.org/10.1093/zoolinnean/zlad062

Camacho, A. E., Dana, D. A., & Matz, M. (2026). Coral species from another ocean may be the only way to save Caribbean reefs. *Proceedings of the National Academy of Sciences*, *123*(4), e2521543123. https://doi.org/10.1073/pnas.2521543123

Davies, S. W., Gamache, M. H., Howe-Kerr, L. I., Kriefall, N. G., Baker, A. C., Banaszak, A. T., Bay, L. K., Bellantuono, A. J., Bhattacharya, D., Chan, C. X., Claar, D. C., Coffroth, M. A., Cunning, R., Davy, S. K., Del Campo, J., Díaz-Almeyda, E. M., Frommlet, J. C., Fuess, L. E., González-Pech, R. A., … Parkinson, J. E. (2023). Building consensus around the assessment and interpretation of Symbiodiniaceae diversity. *PeerJ*, *11*, e15023. https://doi.org/10.7717/peerj.15023

Duvane, J. A., Dupont, S., Sola, E., Ortega-Martinez, O., & Pereyra, R. T. (2025). Genetic diversity and structure among Acropora austera populations in Mozambique suggest low resilience potential of one of the world's most charismatic coral reefs. *Coral Reefs*, *44*(4), 1185–1195. https://doi.org/10.1007/s00338-025-02679-w

Eriksson, S. Y., Matz, M. V., Vize, P. D., & Rosser, N. L. (2025). Whole Genome Sequencing Reveals Genetic Differences Between Symbiodiniaceae Populations Among Reproductively and Geographically Isolated *Acropora* Colonies in Western Australia. *Ecology and Evolution*, *15*(1), e70771. https://doi.org/10.1002/ece3.70771

Fox, M. D., Nelson, C. E., Oliver, T. A., Quinlan, Z. A., Remple, K., Glanz, J., Smith, J. E., & Putnam, H. M. (2021). Differential resistance and acclimation of two coral species to chronic nutrient enrichment reflect life‐history traits. *Functional Ecology*, *35*(5), 1081–1093. https://doi.org/10.1111/1365-2435.13780

González-Pech, R. A., Stephens, T. G., Chen, Y., Mohamed, A. R., Cheng, Y., Shah, S., Dougan, K. E., Fortuin, M. D. A., Lagorce, R., Burt, D. W., Bhattacharya, D., Ragan, M. A., & Chan, C. X. (2021). Comparison of 15 dinoflagellate genomes reveals extensive sequence and structural divergence in family Symbiodiniaceae and genus Symbiodinium. *BMC Biology*, *19*(1), 73. https://doi.org/10.1186/s12915-021-00994-6

Higuchi, T., Agostini, S., Casareto, B. E., Suzuki, Y., & Yuyama, I. (2015). The northern limit of corals of the genus Acropora in temperate zones is determined by their resilience to cold bleaching. *Scientific Reports*, *5*(1), 18467. https://doi.org/10.1038/srep18467

Howells, E. J., Abrego, D., Meyer, E., Kirk, N. L., & Burt, J. A. (2016). Host adaptation and unexpected symbiont partners enable reef‐building corals to tolerate extreme temperatures. *Global Change Biology*, *22*(8), 2702–2714. https://doi.org/10.1111/gcb.13250

Kahng, S. E., Akkaynak, D., Shlesinger, T., Hochberg, E. J., Wiedenmann, J., Tamir, R., & Tchernov, D. (2019). Light, Temperature, Photosynthesis, Heterotrophy, and the Lower Depth Limits of Mesophotic Coral Ecosystems. In Y. Loya, K. A. Puglise, & T. C. L. Bridge (Eds.), *Mesophotic Coral Ecosystems* (Vol. 12, pp. 801–828). Springer International Publishing. https://doi.org/10.1007/978-3-319-92735-0_42

LaJeunesse, T. C., Parkinson, J. E., Gabrielson, P. W., Jeong, H. J., Reimer, J. D., Voolstra, C. R., & Santos, S. R. (2018). Systematic Revision of Symbiodiniaceae Highlights the Antiquity and Diversity of Coral Endosymbionts. *Current Biology*, *28*(16), 2570-2580.e6. https://doi.org/10.1016/j.cub.2018.07.008

McClanahan, T. R., Darling, E. S., Maina, J. M., Muthiga, N. A., 'agata, S. D., Jupiter, S. D., Arthur, R., Wilson, S. K., Mangubhai, S., Nand, Y., Ussi, A. M., Humphries, A. T., Patankar, V. J., Guillaume, M. M. M., Keith, S. A., Shedrawi, G., Julius, P., Grimsditch, G., Ndagala, J., & Leblond, J. (2019). Temperature patterns and mechanisms influencing coral bleaching during the 2016 El Niño. *Nature Climate Change*, *9*(11), 845–851. https://doi.org/10.1038/s41558-019-0576-8

Morikawa, M. K., & Palumbi, S. R. (2019). Using naturally occurring climate resilient corals to construct bleaching-resistant nurseries. *Proceedings of the National Academy of Sciences*, *116*(21), 10586–10591. https://doi.org/10.1073/pnas.1721415116

Nassongole, B. A. F., Buhl-Mortensen, L., Da Silva, I. M., Hilário, A., & McFadden, C. S. (2026). Exploring the diversity and distribution of Mozambique's soft corals (Octocorallia) through an integrative approach. *Marine Biodiversity*, *56*(2), 23. https://doi.org/10.1007/s12526-026-01628-2

Nganhane, I. D. N., & Farooq, H. (2024). Self-advocacy for young African scientists. *Science*, *384*(6697), 748–748. https://doi.org/10.1126/science.adp0406

Pausch, R., Williams, D., & Miller, M. (2018). Impacts of fragment genotype, habitat, and size on outplanted elkhorn coral success under thermal stress. *Marine Ecology Progress Series*, *592*, 109–117. https://doi.org/10.3354/meps12488

Quigley, K. M., Bay, L. K., & Van Oppen, M. J. H. (2019). The active spread of adaptive variation for reef resilience. *Ecology and Evolution*, *9*(19), 11122–11135. https://doi.org/10.1002/ece3.5616

Rassmussen, S. H., Cowman, P. F., Baird, A. H., Crosbie, A. J., Quattrini, A. M., Bonito, V., Sinniger, F., Harii, S., Cabaitan, P. C., Fadli, N., Tan, C.-H., Hung, J. Y.-H., Rongo, T., Huang, D., Halafihi, T., & Bridge, T. C. L. (2025). The tables have turned: Taxonomy, systematics and biogeography of the Acropora hyacinthus (Scleractinia: Acroporidae) complex. *Invertebrate Systematics*, *39*(8), IS24049. https://doi.org/10.1071/IS24049

Strader, M. E., & Quigley, K. M. (2022). The role of gene expression and symbiosis in reef-building coral acquired heat tolerance. *Nature Communications*, *13*(1), 4513. https://doi.org/10.1038/s41467-022-32217-z

Sully, S., Burkepile, D. E., Donovan, M. K., Hodgson, G., & Van Woesik, R. (2019). A global analysis of coral bleaching over the past two decades. *Nature Communications*, *10*(1), 1264. https://doi.org/10.1038/s41467-019-09238-2